(6)
B.S.

RESEARCH ON MOLECULAR LASERS

ANNUAL REPORT

1 November, 1975

Cornell University
Ithaca, N.Y. 14853

521,204

(12)

Sponsored by:

Advanced Research Projects Agency

ARPA Order No. 2062

UNCLASSIFIED

Security Classification

DOCUMENT CONTROL DATA - R&D

(Security classification of title, body of abstract and indexing annotation must be entered when the overall report is classified)

1. ORIGINATING ACTIVITY (Corporate author)

Cornell University
Ithaca, N.Y. 14853

2a. REPORT SECURITY CLASSIFICATION

Unclassified

2b. GROUP

N/A

3. REPORT TITLE

(6) Study of Molecular Lasers.

4. DESCRIPTIVE NOTES (Type of report and inclusive dates)

(9) Annual Report, 1975 ~~1975~~ 1 Oct 74 - 30 Sep 75

5. AUTHOR(S) (Last name, first name, initial)

(10) George J. Wolga, Ross A. McFarlane
Simon H. Bauer, Terrill A. Cool

6. REPORT DATE

(11) Nov~~ember~~ 1975

7a. TOTAL NO. OF PAGES

56

7b. NO. OF REFS

28

8a. CONTRACT OR GRANT NO.

(13) N00014-67-A-0077-0006,

b. PROJECT NO.

c. W/ARPA/ Order-2062

d.

9a. ORIGINATOR'S REPORT NUMBER(S)

N/A (12) 61p.

9b. OTHER REPORT NO(S) (Any other numbers that may be assigned this report)

N/A

10. AVAILABILITY/LIMITATION NOTICES

11. SUPPLEMENTARY NOTES

12. SPONSORING MILITARY ACTIVITY

Office of Naval Research

13. ABSTRACT

Research concerning molecular and chemical lasers was conducted in the following areas:

(1) Vibrational relaxation measurements at T=300 K of HF(v=1), DF(v=1), CO_2(00°1) and HCl(v=1) by atoms including H, D, O, N, F, Cl and Br.

(2) Collisional deactivation of CO(v=1) by oxygen atoms over the temperature range 273K to 390K.

(3) Vibrational relaxation measurements in the HF-DF, HF-CO_2 and DF-CO_2 systems at very low temperatures.

(4) Studies directed toward the measurement of the V→R rates of energy transfer in HF - HF collisions.

(5) Studies directed towards the rapid generation of electronically and/or vibrationally excited boron containing di and triatomics.

(6) Reaction rate studies between B, BH, BH_2 or BH_3 radicals with oxidizers such as NF_3, N_2O and NO_2.

(7) Homogeneous iniation of chemical reactions by pulsed laser heating.

DD FORM 1 JAN 64 1473

Unclassified

Security Classification

098550

14. KEY WORDS	LINK A		LINK B		LINK C	
	ROLE	WT	ROLE	WT	ROLE	WT
Molecular Lasers Chemical Lasers Vibrational Relaxation Energy Transfer Chemical Reaction Rates HF, DF, HCl, HF-CO_2, DF-CO_2, HCl Reactions with Boron Hydrides						

INSTRUCTIONS

1. ORIGINATING ACTIVITY: Enter the name and address of the contractor, subcontractor, grantee, Department of Defense activity or other organization *(corporate author)* issuing the report.

2a. REPORT SECURITY CLASSIFICATION: Enter the overall security classification of the report. Indicate whether "Restricted Data" is included. Marking is to be in accordance with appropriate security regulations.

2b. GROUP: Automatic downgrading is specified in DoD Directive 5200.10 and Armed Forces Industrial Manual. Enter the group number. Also, when applicable, show that optional markings have been used for Group 3 and Group 4 as authorized.

3. REPORT TITLE: Enter the complete report title in all capital letters. Titles in all cases should be unclassified. If a meaningful title cannot be selected without classification, show title classification in all capitals in parenthesis immediately following the title.

4. DESCRIPTIVE NOTES: If appropriate, enter the type of report, e.g., interim, progress, summary, annual, or final. Give the inclusive dates when a specific reporting period is covered.

5. AUTHOR(S): Enter the name(s) of author(s) as shown on or in the report. Enter last name, first name, middle initial. If military, show rank and branch of service. The name of the principal author is an absolute minimum requirement.

6. REPORT DATE: Enter the date of the report as day, month, year, or month, year. If more than one date appears on the report, use date of publication.

7a. TOTAL NUMBER OF PAGES: The total page count should follow normal pagination procedures, i.e., enter the number of pages containing information.

7b. NUMBER OF REFERENCES: Enter the total number of references cited in the report.

8a. CONTRACT OR GRANT NUMBER: If appropriate, enter the applicable number of the contract or grant under which the report was written.

8b, 8c, & 8d. PROJECT NUMBER: Enter the appropriate military department identification, such as project number, subproject number, system numbers, task number, etc.

9a. ORIGINATOR'S REPORT NUMBER(S): Enter the official report number by which the document will be identified and controlled by the originating activity. This number must be unique to this report.

9b. OTHER REPORT NUMBER(S): If the report has been assigned any other report numbers *(either by the originator or by the sponsor)*, also enter this number(s).

10. AVAILABILITY/LIMITATION NOTICES: Enter any limitations on further dissemination of the report, other than those imposed by security classification, using standard statements such as:

(1) "Qualified requesters may obtain copies of this report from DDC."

(2) "Foreign announcement and dissemination of this report by DDC is not authorized."

(3) "U. S. Government agencies may obtain copies of this report directly from DDC. Other qualified DDC users shall request through _____."

(4) "U. S. military agencies may obtain copies of this report directly from DDC. Other qualified users shall request through _____."

(5) "All distribution of this report is controlled. Qualified DDC users shall request through _____."

If the report has been furnished to the Office of Technical Services, Department of Commerce, for sale to the public, indicate this fact and enter the price, if known.

11. SUPPLEMENTARY NOTES: Use for additional explanatory notes.

12. SPONSORING MILITARY ACTIVITY: Enter the name of the departmental project office or laboratory sponsoring *(paying for)* the research and development. Include address.

13. ABSTRACT: Enter an abstract giving a brief and factual summary of the document indicative of the report, even though it may also appear elsewhere in the body of the technical report. If additional space is required, a continuation sheet shall be attached.

It is highly desirable that the abstract of classified reports be unclassified. Each paragraph of the abstract shall end with an indication of the military security classification of the information in the paragraph, represented as *(TS), (S), (C), or (U)*.

There is no limitation on the length of the abstrac .. However, the suggested length is from 150 to 225 words.

14. KEY WORDS: Key words are technically meaningful terms or short phrases that characterize a report and may be used as index entries for cataloging the report. Key words must be selected so that no security classification is required. Identifiers, such as equipment model designation, trade name, military project code name, geographic location, may be used as key words but will be followed by an indication of technical context. The assignment of links, roles, and weights is optional.

ANNUAL REPORT

Reporting Period

1 October 1974 - 30 September 1975

1.	ARPA Order Number	2062
2.	Program Code Number	3E20
3.	Name of Contractor	Cornell University
4.	Effective Date of Contract	1 October 1968
5.	Contract Expiration Date	30 September 1975
6.	Amount of Contract for Current Period	$120,000
7.	Contract Number	N00014-76-C-0426
8.	Principal Investigator	Professor G. J. Wolga
9.	Telephone Number	(607)-256-3962
10.	Project Scientists	Professor S. H. Bauer (607)-256-4028
		Professor T. A. Cool (607)-256-4191
		Professor R. A. McFarlane (607)-256-4075
11.	Title of Work	RESEARCH ON MOLECULAR LASERS

Sponsored by

ADVANCED RESEARCH PROJECTS AGENCY

ARPA Order No. 2062

The views and conclusions contained in this document are those of the authors and should not be interpreted as necessarily representing the official policies, either expressed or implied, of the Advanced Research Projects Agency or the U.S. Government.

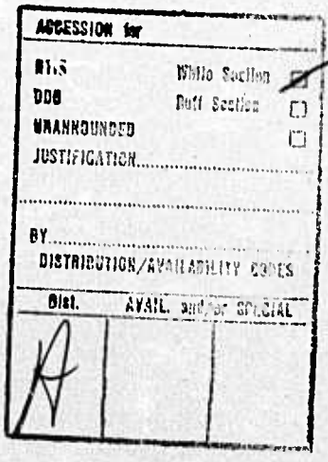

Technical Report Summary

This report describes research conducted at Cornell University on molecular and chemical laser systems. The objective of this work has been to provide precise, quantitative information concerning: the rates, and their temperature dependence, with which vibrational and rotational molecular energy in important laser molecules is transferred to other molecules, redistributed among the degrees of freedom of the same molecule or relaxed by collisions with molecules or atoms; the temperature dependence of these rates; conditions for rapidly generating high densities of electronically and/or vibrationally excited boron containing diatomics and triatomics; the rates of reaction between various boron hydrides and oxidizers to provide kinetic information relevant to new laser systems; homogeneous chemical reaction initiation by means of laser induced gas heating.

The methodology employed consisted of laboratory experiments utilizing: laser induced fluorescence measurements; quantitative EPR determination of atom concentrations; optical double resonance experiments; laser heating with high energy CO_2 laser pulses coupled with chemiluminescence spectroscopy.

Specific technical results obtained were:

1. Vibrational deactivation rates of HF(v=1), DF(v=1) and $CO_2(00^0 1)$ by collisions with atoms such as H,O,F,Cl,Br,N at T=300 K.
2. Vibrational deactivation of CO(v=1) by O atoms over the temperature range 273 K to 390 K.
3. The temperature dependence, at very low temperatures, of vibrational relaxation in the HF-DF, HF-CO_2 and DF-CO_2 systems. These studies clearly established the lower limit for operating temperature of HF chemical lasers. At sufficiently low temperatures HF polymers dominate the deactivation of HF vibrational energy with tetramers and hexamers being the most effective.
4. Preliminary kinetic results on oxidation reactions with boron hydrides producing electronically excited boron containing molecules were obtained.

The rates experimentally determined in these studies can be directly utilized in the comprehensive modeling that is required for the development and scaling of high power HF, DF, CO_2, HF-CO_2, DF-CO_2, and CO lasers.

INDEX

Deactivation of Molecular Vibrational Energy by Atoms

Professor G. J. Wolga

Our primary effort during the past year was to complete our study of the deactivation of HF(v=1), DF(v=1) and $CO_2(00°1)$ by atoms. Initial study of the deactivation of HCl(v=1) by atoms was begun also. All our work employed the technique of laser induced fluorescence in a flow system with atom concentration determination by EPR spectroscopy. The major portion of our results has been published and reprints or preprints of published papers are appended to this report giving complete details of our work. In what follows, the major conclusions to be drawn from these studies will be summarized. Our work on HF, DF and CO_2 deactivation was reported at the St. Louis Chemical Laser Conference and at the Army Symposium on High Energy Lasers held at Huntsville on November 3-4, 1975.

A. HF and DF, v=1

1. The rate constants for deactivation of HF(v=1) and DF(v=1) by O, Cl, F atoms are given below in units of sec^{-1} $Torr^{-1}$:

HF(v=1)		DF(v=1)	
k_{O-HF}	$= 1.1 \pm 0.2 \times 10^{+5}$	k_{O-DF}	$= 2.8 \pm 0.6 \times 10^{+5}$
k_{Cl-HF}	$= 2.6 \pm 0.4 \times 10^{+4}$	k_{Cl-DF}	$= 7.1 \pm 1.0 \times 10^{+4}$
k_{F-HF}	$= 0.99 \pm 0.2 \times 10^{+4}$	k_{F-DF}	$= 2.3 \pm 0.4 \times 10^{+4}$

a) Rotational relaxation cannot explain these results since the heavier molecule, DF, is relaxed more efficiently.

b) Atom exchange or abstraction reactions can be ruled out in the cases of O, Cl and F relaxation because the reactions are endothermic for O and Cl and because the rate constants for O and Cl are much larger than are those for F even though the potential reaction with F becomes exothermic with the addition of one quantum of vibrational energy. In the latter case these results suggest that the potential barrier for reaction exceeds the excitation of the v=1 state.

c) Our H atom experimental results have not shown a measurable change of the HF/DF decay rate when atoms are present. A null experimental result complicates the usual approximate double exponential analysis (appropriate to the HF, H_2, H system) and we believe it is not valid under the experimental conditions usually found in our and other studies. We have recently developed a new method of analysis based upon a Taylor series expansion of the slow and fast time constants which gives promise of permitting a proper rate constant analysis if conditions can be found such that a change in the decay rate is observed. We intend to restudy the H/HF system under conditions of maximum H atom concentration and minimum HF concentration in an effort to settle this issue. Full publication of our H/HF results awaits this better data.

d) In the cases of O, Cl and F atoms both spin-orbit split states must be considered to contribute to the deactivation. The higher lying spin-orbit states are far from resonant with the v=1 states of HF and DF and thus simple and unspecific vibrational relaxation has been assumed in our analysis. This is not true in the case of Br(^2P3/2) deactivating HF(v=1) where the Br(^2P1/2) state is closely resonant with HF(v=1) and we have seen and reported very rapid V→E energy transfer in this system.

B. $CO_2(00°1)$

1. The rate constants for deactivation of $CO_2(00°1)$ by O, Cl, F, H, D and N atoms are given below in units of sec^{-1} $Torr^{-1}$:

$$k_{O-CO_2} = 6.69 \pm 1.2 \times 10^{+3}$$

$$k_{Cl-CO_2} = 4.91 \pm 1.3 \times 10^{5}$$

$$k_{F-CO_2} = 1.04 \pm 0.9 \times 10^{5}$$

$$k_{H-CO_2} = 3.3 \pm 3 \times 10^{3}$$

$$k_{D-CO_2} \leq 2.0 \times 10^{3}$$

$$k_{N-CO_2} \leq 9.6 \times 10^{2}$$

a) In the cases of H, D and N no change in the decay rates were observed when atoms were present in contrast to the experiments with O, Cl and F atoms.

b) Landau-Teller Theory is an unlikely explanation for the very large rate constants observed with O and F and Cl atoms. Unrealistic interaction parameters would be required to explain our experimental results.

c) Chemical reactions are not likely in the cases of Cl and F relaxing CO_2 because of the large endothermicity of the reactions. The reaction

$$CO_2(00°1) + O(^3P) \rightarrow O_2 + CO$$

is only slightly endothermic but the reverse step is known to be very slow which discounts the possibility of the forward reaction.

d) The large rate constants observed with P state atoms (O,Cl,F) and the small rate constants observed with S state atoms (H,D,N) suggests a vibronic mechanism discussed in C below.

e) Nothing definite can be said concerning the relative relaxation efficiencies of the two spin orbit states present in the cases of O, F and Cl. However, a fast V→E energy transfer mechanism is probably ruled out because of lack of energy resonance and because only a single exponential decay was observed.

C. General Conclusions

1. Most of our work so far reported substantiates the view that a vibronic energy transfer mechanism is important when the deactivating atoms possess degenerate orbital angular momentum. This concept was proposed by Nikitin on the basis of data for other systems but ties our work together as well. Thus atoms like O, Cl, and F are more efficient relaxation partners than are H, D and N. A quantitative theory of the vibronic relaxation mechanism for the atom-molecule pairs we have studied does not exist at this time.

2. When the relaxation of HF/DF are compared to that of $CO_2(00°1)$ with the same atoms O, Cl and F we find that O relaxes HF/DF most rapidly and $CO_2(00°1)$, least rapidly. F atoms are least effective in relaxing HF/DF while Cl atoms are the fastest relaxers of $CO_2(00°1)$. It is hard to understand these results without including details of the interaction complex of molecule-atom during the collision. Such details will most likely include effects like Nikitin's vibronic interaction including curve crossings between different electronic states and are unlikely to be effectively described by the rather simple potential surface calculations that are usually invoked to explain and predict experimental results.

D. HCl relaxation by atoms

We have performed preliminary experiments on HCl(v=1) relaxed by H, O, Cl, F and N. In most cases relatively large effects were observed due to the presence of atoms indicating that useful results can be obtained from our experiments. However, these preliminary results suggested that reactive collisions with the atoms were occurring and thus more careful studies were required to separate the rate constants for reactive collisions and ordinary vibrational relaxation. Since reactive collisions can be studied in flow systems like our own we shall continue this work during the next contract period.

Vibrational relaxation of $CO_2(001)$ by atoms

M. I. Buchwald and G. J. Wolga

Cornell University, Ithaca, New York 14853
(Received 17 December 1974)

The laser fluorescence technique coupled with ESR detection of atoms has been used to measure the vibrational relaxation of $CO_2(001)$ by $O(^3P)$, $Cl(^2P)$, and $F(^2P)$. The rates are $k_{CO_2\text{-}O} = 6.69\times10^3$ (sec·Torr)$^{-1}$, $k_{CO_2\text{-}Cl} = 4.91\times10^5$ (sec·Torr)$^{-1}$ and $k_{CO_2\text{-}F} = 1.04\times10^5$ (sec·Torr)$^{-1}$. These rates are much faster than those of rare gas atoms of similar atomic weights. Measurements were also made establishing limits for the relaxation of CO_2 by $H(^2S)$, $D(^2S)$, and $N(^4S)$.

I. INTRODUCTION

Current interest in the rates of vibrational relaxation of molecules by atoms dates from the study of the relaxation of molecular oxygen by atomic oxygen of Kiefer and Lutz[1] in 1967. Researchers in the field of upper atmospheric chemistry and gas lasers have been active in pursuing these data and the recent literature contains several of these rates.

Both electrical discharge and chemical transfer CO_2 lasers involve the production of substantial amounts of atomic and radical species, in the former N atoms, in the latter H, D, and F. Knowledge of atom deactivation rates is therefore required to satisfactorily model these as well as other important laser systems.

Above the stratosphere large concentrations of O atoms are maintained by the photolytic decomposition of ozone.[2] The relaxation rate of atoms on CO_2, O_2, N_2, and O_3 may have an important effect on both the thermal balance and through the vibrational temperature of O_3, on the chemistry and constituents of this important atmospheric layer. Very recent evidence of the presence of freons at this altitude gives the measurement of chlorine atom vibrational relaxation rates additional importance.

Some of these previously measured atom–molecule vibrational relaxation rates[3,4] are anomalously fast and exhibit unusual temperature dependencies. Several suggestions have been made for mechanisms of vibrational relaxation when one of the colliders has an unpaired electron. Chemical theories imply that either a chemical reaction takes place with the aid of vibrational excitation or a stable intermediate is formed. The first type of mechanism can be made apparent by isotopic substitution and the second can usually be detected by spectroscopic means.

As Nikitin[5] has pointed out, vibronic mechanisms of vibrational energy transfer from ground electronic states at thermal velocities become possible when one of the colliding species contains degenerate electronic angular momentum.

We will contrast atom–CO_2 relaxation rates between atoms with $L=0$ and $L\neq0$.

With the addition of the data presented here, $CO_2(00^\circ1)$ vibrational relaxation is probably the most widely studied[6] energy transfer process. Although CO_2 is not the most amenable molecule for quantitative calculation of relaxation rates we can, as a result of the data now available, begin to make some general statement about different classes of relaxers.

II. EXPERIMENTAL

These experiments were made under flowing gas conditions (Fig. 1) at room (298 °K) temperature. The flow tube was 11 mm i.d. quartz with Suprasil in the electron spin resonance (ESR) cavity. Downstream of the microwave discharge the flow tube including the section passing through the ESR cavity was entirely lined with thin Teflon tubing during the atom measurement. During the fluorescence measurement the Teflon lining which obscured the optical cell windows was removed. The cell was constructed from a standard stainless steel "T" vacuum connection and the three optical windows were 1.25 cm Irtran-2 disks.

The optical cell is lined with Teflon during the ESR measurement to eliminate the possibility of effective wall recombination of atoms.

The diatomic gas to be dissociated was mixed with helium upstream of the microwave discharge (a standard Evenson type cavity operating at 2443 MHz) and CO_2 was injected downstream of the observed plasma.

The system is capable of high flow rates (40 m/sec) but the flow was usually throttled downstream of the ESR cavity to less than 10 m/sec by narrow bore tubing. This was done in order to permit long enough window transit times so that the removal of excited CO_2 molecules from the detector field of view by the flow did not compete with vibrational relaxation.

CO_2 pressures were varied from 4 to 15 Torr. The pressure of the diatomic gas plus the helium carrier was always less than 3 Torr. Microwave power delivered to the flow tube varied from 20 to 100 W. Adjusting microwave power allowed us to vary the atom concentrations over a factor of up to 3 without altering the initial constituents. Flow conditions did not change with discharge power because the atom concentration was always a small fraction of the total flow.

The ESR spectrometer was of the homodyne type. The klystron frequency was 8968 MHz and was locked to the ESR cavity. Magnetic field modulation was at 10 kHz. The spectrometer sensitivity was calibrated absolutely with molecular oxygen using the technique detailed by Westenberg.[7]

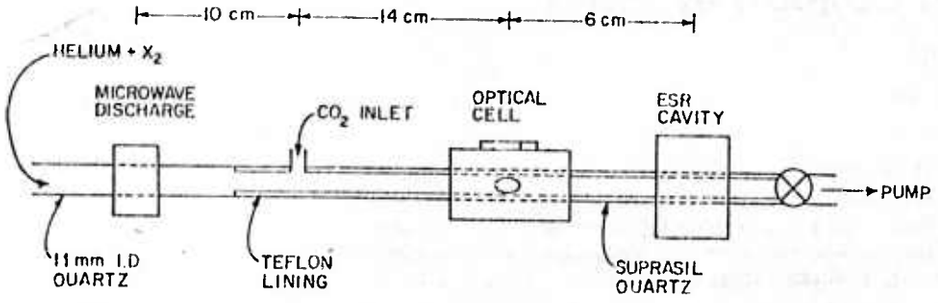

FIG. 1. Schematic representation of the gas flow system used in this work.

The measurement of hydrogen, deuterium, and nitrogen atom concentrations required special care because of the low saturation[8] parameters of the microwave transitions. Microwave power was lowered until a constant (with variation of power) apparent concentration was measured. Saturation could also be detected by an increase in signal strength when molecular oxygen was injected just before the ESR cavity. The oxygen molecules are effective at both broadening the microwave transition and relaxing the upper state.

It was not possible to isolate a single atomic chlorine absorption line due to severe pressure broadening and the close spacing of lines. Instead the entire chlorine spectrum[7] of 24 lines from both isotopes was recorded and reduced to an atom concentration.

Several laser fluorescence decay measurements were made for each initial composition. Fluorescence was first recorded with no microwave discharge, and then under several different levels of microwave excitation. The CO_2 laser was of the transverse pin discharge type. Laser output at 10.6 μ was 40 mJ in each 5 μsec pulse (FWHM) at a frequency of 2 Hz. Fluorescence at 4.3 μ from the $CO_2(001)-(000)$ transition was detected by a photovoltaic 77 °K In–Sb detector and averaged using a Biomation 8100 digital transient recorder and a Northern 575 signal analyzer (see Fig. 2). For each fluorescence decay rate measurement 128 fluorescence pulses were averaged yielding signal to noise ratios of better than 100 to 1. Semilog plots of laser fluorescence counts vs time were made over a range of 40 or more to extract decay rates.

Pressures were measured with a 0.1 to 20 Torr range Bourdon tube type Wallace and Tiernan gauge which was calibrated by a McLeod gauge.

The fractional change in atom concentration between the optical cell and the ESR cavity 6 cm downstream was obtained by use of a measured atom recombination rate coefficient per unit length in the Teflon lined tube. Decreases in atom concentration due to the 6 cm of Teflon lined tube was always less than a 20% correction to the measured atom concentration.

Microwave discharges in the carrier gas alone (helium) made no detectable change in the observed CO_2 relaxation. This attested to both the purity of the carrier gas and the lack of heating downstream of the discharge in the optical cell. This also demonstrated that the CO_2 was being introduced far enough downstream so that it was not being dissociated by the microwave plasma.

CO_2 was Linde Coleman Instrument Grade. Helium was purified through liquid nitrogen cooled activated charcoal. Nitrogen, hydrogen, chlorine, fluorine, and oxygen were Linde ultra high purity grade. Deuterium was Matheson technical grade.

III. ANALYSIS OF RESULTS

Atom–molecule rate constants were easily extracted from measurements. The observed change in fluorescence decay rate due to the microwave discharge is given by

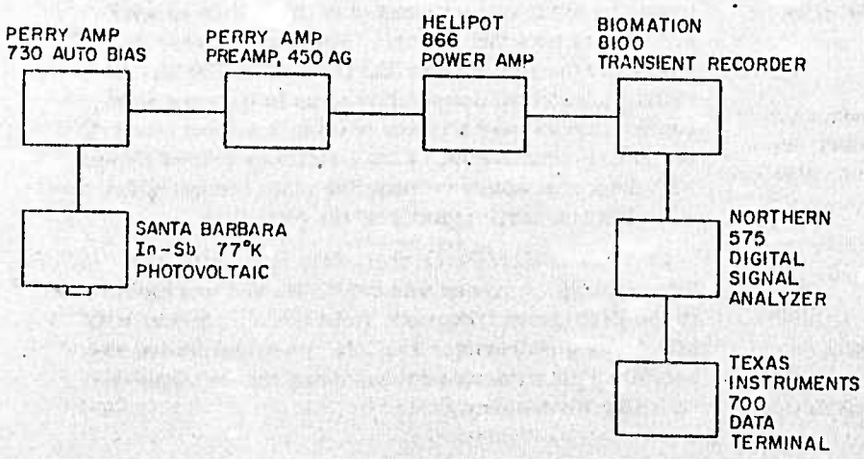

FIG. 2. Schematic diagram of the signal processing electronics used in this work.

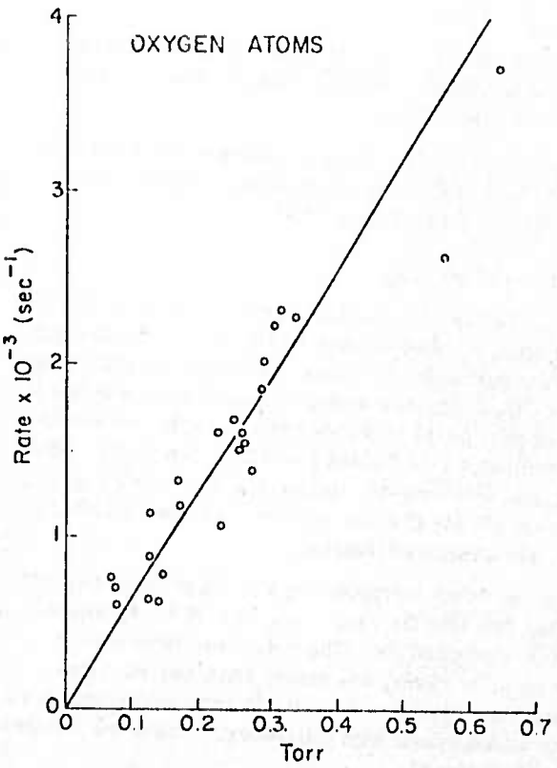

FIG. 3. A plot of the relaxation rate of $CO_2(00°1)$ due to O atoms vs O atom partial pressure.

$$\Delta \text{ Rate} = -k_{CO_2-X_2}\frac{[X]}{2} + k_{CO_2-X}[X], \qquad (1)$$

where [X] is the atom concentration in Torr, Δ Rate is the increase in exponential decay rate in sec^{-1}, $k_{CO_2-X_2}$ is the reduced relaxation rate constant of CO_2 in X_2 in $(sec\text{-}Torr)^{-1}$, and k_{CO_2-X} is the reduced relaxation rate constant of CO_2 in X in $(sec\text{-}Torr)^{-1}$.

The rates of relaxation of $CO_2(001)$ by H_2,[9] D_2,[9] O_2,[9] Cl_2,[10] and F_2[11] have all been measured. In the cases of chlorine, fluorine, and oxygen atom relaxation of CO_2, the loss of diatomic molecules to atoms made only small contributions (<2%) in calculating reduced atom–molecule relaxation rates.

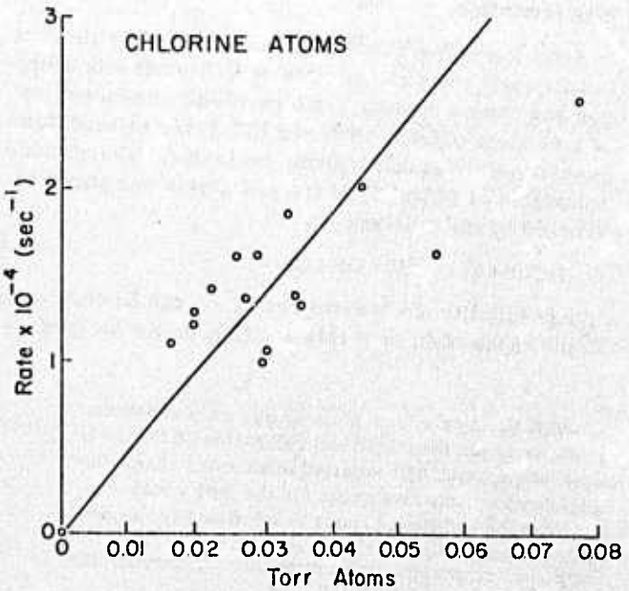

FIG. 4. A plot of the relaxation rate of $CO_2(00°1)$ due to Cl atoms vs Cl atom partial pressure.

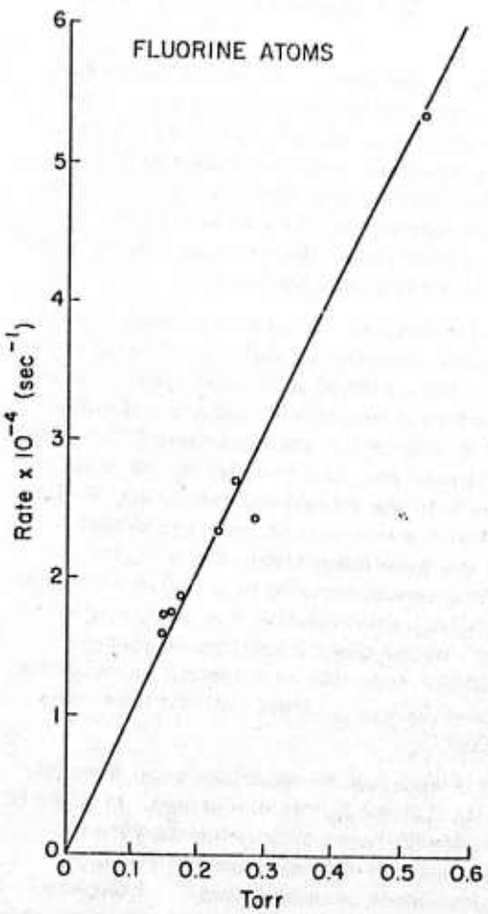

FIG. 5. A plot of the relaxation rate of $CO_2(00°1)$ due to F atoms vs F atom partial pressure.

Figures 3, 4, and 5 give the experimental results for oxygen, chlorine and fluorine atoms deexciting CO_2 and are summarized in Table I.

The relatively large scatter in the chlorine data is attributed to several sources. The microwave discharge in chlorine was both inhomogeneous and unstable depending critically on the tuning of the discharge cav-

TABLE I. A tabulation of measured rate constants for the vibrational relaxation of $CO_2(00°1)$ by atoms with unpaired electrons.

$$CO_2(001) + X \xrightarrow{k_{CO_2-X}} CO_2(m,n,o) + X$$

X	k_{CO_2-X}(this work)	k_{CO_2-X}(other work)
O	$6.69 \pm 1.2 \times 10^3 (sec\text{-}Torr)^{-1}$	$6.25 \times 10^3 (sec\text{-}Torr)^{-1}$ (Ref. 12)
Cl	$4.91 \pm 1.3 \times 10^5$	
F	$1.04 \pm .09 \times 10^5$	
Na		8×10^3 (Ref. 13)

ity and sensitive to vibration. The broadening by CO_2 and the low atom concentrations achieved made atom concentration measurements less reproducible. In addition, effective heterogeneous recombination of chlorine atoms at the tube walls produced a nonuniform radial atom distribution across the tube which influenced both the ESR and fluorescent decay measurements since the observed gas sample was not uniform.

When molecular oxygen, mixed with helium, passes through a microwave discharge $O_2(^1\Delta_g)$ is formed in addition to $O(^3P)$. This excited molecular species is relatively stable with respect to wall and gas collisions and is present in substantial concentrations (~0.1 Torr) together with atomic oxygen. In order to determine if $O_2(^1\Delta_g)$ had a role in the vibrational relaxation, the flow tube was lined with a thin ring of mercuric oxide approximately 1 cm wide downstream of the microwave discharge. Complete absence of oxygen (^3P) atoms with no change in $O_2(^1\Delta_g)$ concentration was confirmed by ESR detection. Under these conditions no change in $CO_2(001)$ relaxation from the no discharge condition was observed, removing $O_2(^1\Delta_g)$ from consideration as an effective relaxer.

No changes in apparent fluorescence rates were observed when H_2, D_2, or N_2 was discharged. In order to maximize sensitivity these measurements were extended to the regime of slowest observed relaxation rates and highest atom concentrations. A limit was reached since maximization of these two conditions conflicted. Increasing the atom concentration requires increasing the flow velocity. Lowering the relaxation rate involves both lowering the pressure and slowing the flow speed to allow an adequate residence time in the optical cell.

Assuming that we can measure a change in rate of more than 2% and using the known values of $k_{CO_2-X_2}$ we can set limits on the H, D, and N relaxation rates of $CO_2(001)$. The results are summarized in Table II.

IV. DISCUSSION

The vibrational relaxation of CO_2 is considerably more complex than that of a diatomic molecule. SSH calculations show that if the process:

$$CO_2(001) + CO_2(000) \rightarrow 2\ CO_2(000) \tag{2}$$

were the only path of relaxation CO_2 would relax as slowly as CO and consequently less than 10^{-4} times as fast as is observed.

Huetz-Aubert and co-workers,[14] by utilizing acoustic, laser fluorescence, and spectrophone data have shown that CO_2 must be treated as having two reservoirs of vibrational energy. One reservoir contains the asymmetric stretching mode, the other the symmetric stretch and bending modes.

Two important routes of relaxing $CO_2(001)$ are

$$CO_2(001) + X \rightarrow CO_2(11^10) + X + 272\ cm^{-1} \tag{3}$$

and

$$CO_2(001) + X \rightarrow CO_2(03^30) + X + 416\ cm^{-1}. \tag{4}$$

These processes as well as other pathways involving multiquantum vibrational state changes are not easily amenable to calculation.

We can however, test some qualitative predictions of relaxation mechanisms by attempting to explain the rates summarized in Tables I and II.

A. Landau-Teller theory

Landau–Teller, or impulsive type theories distinguish between atomic colliders only on the basis of mass and interaction parameters. Since the range for deuterium relaxing CO_2 suggests that the hydrogen rate will fall in the lower part of its range we can separate our results into two classes (see Tables I and II). Hydrogen, deuterium, and nitrogen—all atomic S states—relax CO_2 much more slowly than the atomic P states including oxygen, chlorine, and fluorine.

Estimates from extrapolating rare gas relaxation efficiencies fall into the ranges measured for hydrogen, deuterium and nitrogen. The rates due to atomic P state atoms, however, are faster than any rare gas atom and would require unrealistic interaction parameters to explain their high efficiency. Other mechanisms must be considered.

B. Complex formation and chemical reactions

Complex formation through the existence of strong attractive potentials between CO_2 and O, Cl, or F must be considered. We have, however, measured the pressure broadening coefficient of CO_2 on the atomic fluorine ESR lines. It was found to be 5.85 MHz/Torr. Helium, for comparison broadens F atoms as 2.26 MHz/Torr. No frequency shifts were observed. Oxygen and chlorine showed similar broadening behavior. We would expect line shifts and much more severe broadening effects if long lived complexes formed and, therefore, feel we can discount the possibility of complex formation.

Arnoldi and Wolfrum[15] have measured vibrational relaxation and chemical reaction of $HCl(v=1)$ with hydrogen and oxygen atoms. Time resolved measurements of both atom concentration and HCl laser induced fluorescence were simultaneously recorded. The apparent relaxation of $HCl(v=1)$ by Oxygen atoms was shown to proceed by the reaction:

$$HCl(v=1) + O(^3P) \rightarrow OH + Cl. \tag{5}$$

The possibility of chemical reactions can be dismissed in the cases of Cl or F relaxing CO_2 on the basis of

TABLE II. A tabulation of measured rate constants (this work) for the vibrational relaxation of $CO_2(00^01)$ by S-state atoms with unpaired electrons. These determinations only give limits for the rate constants because the addition of atoms to the flow gave no measurable change to the relaxation rate.

k_{CO_2-H}	$=(3.3\pm3)\times10^3$ (sec-Torr)$^{-1}$
k_{CO_2-D}	$\leq 2.0\times10^3$ (sec-Torr)$^{-1}$
k_{CO_2-N}	$\leq 9.6\times10^2$ (sec-Torr)$^{-1}$

TABLE III. Spin orbit splittings in the ground electronic state of halogen atoms.

Species	Spin orbit splitting(s), cm^{-1}
O	158.5 ($J=1$), 226.5 ($J=0$)
F	404.0
Cl	881.0

large endothermicity.

The reaction:

$$CO_2(001) + O(^3P) \rightarrow O_2 + CO \qquad (6)$$

is only slightly endothermic (2 kcal) but the extremely slow reverse step discounts any possibility of reaction.

Experimental evidence was also obtained which eliminates the possible effect of atoms or some other discharge products reacting with unexcited CO_2. Maximum values of the laser induced fluorescence are quantitative indicators of the CO_2 concentration and may be measured to an accuracy of better than 1%. Under our experimental conditions we did not observe any change in CO_2 concentration. We can, therefore, discount any chemical reaction with CO_2.

C. Vibronic mechanisms

The very effective relaxation of CO_2 by atoms in electronic P states suggests interaction between electronic and vibrational degrees of freedom. Nikitin[5] suggests that relaxation takes place via a potential crossing made possible by the splitting of previously degenerate levels of the atom–molecule system. Other vibronic mechanisms have been suggested. Fisher and Smith[16] have proposed an ionic curve crossing model which predicts very high cross sections for alkali metals relaxing $N_2(v=1)$. This mechanism has been invoked by Benson[13] and co-workers to explain the efficient relaxation of CO_2 by Na atoms (Table I). Adiabatic relaxation efficiencies may be enhanced by vibrational to electronic energy transfer where some of the vibrational energy is converted to excited spin orbit states of the colliding atom. In our case oxygen, chlorine and fluorine have low lying spin orbit states (Table III). This type of process has already been observed in the bromine atom–hydrogen halide system.[17,18]

Calculation of the rates due to vibronic mechanisms demands precise information on atom–molecule potentials and is outside the scope of this paper. We can not distinguish between these mechanisms, all of which may have a share in atom–molecule relaxation processes.

V. CONCLUSION

The coupling of laser induced fluorescence with electron spin resonance has allowed us to measure unusual relaxation processes. Our experiments have shown chlorine and fluorine to rank among the most effective relaxers of $CO_2(001)$.

This experimental technique is both versatile and sensitive and may be extended to other atomic species and free radicals. Measurement of relaxation rates over a temperature range of $-100°$ to 400 °C may be possible with small alterations in procedure. These temperature studies may well produce the best evidence toward understanding the mechanism of vibrational relaxation of molecules by species containing unpaired electrons.

ACKNOWLEDGMENTS

This work was supported by the Advanced Projects Research Agency and monitored by ONR under Contract No. N00014-67-A-0077-006. Support of the Cornell Materials Center is also acknowledged.

[1] J. H. Kiefer and R. W. Lutz, in *Eleventh Symposium (International) on Combustion*, Berkeley, CA, 1966 (Combustion Institute, Pittsburgh, 1967), p. 67.
[2] R. L. Taylor, Can. J. Chem. 52, 1436 (1974).
[3] W. P. Breshears and P. F. Bird, J. Chem. Phys. 48, 4768 (1968).
[4] C. von Rosenberg and K. L. Wray, J. Chem. Phys. 54, 1406 (1971).
[5] E. F. Nikitin, Opt. Spectrosc. 11, 452 (1961).
[6] R. L. Taylor and S. A. Bitterman, Rev. Mod. Phys. 41, 26 (1969).
[7] A. A. Westenberg, Prog. React. Kinet. 7, 23 (1973).
[8] R. L. Brown, J. Res. Natl. Bur. Stand. A 76, 103 (1972).
[9] C. Bradley-Moore in *Fluorescence*, edited by G. G. Guilbrault (Dekker, New York, 1967).
[10] W. C. Rosser and E. I. Gerry, J. Chem. Phys. 54, 4131 (1971).
[11] V. Ya. Agroskin, G. K. Vasilyev, and V. I. Kiryanov Khim. Vysokh. Energ. 8, 283 (1974).
[12] J. H. W. Cramp and J. D. Lambert, Chem. Phys. Lett. 22, 146 (1973).
[13] R. C. Benson, D. J. Benard, and R. E. Walker, J. Chem. Phys. 61, 1652 (1974).
[14] M. Huetz-Aubert and R. Tripodi, J. Chem. Phys. 55, 5724 (1971).
[15] D. Arnoldi and J. Wolfrum, Chem. Phys. Lett. 24, 234 (1974).
[16] E. R. Fisher and G. K. Smith, Chem. Phys. Lett. 6, 438 (1970).
[17] S. R. Leone and F. J. Wodarczyk, J. Chem. Phys. 60, 314 (1974).
[18] G. P. Quigley and G. J. Wolga, Fourth Chem. and Mol. Laser Conference, St. Louis, MO, 1974 (unpublished).

A resonance effect in electronic-to-vibrational energy transfer. Deactivation of HF($v=1$) by Br($^2P_{3/2}$)

G. P. Quigley* and G. J. Wolga

Laboratory of Plasma Studies, Cornell University, Ithaca, New York 14853
(Received 16 January 1975)

This letter reports direct evidence of the existence of a resonance effect in energy transfer from the vibrational to electronic mode. Experiments have been performed in other laboratories[1] which give direct evidence of efficient $E-V$ transfer in the relaxation of Br($^2P_{1/2}$) by HCl and HBr. However, these processes are not resonant.

The spin–orbit splitting in Br($^2P_{1/2}-{}^2P_{3/2}=3685$ cm^{-1}) is highly resonant with several possible vibration rotation transitions in HF. This fact was used to explain the efficiency of Br relaxing HF($v=1$) in recent shock tube experiments.[2]

It should be pointed out that a similar situation exists between these same spin–orbit coupled states of Br and vibration rotation transitions in H_2. Recent theoretical work[3,4] on this system has shown that quantum resonance effects should be expected in electronic-to-vibrational energy transfer processes of this type.

A description of the apparatus used in this experiment has been given elsewhere.[5] Basically, an HF chemical laser was used to excite HF to $v=1$. A microwave discharge in the flowing mixture of Br_2 and an argon diluent was used to produce the Br atoms. The HF was injected into the Br + Br_2 + Ar flow downstream of the discharge and thoroughly mixed before laser excitation.

The results after signal averaging for a typical set of experiments are shown in the oscilloscope photograph in Fig. 1. The top trace is a simple exponential decay of

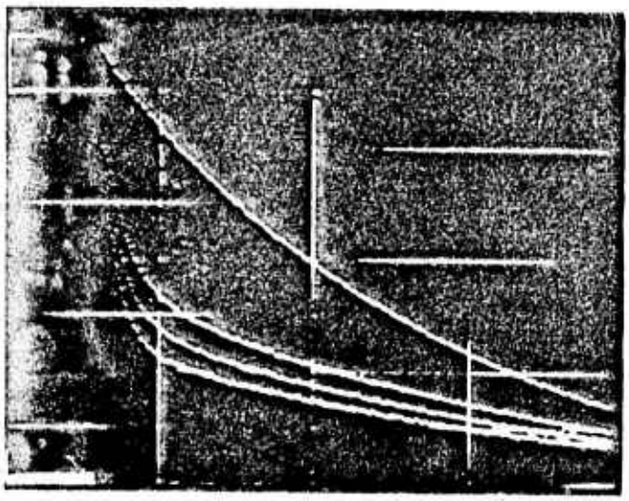

FIG. 1. HF ($v=1$) laser induced fluorescence signal in the presence of HF ($v=0$), Br_2, Br, and Ar, versus time. Top trace without bromine atoms. Succeeding traces display the effect of increasing bromine atom concentration. Total width of trace (including baseline) is 220 μsec for top trace and 110 μsec for bottom three traces.

$HF(v=1)$ in a mixture of $Br_2+Ar+HF(v=0)$, i.e., the discharge is off. In separate experiments, the rate constant for relaxation of $HF(v=1)$ by Br_2 was found to be $3.5\pm0.8\times10^2$ $sec^{-1}\cdot Torr^{-1}$. The rate constants for Ar[6] and $HF(v=0)$[7] have been measured and are ≈ 60 $sec^{-1}\cdot Torr^{-1}$ and 6.0×10^4 $sec^{-1}\cdot Torr^{-1}$, respectively ($T=300°K$ in this experiment). Thus, the partial pressure of HF can be found from the decay time of the single exponential.

Referring again to Fig. 1, the lower three traces are double exponential decays of $HF(v=1)$ in mixtures of $Br_2+Br+Ar+HF(v=0)$. The fast exponential is caused by rapid energy exchange from the vibrational mode of HF to the electronic mode of Br. The slow time constant is due to the $V-R$, T and $E-T$ processes which relax the energy pool set up by the equilibrium between $HF(v=1)$ and $Br(^2P_{1/2})$.

This double exponential behavior is not found in the deactivation of $HF(v=1)$ by O, F[5] or Cl,[8] cases for which a resonant energy transfer process is not available. It is characteristic of systems, e.g., CO_2: N_2,[9] HF: H_2[6] where resonant $v-v$ energy transfer occurs. Since the chemical reaction $Br+HF(v=1)\rightarrow HBr+F$ is 37 kcal endothermic, a reactive collision is not a likely explanation for the fast rate. In combination, these factors support our conclusion that the fast process observed is the resonant $V-E$ energy exchange process (1).

A possible resonant $E\rightarrow V$ process is

$$HF(v=1,\ J=5)+Br(^2P_{3/2}) \underset{k_e'}{\overset{k_e}{\rightleftharpoons}} HF(v=0,\ J=6)+Br(^2P_{1/2})$$

$$\Delta J=1,\ \Delta E=-9\ cm^{-1}. \qquad (1)$$

Other near resonant processes can be found closer to the peak of the Boltzmann distribution in rotational levels, and this experiment cannot identify the relative importance of each of them. It is assumed in what follows that Process (1) is the dominant one. Rotational relaxation consideration aside, the reasons for assuming (1) to be dominant is that the energy defect is smallest and the transition involved is identical to one of the laser lines used to pump the HF(1P6).

Using this, and the consequent assumption that $k_e\approx k_e'$, the analysis of the fast time constant in the usual way[6,10] gives

$$k_e\approx\frac{(1/\tau_f)}{P_{Br}+P_{HF}}\ , \qquad (2)$$

where τ_f is the time constant for the fast decay, P_{HF} is the partial pressure of HF, and P_{Br} is the partial pressure of Br. P_{Br} is measured by an electron paramagnetic resonance spectrometer.[5] The assumption that $E\rightarrow V$ processes are much faster than all $V-R$, T processes is implicit in (2).

Figure 2 shows a semilog plot of the HF $1-0$ R-branch laser induced fluorescence as a function of time for the single exponential decay and one of the double exponential decays (the top one). These and other data are readily analyzed to give a preliminary number of $k_e=1.0$

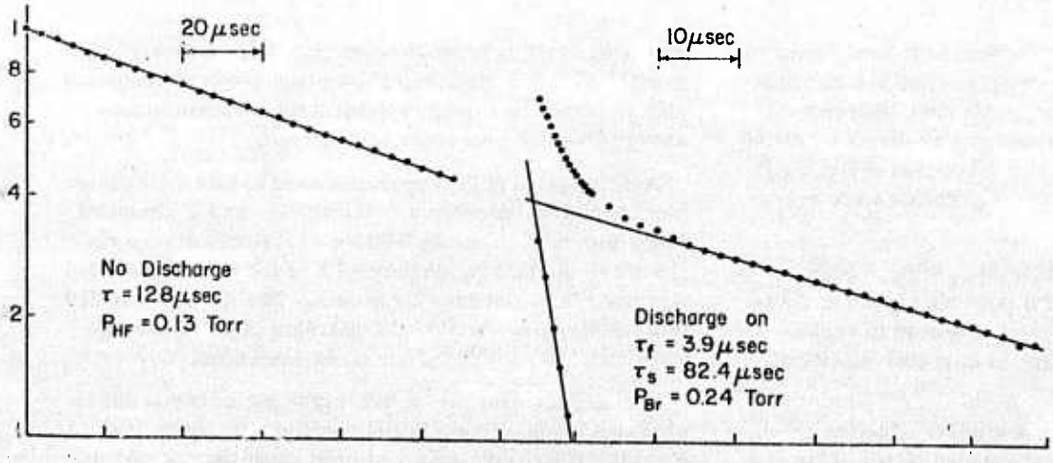

FIG. 2. Semilog plot of laser induced fluorescence signal versus time. The data plotted are the top two traces of Fig. 1.

$\pm 0.5\times10^{6}$ sec$^{-1}\cdot$Torr^{-1}. Thus the $E \rightarrow V$ transfer process occurs in about six or seven gas kinetic collisions.

This work was supported by ARPA and was monitored by ONR under Contract No. N00014-67-A-0077-0006. We also acknowledge support by the Cornell Materials Science Center through their Central Facilities.

*Now at Laboratory for Laser Energetics, The University of Rochester, Rochester, NY 14627.

[1]S. R. Leone and F. J. Wodarczyk, J. Chem. Phys. 60, 314 (1974).
[2]J. A. Blauer and W. C. Solomon, Proc. Interm. Symp. Combust., 14th, University Park, PA, 1972 (1973).
[3]I. H. Zimmerman and T. F. George, J. Chem. Phys. 61, 2468 (1974).
[4]I. H. Zimmerman and T. F. George, Chem. Phys. (to be published).
[5]G. P. Quigley and G. J. Wolga, Chem. Phys. Lett. 27, 276 (1974).
[6]J. K. Hancock and W. H. Green, J. Chem. Phys. 57, 4515 (1972).
[7]R. Lucht and T. Cool (to be published).
[8]G. P. Quigley, Ph.D. thesis (unpublished).
[9]C. B. Moore, R. E. Wood, B.-L. Hu, and J. T. Jardley, J. Chem. Phys. 46, 4222 (1967).
[10]H. L. Chen and C. B. Moore, J. Chem. Phys. 54, 4072 (1967).

The deactivation of HF($v=1$) and DF($v=1$) by O, Cl, and F atoms

G. P. Quigley* and G. J. Wolga

Laboratory of Plasma Studies, Cornell University, Ithaca, New York 14853
(Received 24 June 1975)

The relaxation of vibrationally excited HF and DF by O, Cl, and F atoms at $T = 300$°K has been measured by the laser induced fluorescence method. The rate constants in units of cm^3 molecule^{-1}·sec^{-1} for HF($v=1$) are $k_{O\text{-}HF} = 3.1 \pm 0.6 \times 10^{-12}$, $k_{Cl\text{-}HF} = 7.4 \pm 1.6 \times 10^{-13}$, $k_{F\text{-}HF} = 2.8 \pm 0.6 \times 10^{-13}$; for DF($v=1$) they are $k_{O\text{-}DF} = 7.8 \pm 2.2 \times 10^{-12}$, $k_{Cl\text{-}DF} = 2.0 \pm 0.3 \times 10^{-12}$, $k_{F\text{-}DF} = 6.5 \pm 1.2 \times 10^{-13}$. The results provide further evidence for the validity of a vibronic to translational energy transfer mechanism. Atom transfer reactions are shown to be of no importance.

I. INTRODUCTION

The relaxation of vibrationally excited molecules by potentially reactive atoms has attracted wide interest.[1-10] These processes are particularly important from the standpoint of elucidating the mechanisms for energy transfer involving chemically reactive species, of which little is known.

Chemical lasers contain large concentrations of highly reactive atoms. It is important to know the effect of these atoms on the decay of the vibrationally excited molecules in order to accurately characterize these laser systems for the purpose of predicting performance and optimizing efficiency.

Another area of intensive study is in determining the importance of reagent vibrational energy in chemical reaction rates. Since the vibrational relaxation of a molecule by an atom can in some cases proceed via a reactive route, experiments on these systems can shed some light on the efficiency (or lack thereof) of vibrational energy in accelerating chemical reaction rates.

The experiments reported here involve the measurement at room temperature of the rates for relaxation of HF and DF by F, Cl, and O atoms. The relative quenching efficiencies of these atoms, as well as the isotope effect on going from HF to DF, lends further support to the vibronic mechanism[5] first proposed by Nikitin.[11,12] Further, it is shown that the reactive channel for relaxation is not of importance for interaction between O, F, and Cl atoms and HF($v=1$) or DF($v=1$).

II. EXPERIMENTAL

In an earlier paper,[5] a simple expression was obtained for the rate constant for deactivation of HF (or DF) by an atom X. This is given by Eq. (7) of Ref. 5 as

$$k_{14} = \frac{1}{[X]}\left|\frac{1}{\tau_D} - \frac{1}{\tau_0}\right| + \tfrac{1}{2}\,k_{12}\,, \qquad (1)$$

where k_{12} is the rate constant for deactivation of HF($v=1$) or DF($v=1$) by the parent molecule (X_2), [X] is the atom concentration, τ_D is the laser induced fluorescence decay time of HF(DF) in the presence of atoms, and τ_0 is the laser induced fluorescence decay time of HF(DF) with no atoms present. This expression is correct for all cases except those which involve near resonant energy transfer processes resulting in double exponential fluorescence decays. All of the systems reported here exhibit a single decay, and the rate constant for atom deactivation is given by (1). Thus, the determination of k_{14} involves the measurement of four quantities (k_{12}, τ_0, τ_D, [X]).

The rate constant for relaxation by the parent molecule is found by a laser induced fluorescence (LIF) measurement under quasistatic flow conditions. Table I gives the results. In all cases, these made a negligible contribution to k_{14}.

The other three quantities were measured under fast flow conditions in a system whose over-all block diagram is shown in Fig. 1. A brief description of this system was given in Ref. 5. Both the decay time by LIF and atom concentration measurements were made using the same flow system. The LIF measurement was done in the downstream section with the flow rates set by the pressures P_2 and P_1. The HF(DF) was excited by a transverse discharge chemical laser which was operated multiline and whose gas flow, SF_6 and H_2 (D_2) mixture, and pulse repetition rate were adjusted to give optimum $v=1 \rightarrow v=0$ laser output.

The decay time of the fluorescence was first measured in the flowing Ar + X_2 + HF(DF) mixture. This yielded τ_0. The decay time in the presence of atoms (τ_D) was then found by striking a microwave discharge upstream of the HF(DF) injection port in the Ar + X_2 flow. The flow conditions before and after the discharge was turned on were identical since the dissociation of X_2 resulted in a negligible change compared to the total flow which was dominated by the argon diluent.

TABLE I. Relaxation ratos for parent molecules.[a]

X_2	k_{12} for HF	k_{12} for DF
Cl_2	$1.0 \pm 0.2 \times 10^{-14}$ [b]	$< 1.2 \times 10^{-14}$ [b]
F_2	$< 3.1 \times 10^{-15}$ [13]	$< 8 \times 10^{-15}$ [b]
O_2	1.2×10^{-14} [14]	$< 1.6 \times 10^{-14}$ [b]

[a] Rato constants are in units of cm^3 molecule^{-1} · sec^{-1}.
[b] This work.

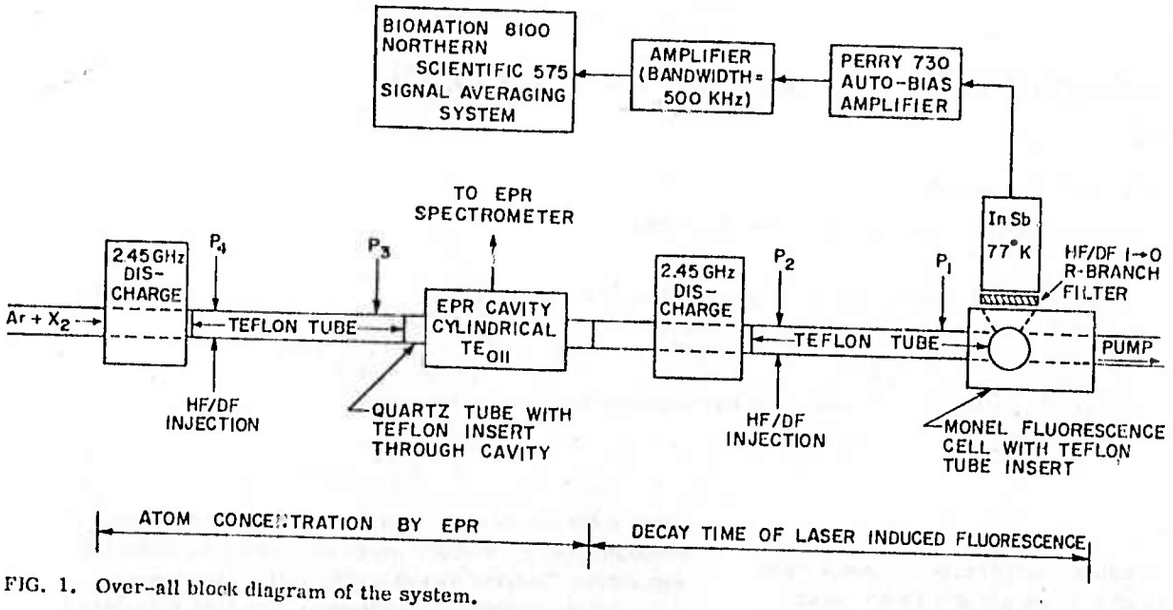

FIG. 1. Over-all block diagram of the system.

The atom concentration was measured by EPR methods[15] in the upstream section of the flow tube. All flow conditions determined by pressure measurements P_2 and P_1 were reproduced exactly at P_4 and P_3, respectively. This section of flow tube was identical to the downstream section except that an EPR microwave resonant cavity was in the same location relative to the microwave discharge and HF/DF injection port as was the sapphire window of the monel fluorescence cell.

Figure 2 shows a detailed block diagram of the EPR spectrometer. This spectrometer is of the homodyne type which uses an X-band klystron locked by a commercial stabilizer to the resonant frequency (8.975 GHz) of the high Q cylindrical cavity. Thus, the spectrometer is sensitive only to the absorption and not the dispersion of the paramagnetic atom. As the amplitude modulated (10 kHz) dc magnetic field is slowly swept through a resonance, the output of the lock-in amplifier traces out a curve which is proportional to the first derivative with respect to the magnetic field of the imaginary part of the paramagnetic susceptibility χ''_{ij}. The absolute atom concentration is proportional to the double integral of the recorded output of the spectrometer. The proportionality constant is dependent on instrumental parameters and can be eliminated by calibrating the system with the paramagnetic molecule O_2 filling the sample volume at a known pressure.[15] The sample volume is a 10 mm i.d. quartz tube (with a thin walled Teflon tube insert) passing through the EPR cavity

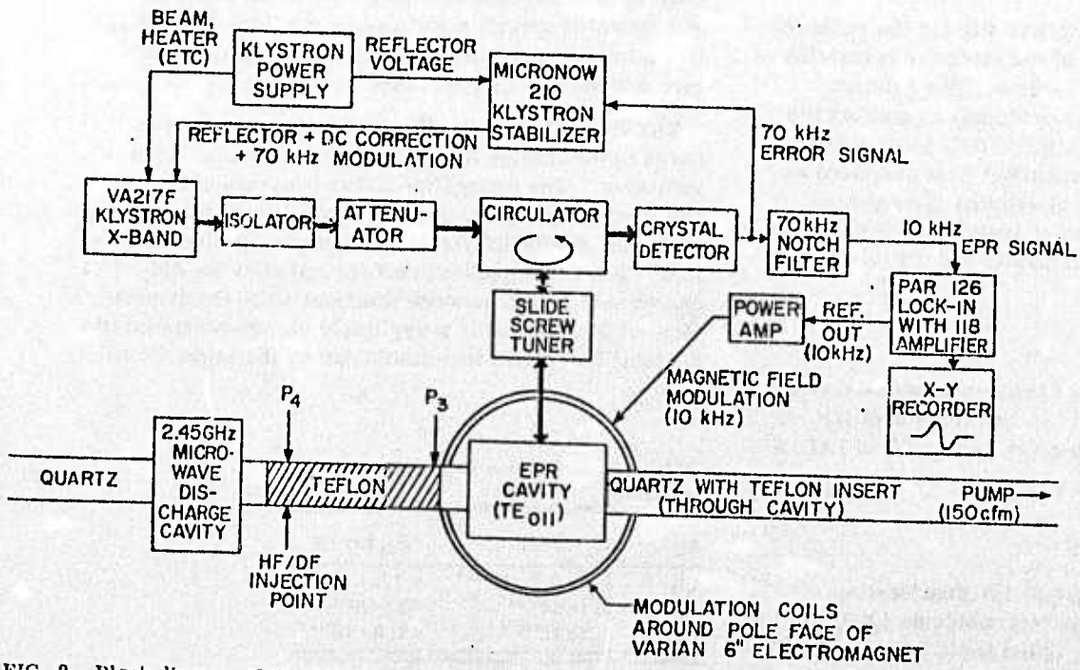

FIG. 2. Block diagram of the EPR spectrometer.

along the cylinder axis. Owing to wall recombination, the filling factor for the atoms is not the same as that for O_2 since, for the former, there is a density gradient along the radial and longitudinal (flow) directions. The error introduced by this discrepancy is made negligible by the Teflon insert which reduces wall recombination significantly. The loaded cavity Q (12 000 without the Teflon tube) is degraded by 15% as a result of the Teflon, and since the minimum detectable signal is proportional to Q^{-1}, the sensitivity suffers somewhat. However, the atom concentration was so large in all cases (≥ 0.1 Torr) that it was nowhere near the minimum detectable concentration (≤ 0.01 Torr), and hence excellent signal to noise ratios were obtained with moderate lock-in-amplifier time constants (≤ 100 msec).

Taking the ratio of the unknown atom concentration to the known O_2 concentration, one finds

$$\frac{N_X}{N_{O_2}} = \frac{Q_X}{Q_{O_2}} \frac{\iint S_X dH' dH}{\iint S_{O_2} dH' dH} , \tag{2}$$

where Q_X and Q_{O_2} are the theoretical intensity factors for the atom and O_2 resonances, respectively; S_X and S_{O_2} are the recorded EPR signals which are proportional to the corresponding resonance derivatives $d\chi''_j/dH$. The Q factors are tabulated by Westenberg[15] for all species of interest.

The above analysis assumes that the Zeeman levels are in thermodynamic equilibrium. Thus, effects such as saturation of the spin system owing to high intensity microwave fields will lead to significant errors. This problem is particularly important for paramagnetic species which have spin–lattice relaxation times on the order of the residence time in the EPR cavity. The microwave powers used here are well within the limits imposed by such saturation effects and do not constitute a problem. For a more detailed account of the experimental techniques used with this EPR spectrometer, consult Ref. 16.

Most of the gases used were described in Ref. 5. To that list, the following should be added: Cl_2: Matheson Ultra High Purity (purity >99.9%), no further purification; DF: Merck, Sharpe and Dohm (purity >98%), further purification by trap to trap distillation between 77 °K and 195 °K.

Typical dimensions in the flow system were as follows: the distance from the HF/DF injection port to the EPR cavity or the fluorescence window was about 20 cm; the microwave discharge took place in a 10 mm i.d. quartz tube and was located approximately 10 cm from the HF/DF injection port. All other tubing was either quartz with a Teflon insert or solid thick-walled Teflon tubing. The flow did not come into contact with any metal surfaces.

Typical flow speeds were on the order of 10 m/sec. The HF(DF) concentration was rarely more than 1% of the total flow. Atom concentrations were typically greater than the HF(DF) concentrations.

The heating of the gas by the microwave discharge could have presented a problem since the expression for the atom concentration (2) is temperature dependent. Also, the self-relaxation rates for HF and DF are highly temperature dependent,[17] and this would give a false change in the LIF decay time. This was not considered to be a significant problem, since many different discharge and flow conditions yielded consistent data, as shown in Fig. 3 of Ref. 5.

Finally, an additional source of concern was the possibility of an effect due to the production of electronically and vibrationally excited metastables in the microwave discharge which could survive long enough to transfer their energy to HF(DF) in the fluorescence region and result in a change in the LIF decay time independent of atom effects. It was assumed that all vibrationally excited molecules produced in the discharge were collisionally quenched by the HF(DF) or the atoms before they reached the laser illuminated region.

The only electronically excited metastable which could have presented a problem was $O_2(^1\Delta_g)$. Experiments in this laboratory indicate that this electronic energy is rapidly transferred by near resonant $E \rightarrow V$ processes to $v=2$ of HF (and perhaps to $v=2$ of DF). Subsequent rapid quenching of the HF and DF by the atoms and ground state HF or DF completes the relaxation process. Furthermore, the insensitivity of our atom deactivation efficiencies to widely varying experimental conditions (partial pressures including that of the diluent, and discharge power) that would affect the relative atom to $O_2(^1\Delta_g)$ concentration suggest that $O_2(^1\Delta_g)$ was not an important factor in our results.

III. RESULTS AND DISCUSSION

A typical example of a semilogarithmic plot of the laser induced fluorescence as a function of time is shown in Fig. 3 for the deactivation of HF($v=1$) by Cl atoms. Each curve represents the average of 128 pulses. The DF data generally required considerably more signal averaging to get similar results, since the DF laser produced about one-fifth the intensity of the HF laser.

Table II summarizes the results for O, F, and Cl deactivating HF($v=1$) and DF($v=1$). Notice that Cl atoms are more effective than F atoms, and O atoms are the most effective. Also, in all cases, a particular atom relaxes DF($v=1$) more effectively than HF($v=1$).

A relevant question concerns the importance of atom exchange or abstraction reactions as possible contributions to the observed rates. Consider the following:

$$O + HF(v=0) \rightarrow OH(v=0) + F, \quad \Delta H = 33 \text{ kcal/mole}, \tag{3}$$

$$Cl + HF(v=0) \rightarrow ClH(v=0) + F, \quad \Delta H = 32 \text{ kcal/mole}, \tag{4}$$

TABLE II. Summary of results ($T=300$ °K).

X	k_{14} for HF (cm^3 molecule^{-1} · sec^{-1}	k_{14} for DF (cm^3 molecule^{-1} · sec^{-1}
O (^3P)	$3.1 \pm 0.6 \times 10^{-12}$	$7.8 \pm 2.2 \times 10^{-12}$
F (^2P)	$2.8 \pm 0.6 \times 10^{-13}$	$6.5 \pm 1.2 \times 10^{-13}$
Cl (^2P)	$7.4 \pm 1.6 \times 10^{-13}$	$2.0 \pm 0.3 \times 10^{-12}$

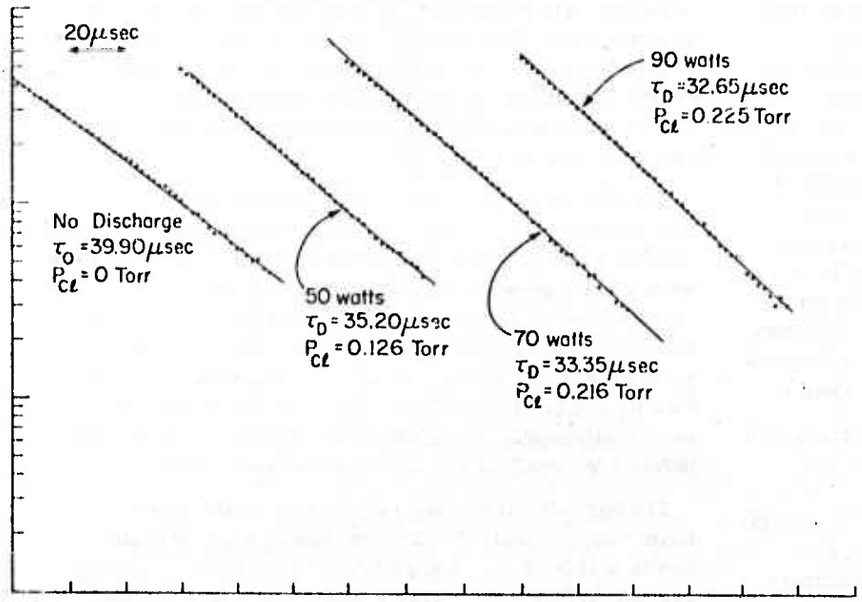

FIG. 3. Semilog plot of laser induced fluorescence in HF ($v=1$) as a function of time for different discharge conditions in Ar + Cl_2.

$$F^1 + HF(v=0) \rightarrow F^1H(v=0) + F, \quad \Delta H = 0. \tag{5}$$

Since the H atom exchange reactions involving O and Cl atoms are substantially endothermic, it is unlikely that these reactions are important even with the addition of a quantum of vibrational energy in the HF or DF (about 12 kcal/mole and 9 kcal/mole, respectively). However, both O and Cl are more effective than F atoms in relaxing both HF and DF, even though in the latter case the addition of a vibrational quantum makes this reaction exothermic by 12 kcal/mole and 9 kcal/mole, respectively. This supports the conclusion that for HF($v=1$) and DF($v=1$) one is observing pure vibrational relaxation processes and that the atom exchange reactions do not make a significant contribution. Also, the results suggest that in the F atom case, either the vibrational energy is ineffective in enhancing the reaction rate for exchange, or the potential barrier to exchange is larger than a single vibrational quantum and one may need excitation to higher vibrational levels to see a significant contribution from the reactive channel to the over-all relaxation rate. The calculations of O'Neil *et al.*[18] support the latter conclusion, since they show that the minimum barrier height for Reaction (5) is 18 kcal/mole.

One can suggest a qualitative explanation for the difference in the Cl and F atom rates on the basis of the larger attractive forces prevailing in the Cl–HF(DF) encounters. A simple calculation of the van der Waals constant[19] C_6 including induction and dispersion effects gives for Cl–HF encounters $C_6 = 106\times10^{-60}$ erg · cm^6, and for F–HF encounters $C_6 = 22\times10^{-60}$ erg · cm^6.[20] Thus, the long range attractive forces are 5 times larger for Cl atoms than for F atoms. This could account for the increased efficiency of Cl over F through an effective increase in the collision frequency.

If one considers for HF or DF the ratio of the rate constants for the different atoms, one finds that the data is remarkably consistent. Table III shows the bounds on such ratios as determined from the error bounds of the rate constants. Thus it appears that the taking of the ratio has eliminated all of the isotopic dependence and one is left with a quantity which depends on the interaction of the atom with the electronic cloud of HF or DF. Therefore, these ratios depend on the details of the electronic potential energy of interaction between the atom and the molecule.

One of the most important results of these atom molecule relaxation studies has been the conclusion that in nonreactive encounters, vibrational relaxation is dominated by a vibronic to translational energy transfer mechanism.[5] This was first proposed by Nikitin[11,12] to explain the anomalously high probability for vibrational relaxation in systems such as $NO(^2\pi) + Ar(^1S)$, $N_2(^1\Sigma) + O(^3P)$, and $O_2(^3\Sigma) + O(^3P)$, where at least one of the colliding partners has electronic orbital angular momentum degeneracy. The essence of this theory as it applies to this experiment is that atoms which are in degenerate electronic orbital angular momentum states [e.g., $O(^3P)$, $Cl(^2P)$, and $F(^2P)$] are more effective in vibrational relaxation than those which are in states without this degeneracy [e.g., $H(^2S)$, $N(^4S)$, and $Ar(^1S)$]. This model assumes that during the collision the electrostatic fields act to split the degeneracy such that when the colliding partners reach a point in their trajectory where the splitting equals the vibrational quantum (termed the "resonance distance"), an enhancement in the cross section for vibrational energy transfer occurs.

TABLE III. Ratios of the atom relaxation rates.

$7.4 < \frac{k_{O-HF}}{k_{F-HF}} < 16.8$	$7.3 < \frac{k_{O-DF}}{k_{F-DF}} < 18.9$
$1.7 < \frac{k_{Cl-HF}}{k_{F-HF}} < 4.1$	$2.2 < \frac{k_{Cl-DF}}{k_{F-DF}} < 4.3$
$2.8 < \frac{k_{O-HF}}{k_{Cl-HF}} < 6.4$	$2.4 < \frac{k_{O-DF}}{k_{Cl-DF}} < 5.9$

Thus, for the systems with angular momentum degeneracy, the total cross section for vibrational energy transfer can be pictured as the sum of the usual adiabatic term (describable by a Landau–Teller[21] or SSH[22] model) and the dominant nonadiabatic term which considers transitions between the crossing adiabatic potential energy surfaces. Actual values of the probability for vibrational energy transfer depend on the details of the potential surfaces and the interactions and selection rules which couple the different adiabatic states. A complete solution to this theoretical problem is not available.

The isotope effect that one expects in the Nikitin model is that for a given atom the molecule with the smaller quantum relaxes faster. This is a consequence of the fact that a smaller vibrational quantum requires a smaller electrostatic field to produce the required resonant splitting. Thus the resonance distance is greater and more collisions are effective in the nonadiabatic mechanism. Reference to Table II shows that in all cases DF relaxes faster than HF by a factor of 2.5 for a given atom. This provides further evidence for the Nikitin model.

The usual isotope effect for the hydrogen halides[23] is based on the observation that the molecule with the smaller moment of inertia relaxes faster. The small moment of inertia results in a rotational velocity of the hydrogen atom which is greater than the relative translational velocity at low enough temperatures. In this case, the relevant energy transfer process is from vibration into rotation, and therefore, one would expect the hydrogen containing molecule to relax faster than the deuterium containing one. The observed isotope effect is opposite to this and hence this rules out the importance of $V-R$ processes in collisional quenching of vibrational energy by atoms with orbital angular momentum degeneracy.

All of the atoms considered here have ground states which are split by the spin–orbit coupling interaction. In all cases, each of the excited states has appreciable population at room temperature (see Table IV). It is not possible from this experiment to tell whether these excited states are more or less effective than the lowest state in vibrational energy transfer. Such differences should be considered since calculations have shown,[24] for example, a difference in the reactivity for the $^2P_{3/2}$ and $^2P_{1/2}$ states of F atoms.

Another important electronic effect to consider is the possibility of vibration to electronic energy transfer leaving an electronically excited atom. Reference to Table IV shows that the low lying spin–orbit states are far from resonant with HF($v=1$) or DF($v=1$) and $V-E$ processes are not expected to be important. In the case of Br($^2P_{3/2}$) relaxing HF($v=1$), the levels are closely resonant, and rapid $V-E$ processes are observed.[6]

TABLE IV. Thermally accessible states of F, Cl, and O atoms.[a]

X	States	Energy level (cm^{-1})	Boltzmann factor
F	$^2P_{3/2}$	0	1
	$^2P_{1/2}$	404	6.7×10^{-2}
Cl	$^2P_{3/2}$	0	1
	$^2P_{1/2}$	881	7.3×10^{-3}
O	$^3P_2$	0	1
	$^3P_1$	159	0.47
	$^3P_0$	226	0.34

[a] $\nu_{HF}=4138\ cm^{-1}$, $\nu_{DF}=2998\ cm^{-1}$.

IV. CONCLUSIONS

The experiments reported here provide further evidence for the validity of the vibronic to translation energy transfer model of Nikitin in accounting for the quenching efficiency of atoms with ground states which have electronic orbital angular momentum degeneracy. Both the order of magnitude of rates for P-state atoms relative to those for S-state atoms and the molecular isotope effect support this conclusion.

Also, it has been shown unambiguously that for HF and DF, atom transfer reactions are not an important channel in vibrational relaxation of HF($v=1$) or DF($v=1$). However, for F atoms attacking HF or DF excited to higher vibrational levels, H or D atom exchange reactions become a distinct possibility and may result in a significant increase in the relaxation rate.

ACKNOWLEDGMENTS

This work was supported by the Advanced Research Projects Agency under ARPA Order 660. We acknowledge support by the Cornell Materials Science Center for the use of Central Facilities.

*Now at the Los Alamos Scientific Laboratory, Los Alamos, NM.

[1] R. D. H. Brown, G. P. Glass, and I. W. M. Smith, "The Relaxation of HCl ($v=1$) and DCl ($v=1$) By O Atoms Between 196 and 400 °K, Chem. Phys. Lett. (to be published).
[2] D. Arnoldi and J. Wolfrum, Chem. Phys. Lett. 24, 234 (1974).
[3] N. C. Craig and C. B. Moore, J. Phys. Chem. 75, 1622 (1971).
[4] J. A. Blauer and W. C. Solomon, in *Fourteenth Symposium (International) on Combustion* (The Combustion Institute, 1973), p. 189.
[5] G. P. Quigley and G. J. Wolga, Chem. Phys. Lett. 27, 276 (1974).
[6] G. P. Quigley and G. J. Wolga, J. Chem. Phys. 62, 4560 (1975).
[7] M. I. Buchwald and G. J. Wolga, J. Chem. Phys. 62, 2828 (1975).
[8] J. H. W. Cramp and J. D. Lambert, Chem. Phys. Lett. 22, 146 (1973).
[9] S. R. Leone and F. J. Wodarczyk, J. Chem. Phys. 60, 314 (1974).
[10] R. C. Benson, D. J. Benard, and R. E. Walker, J. Chem. Phys. 61, 1652 (1974).
[11] E. E. Nikitin, Opt. Spectros. 9, 8 (1960).
[12] E. E. Nikitin and S. Ya Umanski, Faraday Discuss. Chem. Soc. 53, 1 (1972).
[13] S. S. Fried, J. Wilson, and R. L. Taylor, IEEE J. Quantum

Electron. QE-9, 59 (1973).
[14]W. H. Green and J. K. Hancock, IEEE J. Quantum Electron. QE-9, 60 (1973); J. F. Bott and N. Cohen, J. Chem. Phys. 58, 4539 (1973).
[15]A. A. Westenberg, Prog. React. Kinet. 7, Part 1, 23 (1973).
[16]G. Quigley, "The Deactivation of Vibrationally Excited HF by Reactive Atoms," Ph. D. thesis, Cornell University, 1975.
[17]R. A. Lucht and T. A. Cool, J. Chem. Phys. 60, 1026 (1974).
[18]S. V. O'Neil, H. F. Schaefer III, and C. F. Bender, Proc. Natl. Acad. Sci. USA 71, 104 (1974).
[19]J. O. Hirschfelder, C. F. Curtiss, and R. B. Bird, *Molecular Theory of Gases and Liquids* (Wiley, New York, 1954).
[20]$C_6 = r^6[\phi^{(\mathrm{dis})} + \phi^{(\mathrm{ind})}]$, where $\phi^{(\mathrm{dis})}$ is the potential energy for the London dispersion interaction and $\phi^{(\mathrm{ind})}$ is the potential energy for the induction interaction. It can be shown[19] that $C_6 = \frac{3}{2}\alpha_X\,\alpha_{HF}[I_X I_{HF}/(I_X + I_{HF})] + \alpha_X\,\mu_{HF}^2$ where α_X, α_{HF} are the polarizabilities of the atom and HF, respectively, μ_{HF} is the dipole moment for HF, and I_X and I_{HF} are the ionization potentials for the atom and HF, respectively. The variation in the long range attractive forces for different atoms is dominated by the change in the atomic polarizability. The values used in the calculation are $\alpha_F = 0.43$ (Å)^3 and $\alpha_{Cl} = 2.33$ (Å)^3.
[21]L. Landau and E. Teller, Phys. Z. Sowjetunion 10, 34 (1936).
[22]R. Schwartz, Z. Slawsky, and K. Herzfeld, J. Chem. Phys. 20, 1951 (1952).
[23]H. L. Chen and C. B. Moore, J. Chem. Phys. 54, 4072 (1971).
[24]J. C. Tully, J. Chem. Phys. 60, 3042 (1974).

Deactivation of Vibrationally Excited CO Molecules by Atomic Oxygen

Professor R. A. McFarlane

Introduction

During the past contract period measurements were carried out on the temperature dependence of the rate of collisional deactivation of CO(v=1) molecules by oxygen atoms. The rate was found to be substantially faster than the deactivation rate for collisions with oxygen molecules and can now be included in any kinetic modelling of carbon monoxide chemical lasers. The first set of measurements which we report here are over a limited range of temperature, 273°K to 390°K and it is planned to extend the range both higher and lower for oxygen and for other atoms during this contract period.

When the present data is compared with high temperature data from shock tube experiments, it is found that both sets of data can be accommodated on a $T^{-1/3}$ Landau-Teller plot. Because of the limited temperature range for the present measurements however, this result is not surprising and future measurements may indicate a deviation from strict Landau-Teller behavior.

Although the experimental technique using laser induced fluorescence, which was employed for this work, is in principle similar to that employed for related studies on other molecules in this laboratory, it was found that because of the long spontaneous emission lifetime for CO(v=1) molecules, the observed fluorescence decay signals were dominated by a loss rate due to the flow of gas out of the observation cell and not by spontaneous emission or collisional deactivation. It was necessary to abandon therefore the usual analysis of the time dependence of the fluorescence which looks simply at the difference in two exponential decay rates and ascribes this to collisions with the species being examined and to go to a modified analysis which permits a non exponential functional dependence to be used and still allows the extraction of quenching effects due to collisions with atoms.

The Experiment

A block diagram of the experiment is shown in Figure 1. As it has been described in detail in earlier reports it will be only briefly discussed here. A stream of molecular oxygen in an argon diluent is dissociated by a microwave discharge, mixed with injected CO molecules, passes through a furnace for varying the temperature and is excited by a 4.8 micron laser source at the fluorescence cell. This excitation is provided by frequency doubling the output of a CO_2 TEA laser operating on the P(24) 00°1 → 02°0 transition and corresponds to absorption by CO on P(14) 0 → 1 . Fluorescence is observed as a function of time with an InSb detector and signals are digitized and averaged for further analysis on an IBM 360 computer. In the same flow system, all conditions are reproduced downstream to permit atom concentration determination with an ESR spectrometer.

The furnaces shown in Figure 1 consist of both heating and cooling elements and operating conditions are calibrated by actually placing a thermocouple in the fluorescence cell to measure the flowing gas temperature at the point of observation of the laser induced fluorescence. Not shown in Figure 1 are gas mass flow meters and pressure gauges used to permit the duplication of conditions in both the ESR and fluorescence cell sections. Similar temperature calibration is employed in the ESR cavity.

It was found that the addition of CO into the stream of oxygen caused the oxygen atom ESR signal to disappear within a few seconds and it did not reappear with the removal of the CO. It was concluded that iron carbonyl from the CO storage cylinder was dissociating in the region of elevated temperature immediately downstream of the microwave discharge and the iron which plated onto the quartz tube was oxidized and provided an effective site for the recombination of the oxygen atoms. A reactor chamber filled with glass wool and heated to 180°F, the dissociation temperature of iron carbonyl, was placed in the CO gas flow line. This has been totally effective in eliminating the degradation of oxygen atom concentration during months of use.

Purification of the oxygen and argon was carried out using a dry ice cold trap to remove condensable impurities such as H_2O, CO_2 or oil.

The first set of fluorescence traces which were observed showed an unexpected initial slow rise in the intensity followed by the usual decay. This was interpreted as being due to 4.3 micron emission from a CO_2 impurity which was excited by rapid V-V energy exchange from the excited CO. As the Einstein A coefficient for this emission from CO_2 is about ten times that for CO, relatively small CO_2 concentrations can be significant. Indeed, the deliberate introduction of quantities of CO_2 too small to be reliably measured in the pressure gauges gave exactly similar fluorescence risetime effects. The reaction of oxygen atoms and the injected carbon monoxide, although known to be slow, was producing sufficient CO_2 to be observed.

As the gas flow velocity was lowered, thus increasing the time the CO was present with the oxygen atoms prior to reaching the fluorescence cell, the larger was the intensity of the 4.3 micron radiation. Two changes in experimental conditions were possible to eliminate the unwanted effect. By lowering the CO pressure the unwanted signal could be made relatively smaller compared to the desired fluorescence. The CO_2 emission would be expected to depend quadratically on the CO pressure while the desired CO fluorescence would vary linearly. At a flow velocity of 6 meters per second, a CO pressure of 0.05 Torr, an O_2 pressure of 0.4 Torr and an O atom pressure of 0.04 Torr at the cell eliminated the leading edge distortion. Further reduction of CO pressure was difficult because of the reduction of the desired signal.

A second alternative was an increase in flow velocity to minimize the time available for CO_2 production. This has its own problems associated with the flow dominated fluorescent decays discussed below.

After analyzing several sets of fluorescence data taken at room temperature, tests for goodness of fit showed that a single exponential time decay function was not a good representation of the data. Further, the observed decay time constant depended upon flow velocity. It was then realized that because of the very long spontaneous emission lifetime of CO(v=1) and the relatively slow absolute quenching rates by any species, the observed decays were simply due to the excited CO being carried out of the viewing region and would be expected to depend in only a small way

on atom quenching. Decreasing the flow velocity to 2.5 meters per second introduced the CO_2 fluorescence again and had the additional consequence of limiting the temperature range that could be obtained for the gas at the fluorescence cell downstream of the furnace. A procedure was required which permitted the experiment to be carried out at high flow velocities.

A series of room temperature measurements were carried out in which the cell was replaced with a sapphire cylinder and fluorescence observations were made at two points downstream from the point of laser excitation. This will be referred to as the Time of Flight or TOF experiment and employed a four point analysis. That is to say four fluorescence traces were taken.

1 - Position x_1 without 0 atoms
2 - Position x_2 without 0 atoms
3 - Position x_1 with 0 atoms
4 - Position x_2 with 0 atoms

Laser power measurements were made for each trace.

Letting t be the time interval between the laser pulse and a point on a given trace, the same time t_1 was taken for traces 1 and 3 and another time t_2 for traces 2 and 4. The intensities at these positions and times are then

$$I_1 = L_1 f(x_1 t_1) e^{-t_1/\tau_1}$$
$$I_2 = L_2 f(x_2 t_2) e^{-t_2/\tau_1}$$
$$I_3 = L_3 f(x_1 t_1) e^{-t_1/\tau_2}$$
$$I_4 = L_4 f(x_2 t_2) e^{-t_2/\tau_2}$$

L represents the laser power for each run, f is a function of detector position along the flow tube and also the time. It further depends on flow velocity and diffusion among other parameters which are maintained the same for the four traces. τ_1 and τ_2 are the exponential decay constants associated with spontaneous emission and quenching.

For pairs of times t_1 and t_2 define

$$\Delta t = t_2 - t_1$$

and also

$$\Delta\left(\frac{1}{\tau}\right) = \frac{1}{\tau_2} - \frac{1}{\tau_1}$$

which for the present experiment will be equal to k[0].

$$\therefore \quad \Delta\left(\frac{1}{\tau}\right) = -\frac{1}{\Delta t} \ln\left\{\frac{I_1 I_4}{I_2 I_3} \frac{L_2 L_3}{L_1 L_4}\right\}$$

Any set of points (x_1 , x_2 , t_1 , t_2) yield the same results. For fixed x_1 and x_2 , a number of pairs of t_1 , t_2 points can be taken near the peak of fluorescence intensity curve and the results averaged in determining $\Delta\left(\frac{1}{\tau}\right)$.

It was then realized that data taken on the fluorescence cell could be analyzed in a related way. The observation position $x_1 = x_2$ and the function f is now simply g(t).

$$I_1 = L_1 \, g(t_1) \, e^{-t_1/\tau_1}$$
$$I_2 = L_1 \, g(t_2) \, e^{-t_2/\tau_1}$$
$$I_3 = L_2 \, g(t_1) \, e^{-t_1/\tau_2}$$
$$I_4 = L_2 \, g(t_2) \, e^{-t_2/\tau_2}$$

Again for pairs of times t_1 and t_2

$$\Delta\left(\frac{1}{\tau}\right) = -\frac{1}{\Delta t} \ln\left(\frac{I_1 I_4}{I_2 I_3}\right)$$

where the laser powers now cancel since I_1 and I_2 are taken from the same trace as are I_3 and I_4. An average over t_1, t_2 pairs is also taken here.

To be strictly accurate we should write the rate constant for quenching of CO(v=1) by O atoms as

$$k = \frac{1}{[O]} \left(\frac{1}{\tau_2} - \frac{1}{\tau_1}\right) + \frac{1}{2} k_1$$

where k_1 is the quenching rate due to O_2. It has been measured by Hancock and Green[1] to be 2.75 $sec.^{-1}$ $Torr^{-1}$. This is very much less than our measured k values and has been ignored in our data analysis.

A plot was made of the measured averaged values of $\Delta(\frac{1}{\tau})$ as a function of oxygen atom pressure P_O for each temperature. A least squares straight line fit to the data provided a value of the slope from which the second order quenching rate constant was derived. The plots for four temperatures are shown in Figure 2.

In carrying out these measurements, the atom pressure was varied by changing the microwave power used to dissociate O_2 molecules between zero and twelve watts. All of the lines plotted in Figure 2 show a non zero intercept suggestive of some impurity which is formed when the discharge is turned on. The reference condition for these measurements was the "microwave discharge off" situation. It was found that with no oxygen present a change occurred in the observed decay rate of the CO fluorescence when the discharge was turned on. While this change depended upon the flow conditions of a particular run, it showed no systematic dependence on the microwave excitation level once a discharge had been initiated. It was concluded that a change in temperature over a distance of a few centimeters led to a local pressure rise and a larger pressure gradient in the region of the fluorescence cell resulted in a slight increase in flow velocity of CO molecules out of the cell. In a computer simulation of this velocity change by the simple expedient of offsetting channels in the comparison of otherwise identical traces, it was estimated that out of a flow velocity of six meters per second a change on the order of 0.2 meters per second was taking place.

The second order quenching rate of constants determined using the slopes in Figure 2 were found to be identical to those derived from comparing traces with the microwave discharge on but differing O atom concentrations.

Results

The measured second order quenching rate constants for [1] atoms deactivating CO(v=1) at several temperatures are presented in Table 1. Figure 3 collects several of the shock tube data points found by Center [2] and the results of the present work. When a best fit is made to Center's data and extrapolated to lower temperatures in a Landau-Teller Plot, it is found that the measured room temperature rate is about two times faster than would be predicted. Within the error limits of both sets of data it is possible to construct a single straight to represent the temperature behavior. More data is needed to establish whether this is reasonable and work is underway to extend the temperature range of the measurements.

References

1. W. H. Green and J. K. Hancock, J. Chem. Phys. 59 4326, (1973).

2. R. E. Center, J. Chem. Phys. 58 5230, (1973).

TABLE 1

DEACTIVATION OF CO(v=1) BY OXYGEN ATOMS

TEMPERATURE °K	DEACTIVATION RATE CONSTANT Sec^{-1} $Torr^{-1}$
398	$(4.2 \pm 1.0) \times 10^3$
359	$(2.1 \pm 0.8) \times 10^3$
306	$(1.3 \pm 0.4) \times 10^3$
273	$(8.9 \pm 2.2) \times 10^2$

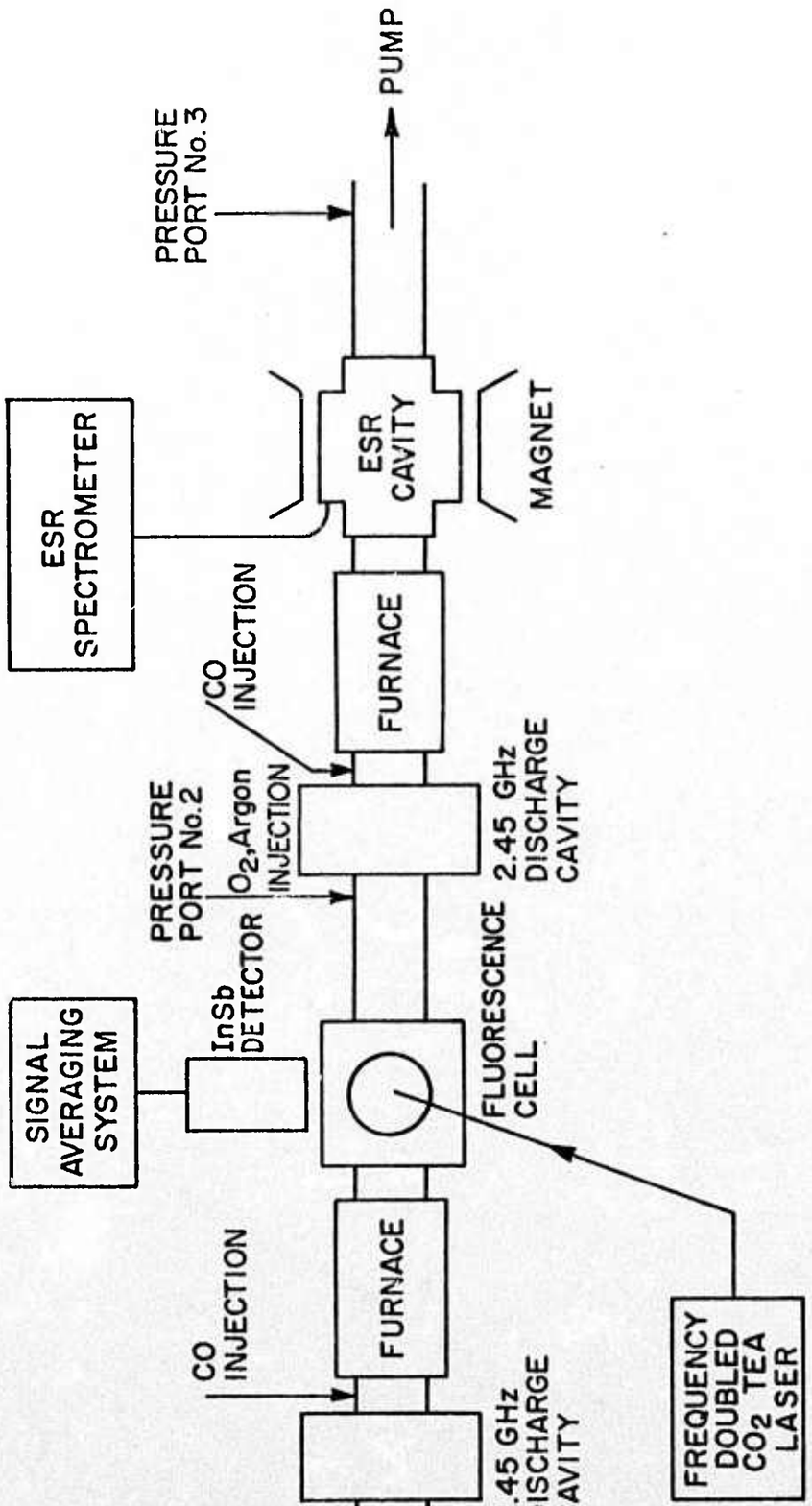

FIGURE 1. BLOCK DIAGRAM OF THE EXPERIMENT

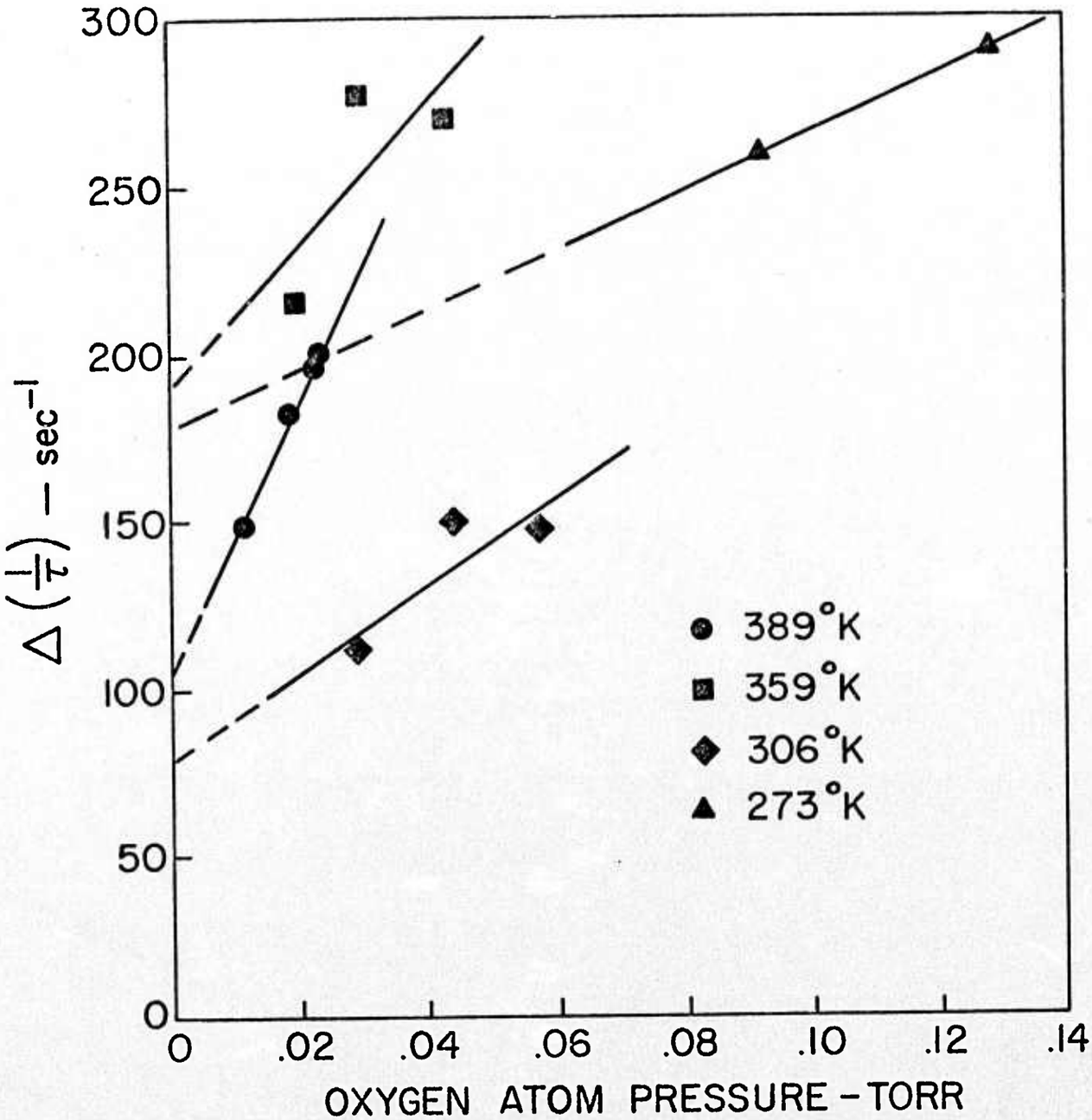

FIGURE 2. CHANGE IN DECAY RATE AS A FUNCTION OF OXYGEN ATOM PRESSURE FOR THE INDICATED TEMPERATURES

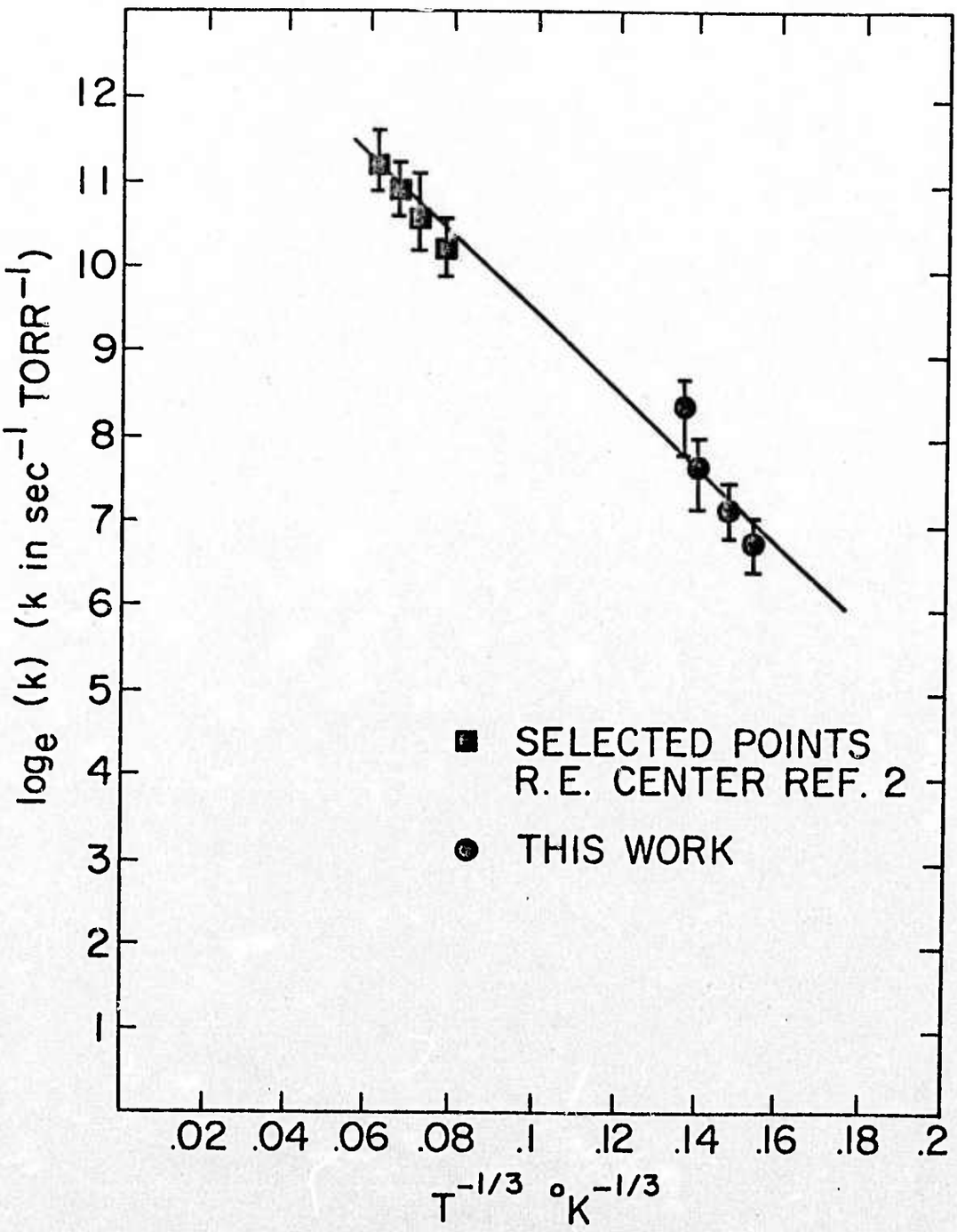

FIGURE 3. CO(v=1) DEACTIVATION BY O ATOMS $\log_e k$ vs $T^{-1/3}$

Molecular Energy Transfer and Chemical Lasers

Professor T. A. Cool

Abstract of Research

The research completed this past year consisted of two studies of importance for the development of energetic chemical laser systems. The most successful of these studies was an examination of the temperature dependence, at very low temperatures, of vibrational relaxation in the HF-DF, HF-CO_2, and DF-CO_2 systems. These measurements complement earlier work at higher temperature and provide a sound basis for comparison of current theories of multiquantum V→V,R energy transfer. This work also clearly establishes the lower limit for operatin, temperature of HF chemical lasers at which the detrimental effects of deactivation by HF polymers dominate all other kinetic processes. It was found that the dominant polymer species for deactivation are HF tetramers and hexamers; large concentrations of dimers do not appear to be present at pressures near 1 Torr.

The second study undertaken was directed toward the measurement of the V→R rates of energy transfer believed to be of importance in the design of pulsed HF chemical lasers with useful spectral output characteristics. This work is incomplete and only partially successful at the present time. A laser double resonance experiment was designed and performed in the effort to measure the distribution of HF molecules among the rotational states of the ground vibrational relaxation by the V→R processes

$$HF(v=1,J_1) + HF(v=0,J_2) \rightarrow HF(v=0,J_1') + HF(v=0,J_2')$$

The initial results of these experiments were inconclusive and further experiments have been postponed pending the results of computer modeling of the transient behavior of the HF rotational populations.

A Description of Research

A. Studies of energy transfer at low temperature in the HF-DF, HF-CO_2, and DF-CO_2 systems.

Vibrational (V→V) energy transfer between HF and DF and the asymmetric stretching mode of CO_2 is quite rapid despite the large

differences in vibrational energy between initial and final states. This circumstance has been cited as additional evidence for the existence of efficient multiquantum vibration-to-rotation (V → R) energy transfer in HF and DF,[1] already inferred from measurements of the V→R, T self-deactivation of HF and DF.[2,3] Similar observations of rapid rates for vibrational energy transfer from HF in collisions with DF[4-7,9,21] also indicate a rapid coupling between vibrational and rotational motions.

Progress in understanding such processes is hampered by the complexities of theoretical description and by the absence of direct experimental information concerning V→R transfer probabilities to specific rotational states. Nevertheless, the experimental determination of the temperature dependence of V→V transfer processes can be useful in theoretical modeling of intermolecular interactions. Moreover, an accurate knowledge of these energy transfer probabilities over a wide range of temperatures is needed in chemical laser development. Several recent studies of the temperature dependence of V→V and V→R processes in gas mixtures containing HF and DF for temperatures above 300 °K have been reported.[7-16] In a recent paper[1] we presented measurements of vibrational energy transfer over the range from 295-670 °K. In the present work measurements have been extended to lower temperatures, and certain systematic corrections have been made to measurements we have reported previously.[1,7]

The present results show that the inverse temperature dependence observed at higher temperatures for processes involving HF and DF monomers continues smoothly to temperatures near 200 °K. The effects of HF polymers in deactivation of HF and DF are clearly discernible in the 200-220 °K range; the probabilities for deactivation by polymers appear to exceed 0.1 at these temperatures.

The temperature dependence of several energy transfer processes in the HF-DF, HF-CO_2, and DF-CO_2 systems are shown in Figures 1-5 which contain the results of the present study along with previously reported action of other investigations.

The interactions between HF-HF, DF-DF, and HF-DF pairs and between HF(DF) and CO_2 are characterized by inverse temperature dependences for energy transfer probabilities that are stronger than T^{-1} (See Figs. 3 and 4). No presently available theories for energy transfer predict the strong inverse temperature dependence observed for these processes.[23] Until the effects of short range anisotropies in the intermolecular potentials can be included in a realistic way, it is doubtful that good agreement between experiment and theory will be obtained. Fortunately, progress in a priori calculations of energy surfaces has been rapid and perhaps reasonable interaction potentials for the F-H···F-H and F-H···O=C=O systems are near at hand.[24]

B. Continued Study of V→R and R→R Relaxation in HF

We are currently engaged in experimental studies of the V→R processes

$$HF(1,J_1) + HF(0,J_2) \rightleftharpoons HF(0,J_1') + HF(0,J_2') \qquad (1)$$

and R→R processes

$$HF(0,J_1) + HF(0,J_2) \rightleftharpoons HF(0,J_1') + HF(0,J_2') \qquad (2)$$

of importance in high energy HF laser systems.

A schematic diagram of the experimental apparatus is shown in Figure 6. The object of the experiments is the direct observation of nonthermal populations of high rotational states $9 \leq J \leq 14$ produced by the V→R processes (1). The temporal behavior of these rotational state populations would permit the estimation of the rate constants for the processes (1) and (2). The experimental technique is based upon the use of two lasers; a pump laser is used to produce the $HF(1,J_1)$ initial population and a sec ond laser is used to monitor the populations of $HF(0,J_1')$ and $HF(0,J_2')$. This monitoring is accomplished by observation of the R-branch fluorescence $h\nu_3$ produced by process (5) below: That is, subsequent to the pump pulse $h\nu_1$, the probe pulse $h\nu_2$ is employed to produce

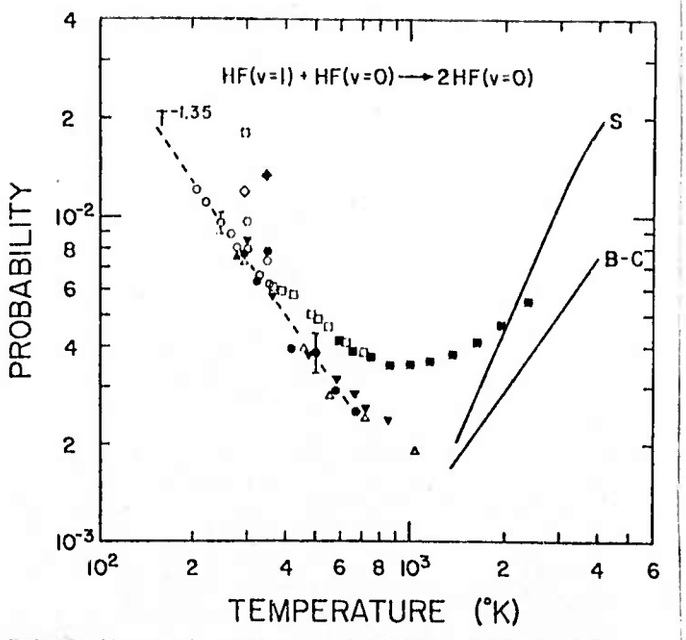

FIG. 1. Temperature dependence of the probability for self-deactivation of HF: line B–C, Bott and Cohen, Ref. 10; line S, Solomon *et al.*, Ref. 8; ■, Blair *et al.*, Ref. 13; △, Bott, Ref. 12; ▼, Hinchen, Ref. 15; □, Fried *et al.*, Ref. 14; ●, Lucht and Cool, Ref. 1; ○, present data; ♦, Airey and Fried, Ref. 2; ●, Stephens and Cool, Ref. 19; ○, Ahl and Cool, Ref. 6; ◇, Hancock and Green, Ref. 20; ▲, Osgood *et al.*, Ref. 22.

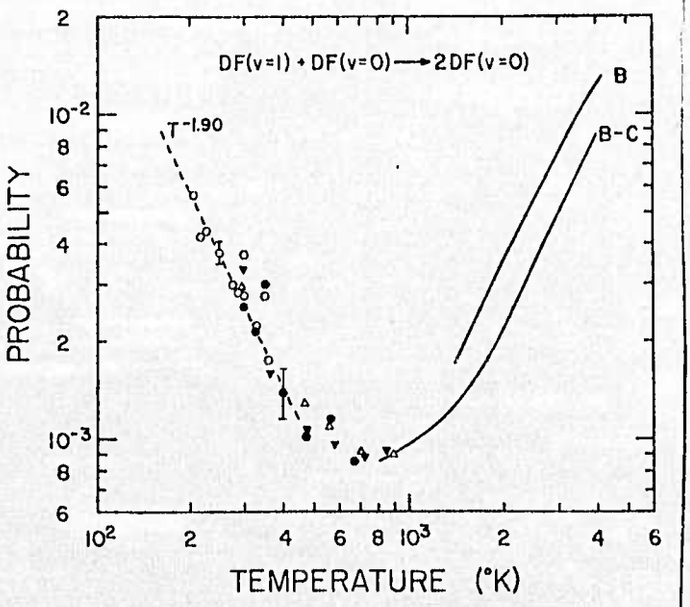

FIG. 2. Temperature dependence of the probability for self-deactivation of DF: line B, Blauer *et al.*, Ref. 9; line B–C Bott and Cohen, Ref. 11; △, Bott and Cohen, Ref. 10; ▼, Hinchen, Ref. 15; ○, Ahl and Cool, Ref. 6; ●, Stephens and Cool, Ref. 19; ●, Lucht and Cool, Ref. 1; ○, present data.

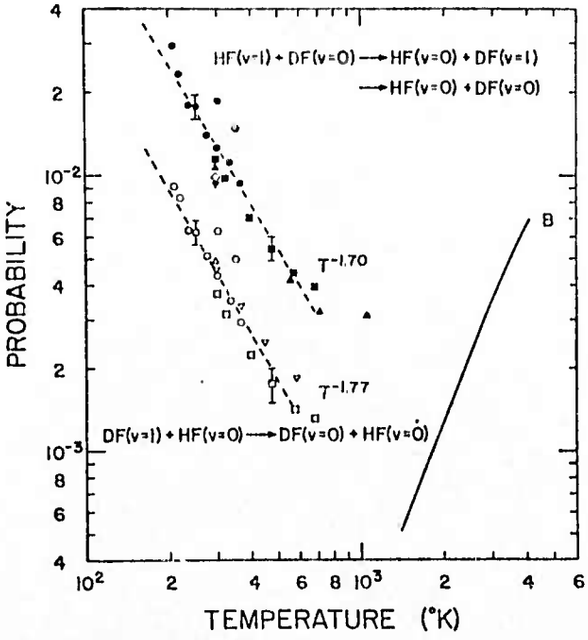

FIG. 3. Temperature dependences of probabilities for energy transfer in HF–DF mixtures: line B, Blauer *et al.*, Ref. 9; ▲, △, Bott and Cohen, Ref. 4; ○, ●, Ahl and Cool, Ref. 6; ◇, Airey and Smith, Ref. 21; ▼, Hinchen, Ref. 5; ▽, Hinchen, Ref. 15; ■, □, Lucht and Cool, Ref. 7; ◓, ○, present data.

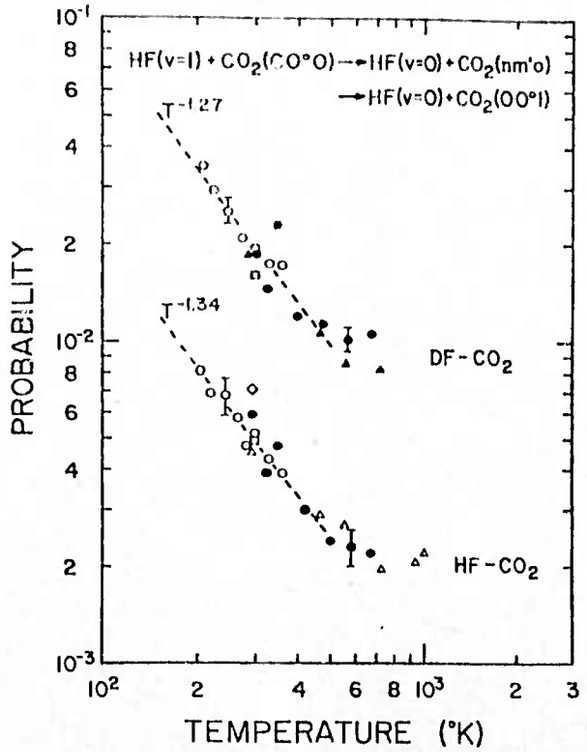

FIG. 4. Temperature dependence of the probabilities for energy transfer between HF(DF) and CO_2: Δ, Bott and Cohen, Ref. 4; ▲, Bott and Cohen, Ref. 16; ◊, Hancock and Green, Ref. 20; ◆, Stephens and Cool, Ref. 19; ●, Lucht and Cool, Ref. 1; ○, present data; □, Airey and Smith, Ref. 21.

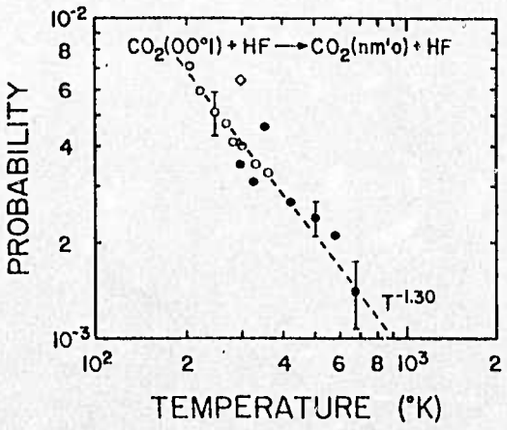

FIG. 5. Temperature dependence of the probabilities for $CO_2(00°1)$ deactivation by HF: Δ, Bott nnd Cohen, Ref. 4; ◊, Hancock and Green, Ref. 20; ◆, Stephens and Cool, Ref. 19; ●, Lucht and Cool, Ref. 1; ○, present data.

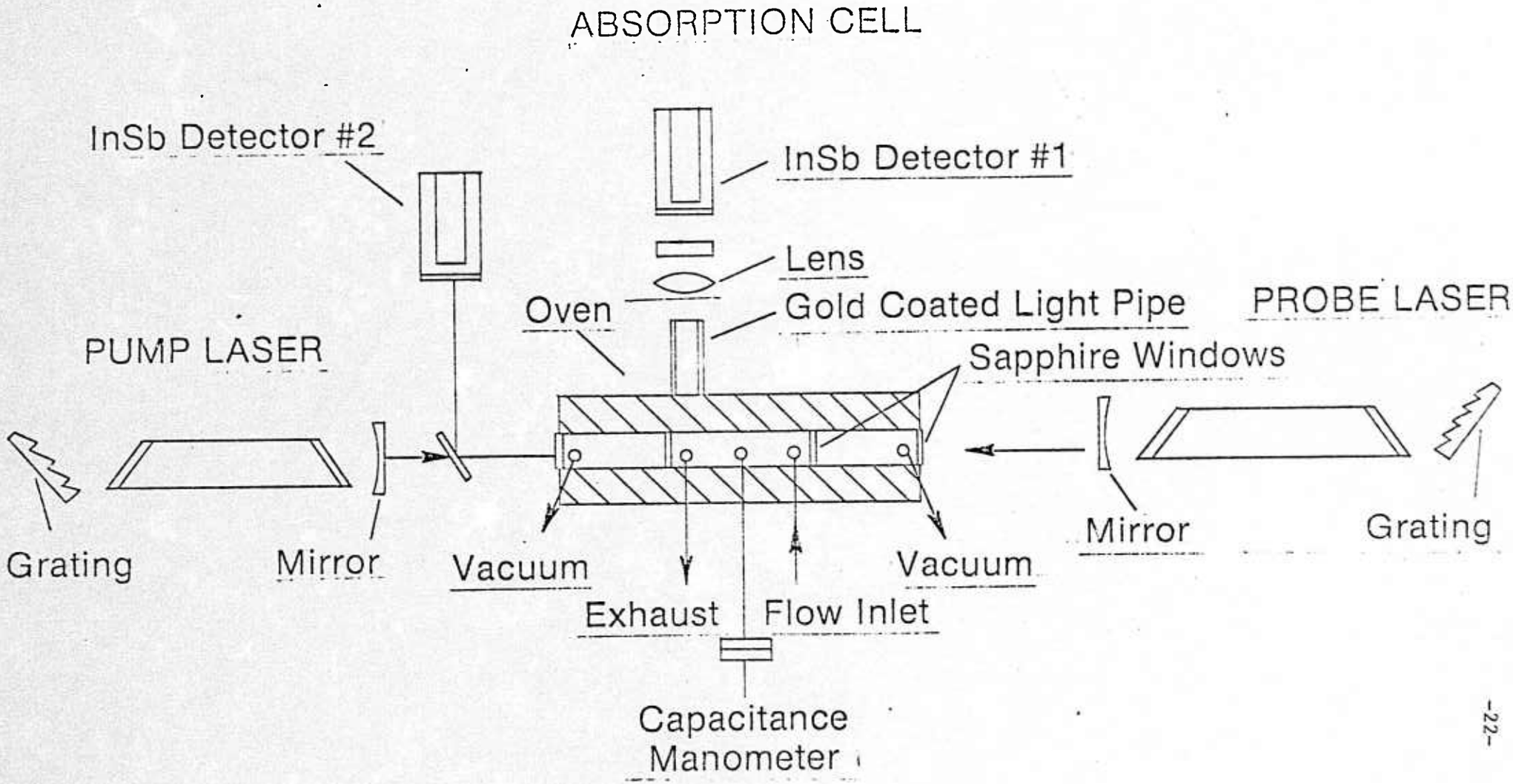
ABSORPTION CELL
InSb Detector #2
InSb Detector #1
Lens
Oven
Gold Coated Light Pipe
PROBE LASER
PUMP LASER
Sapphire Windows
Grating
Mirror
Vacuum
Vacuum
Mirror
Grating
Exhaust
Flow Inlet
Capacitance
Manometer

FIGURE 6

HF(1,J-1) from HF(0,J) where $9 \leq J \leq 14$;

$$HF(0,J) + h\nu_2 \longrightarrow HF(1,J-1). \qquad (3)$$

The resulting fluorescence from HF(1,J-1) is eith P-branch;

$$HF(1,J-1) \longrightarrow HF(0,J) + h\nu_{2'} \qquad (4)$$

or R-branch;

$$HF(1,J-1) \longrightarrow HF(0,J-2) + h\nu_3 \qquad (5)$$

This technique has turned out to be much more sensitive than the usual double-resonance absorption experiment. We have successfully observed fluorescence in step (5) when this technique is used with a thermal population in HF(0,9) of less than 10^{12} cm^{-3}. In spite of this sensitivity we have not yet been successful in our experimental goals[25] and we have decided to get a better idea of what might be expected from such experiments with the use of a computer model for processes (1) and (2). The model is based on the Polyani-Woodall kinetic expression for $R \rightarrow T$ relaxation[26] found to be useful in analysis of rotational relaxation in HCl.

In brief, we plan to solve the nonlinear equations of rotational relaxation associated with processes (1) and (2) for various assumptions for the nascent distribution of rotational states produced by the $V \rightarrow R$ processes (1). As an example, we will use simple trial distributions such as a delta-function corresponding to exclusive production of HF(0,J=13), along with other assumed distributions. We then will examine the sensitivity to such simple assumptions of the computed nonthermal populations in the presence of processes (2). By this means we hope to assess the significance of any experimentally observed departures from the thermal distribution, and, more importantly, to determine the feasibility of any further experiments.

It should be recognized that the information sought from these experiments has never been achieved before; direct observations of the J-dependence of $V \rightarrow R$ and $R \rightarrow R$ relaxation in HF will contribute greatly to the

theoretical understanding of such processes. Analysis of rotational relaxation and line broadening in high pressure HF and DF laser operation is essential for rapid progress in application of high energy lasers to laser initiated fusion and photochemistry.

References

1 R. A. Lucht and T. A. Cool, J. Chem. Phys. 60, 1026 (1974).

2 J. R. Airey and S. S. Fried, Chem. Phys. Lett. 8, 23 (1971).

3 H. L. Chen and C. B. Moore, J. Chem. Phys. 54, 4072 (1971).

4 J. F. Bott and N. Cohen, J. Chem. Phys. 58, 4539 (1973).

5 J. J. Hinchen, J. Chem. Phys. 59, 233 (1973).

6 J. L. Ahl and T. A. Cool, J. Chem. Phys. 58, 5540 (1973).

7 R. A. Lucht and T. A. Cool, J. Chem. Phys. 60, 2554 (1973).

8 W. C. Solomon, J. A. Blauer, F. C. Jaye, and J. G. Hnat, Int. J. Chem. Kinet. 3, 215 (1971).

9 J. A. Blauer, W. C. Solomon, and T. W. Owens, Int. J. Chem. Kinet. 4, 293 (1972).

10 J. F. Bott and N. Cohen, J. Chem. Phys. 55, 3698 (1971).

11 J. F. Bott and N. Cohen, J. Chem. Phys. 58, 934 (1973).

12 J. F. Bott, J. Chem. Phys. 57, 96 (1972).

13 L. S. Blair, W. D. Breshears, and G. L. Schot, J. Chem. Phys. 59, 1582 (1973).

14 S. S. Fried, J. Wilson, and R. L. Taylor, IEEE J. Quantum Electron. QE-9, 59 (1973).

15 J. J. Hinchen, J. Chem. Phys. 59, 2224 (1973).

16 J. F. Bott and N. Cohen, J. Chem. Phys. 59, 447 (1973).

17 We are indebted to Dr. J. K. Hancock for suggesting this technique for temperature measurement.

18 J. F. Bott, J. Chem. Phys. 61, 3414 (1974).

19 R. R. Stephens and T. A. Cool, J. Chem. Phys. 56, 5863 (1972).

20 J. K. Hancock and W. H. Green, J. Chem. Phys. 56, 2474 (1972).

21 J. R. Airey and I. W. M. Smith, J. Chem. Phys. 57, 1669 (1972).

22 R. M. Osgood, Jr., A. Javan, and P. B. Sackett, Appl. Phys. Lett. 20, 469 (1972).

23 S. Ormonde, Rev. Mod. Phys. 47, 193 (1975).

24 D. R. Yarkony, S. V. O'Neil, H. F. Schaefer III, C. P. Baskin, and C. F. Bender, J. Chem. Phys. 60, 855 (1974).

25 R. A. Lucht, "Vibrational Energy Exchange and Deactivation Processes in the HF-DF, HF-CO_2, and DF-CO_2 Systems from 205°K to 675 °K, Ph.D. Thesis, Cornell University, January 1976.

26 J. C. Polanyi and K. B. Woodall, J. Chem. Phys. 56, 1563 (1972).

List of Publications and Conference Papers for
the Period January 1, 1975 to December 31, 1975

1. K. K. Hui, D. I. Rosen, and T. A. Cool, "Intermode Energy Transfer in Vibrationally Excited O_3", Chem. Phys. Lett. 32, 141 (1975).

2. M. S. Chou and T. A. Cool, "Laser Operation by Dissociation of Metal Complexes: New Transitions in As, Bi, Ga, Ge, Hg, In, Pb, Sb, and Tl", to be published, J. Appl. Phys.

3. R. N. Sileo and T. A. Ciol, "Overtone Emission Spectroscopy of HF and DF: Vibrational Matrix Elements and Dipole Moment Function", to be published, J. Chem. Phys.

4. D. I. Rosen and T. A. Cool, "Vibrational Deactivation of O_3 Molecules in Gas Mixtures II", J. Chem. Phys. 62, 466 (1975).

5. R. A. Lucht and T. A. Cool, "Temperature Dependence of Vibrational Relaxation in the HF-DF, HF-CO_2 and DF-CO_2 Systems II," to be published, J. Chem. Phys.

6. T. A. Cool, "Prospects for Electronic Transition Chemical Lasers", 5th Winter Colloquium on Quantum Electronics, Sno Mass, Colorado, Feb. 1975.

7. M. S. Chou and T. A. Cool, "New Metal Atom Laser Transitions in As, Bi, Ga, Ge, Hg, In, Pb, Sb, and Tl", 2nd Summer Conference on Electronic Transition Lasers, Woods Hole, Mass. Sept. 1975.

8. J. S. Whittier and T. A. Cool, "Initiation with an Electron Beam of Chemical Reactions of Interest for Visible Wavelength Lasers", 2nd Summer Conference on Electronic Transition Lasers, Woods Hole, Mass., Sept. 1975.

Temperature dependence of vibrational relaxation in the HF–DF, $HF–CO_2$, and $DF–CO_2$ systems. II*

Roy A. Lucht and Terrill A. Cool

School of Applied and Engineering Physics, Cornell University, Ithaca, New York 14853
(Received 27 June 1975)

Measurements of vibrational energy transfer probabilities are presented for the temperature range 205–360°K for HF–DF, HF–CO_2, and DF–CO_2 gas mixtures. The present results provide an accurate determination of the inverse temperature dependence of the energy transfer probabilities exhibited by these systems. Large deactivation effects caused by HF (DF) polymers were observed for temperatures below 220°K.

I. INTRODUCTION

Vibrational ($V \rightarrow V$) energy transfer between HF and DF and the asymmetric stretching mode of CO_2 is quite rapid despite the large differences in vibrational energy between initial and final states. This circumstance has been cited as additional evidence for the existence of efficient multiquantum vibration-to-rotation ($V \rightarrow R$) energy transfer in HF and DF,[1] already inferred from measurements of the $V \rightarrow R, T$ self-deactivation of HF and DF.[2,3] Similar observations of rapid rates for vibrational energy transfer from HF in collisions with DF[4–7,9,21] also indicate a rapid coupling between vibrational and rotational motions.

Progress in understanding such processes is hampered by the complexities of theoretical description and by the absence of direct experimental information concerning $V \rightarrow R$ transfer probabilities to specific rotational states. Nevertheless, the experimental determination of the temperature dependence of $V \rightarrow V$ transfer processes can be useful in theoretical modeling of intermolecular interactions. Moreover, an accurate knowledge of these energy transfer probabilities over a wide range of temperatures is needed in chemical laser development. Several recent studies of the temperature dependence of $V \rightarrow V$ and $V \rightarrow R$ processes in gas mixtures containing HF and DF for temperatures above 300 °K have been reported.[7–16] In a recent paper,[1] hereafter referred to as I, we presented measurements of vibrational energy transfer over the range from 295–670 °K. In the present work measurements have been extended to lower temperatures, and certain systematic corrections have been made to measurements we have reported previously.[1,7]

The present results show that the inverse temperature dependence observed at higher temperatures for processes involving HF and DF monomers continues smoothly to temperatures near 200 °K. The effects of HF polymers in deactivation of HF and DF are clearly discernible in the 200–220 °K range; the probabilities for deactivation by polymers appear to exceed 0.1 at these temperatures.

II. EXPERIMENTAL APPARATUS

The laser fluorescence apparatus and procedures used in the present work were modified in three respects from those previously described.[1] First the fluorescence cell described in I was provided with cooling coils to permit operation down to temperatures of 200 °K. Secondly, the measurements of partial gas pressure within the fluorescence cell were corrected to include compressible flow effects associated with the sonic orifice used for exhaust flow control of the fluorescence cell. Finally, in the course of flow calibrations, flows metered with the valves used in the experiments described in I and Ref. 7 were found to be subject to significant corrections because of viscous effects. This problem was eliminated for the present work; however, some of the previously given results[1,7] were found to be systematically in error. Fortunately, it was possible to make complete corrections to those data; the corrected measurements are given in Sec. III. Except for these modifications, the present experiments were performed in a fashion identical to that described in I.

A. Fluorescence cell temperature control

The solid nickel fluorescence cell of I was easily adapted to low temperature operation. The cell was wrapped with 3/16 in. o.d. copper cooling coils which were soldered to the cell body to ensure good thermal contact. Cell cooling was accomplished by a recirculating flow of methanol between the cell and a cold bath. For temperatures from 200 to 250 °K a methanol–dry-ice bath was employed; an ice-water bath was used from 275 to 300 °K; some data were also taken from 300 to 360 °K with use of a heated water bath. Precise temperature selection and control (±1.0 °K) was accomplished with use of electrical heating tapes wrapped around the entering coolant flow line which connected the cell with the cold bath. Cell temperatures were monitored with a thermocouple immersed in the fluorescence cell gas flow. Temperatures measured for flowing gas conditions within the cell were identical to those for the static cell for all flow rates employed here.

A simple check was performed[17] on the accuracy of the thermocouple reading. The cooled fluorescence cell was first filled with static propane gas. The vapor pressure of the propane was then measured to give an accurate indication of the cell temperature. The temperature given from the propane vapor pressure was 2 °K lower than the thermocouple temperature for temperatures near 200 °K. This small discrepancy was apparently caused by heat conduction along the thermocouple leads. Compensation for this was made with a correction which varied linearly with the temperature

difference between the cell and its surroundings.

B. Partial pressure measurements

Following a suggestion by Bott[18] we have modified our method of partial pressure measurement to include corrections for gasdynamic effects. In the present apparatus a sharp-edged sonic orifice located at the exhaust of the fluorescence cell was used for control of the gas flow rate through the cell. A primary flow of argon was established at a pressure of 30 Torr within the fluorescence cell. The desired cell composition of the added gases HF, DF, or CO_2 was then established for a given run. This was accomplished by recording the changes in cell static pressure as each secondary flow compoenet was successively established. Because the cell gas flow rate was controlled by the sonic orifice, the change in cell static pressure was determined by the change in sonic flow conditions before and after the secondary flow was added. The effect of a given added gas flow rate on the sonic conditions and on the cell static pressure depends on the specific heat ratios and molecular weights of both the added gas and the initial cell gas flow to which it is added. When viscous effects at the orifice can be ignored, isentropic flow relationships may be employed to calculate a correction factor by which the measured cell pressure change must be multiplied to determine the actual partial pressure of added gas.[18]

This procedure was tested by performing measurements of HF self-deactivation rates for five helium–argon mixtures of various atomic weights.[18] The sharp-edged sonic orifice used in the present work exhibited flow characteristics accurately described by the inviscid compressible flow relationships. This orifice was a 0.024 in. diam hole drilled in a flat disk of 0.003 in. thickness. In the work reported in I and Ref. 7, however, a Granville Phillips Series 203 variable leak valve was used instead of a sharp-edged orifice for fluorescence cell flow control. Unfortunately, the flow characteristics for this valve were significantly different from those exhibited by the sharp-edged orifice, and additional corrections had to be made point by point to the HF–CO_2 and DF–CO_2 data reported in I and the HF–DF data of Ref. 7. We have found other types of valves (e.g., Whitey 21RS4) which appear to have flow characteristics quite similar to those of the sharp-edged sonic orifices; however, enough variation exists between different valves and valve settings that the compressible flow corrections of Ref. 18 cannot be applied indiscriminately.

III. EXPERIMENTAL RESULTS

The data reduction techniques employed here have been fully presented in I. These methods permit the direct determination of the exponential decay constants λ_1 and λ_2 used for the description of the temporal variations in the populations of HF ($v=1$), DF ($v=1$), and CO_2 (00°1) molecules in the gas mixtures of present interest. In the following presentation the notation and rate constant definitions are the conventional ones given in I.

A. Self-deactivation of HF and DF

Previous measurements[1,2,7–16,19–22] of the self-deactivation processes

$$HF(v=1)+HF(v=0) \xrightarrow{k_{11}} 2HF(v=0)+\Delta E_v = 3962\ \text{cm}^{-1} \quad (1)$$

and

$$DF(v=1)+DF(v=0) \xrightarrow{k_{11}} 2DF(v=0)+\Delta E_v = 2907\ \text{cm}^{-1} \quad (2)$$

have been for sufficiently high temperatures that the influences of HF polymers on deactivation were negligible. In the present work an attempt was made to extend measurements of k_{11} to temperatures as low as possible before polymers become the dominant source of deactivation.

The equilibrium composition of HF is described in terms of the equilibrium constants for the association equations

$$n\text{HF} \rightleftharpoons (\text{HF})_n \quad (3)$$

defined in terms of the partial pressures of nth order polymers,

$$p_n = K_n p_1^n , \quad (4)$$

where p_1 is the partial pressure of HF monomers.

Thus at low temperatures the experimental deactivation rates of $HF(v=1)$ and $DF(v=1)$ ought to follow the relationship

$$(p\tau)^{-1} = k_{1m}(p_m/p) + k_{11}(p_1/p) + \sum_{n>1} (k_{11})_n K_n p_1^n/p , \quad (5)$$

where k_{1m} and k_{11} are the respective rate constants ($\text{sec}^{-1}\cdot\text{Torr}^{-1}$) for deactivation by argon and by HF monomers present with partial pressures p_m and p_1; p is the total pressure. The rate constant $(k_{11})_n$ refers to deactivation of $HF(v=1)$ or $DF(v=1)$ by the nth order polymer $(HF)_n$ or $(DF)_n$.

In the present experiments p was nearly constant since p_m was 30 Torr and the HF(DF) pressures did not exceed 1 Torr. Moreover, at temperatures above 200 °K, the use of total HF pressure in place of p_1 in Eq. (5) introduces a negligible error.[23] Therefore, in analysis of the experiments, the approximate expression

$$(p\tau)^{-1} = k_{1m}X_m + k_{11}X_{\text{HF}} + \sum_{n>1} (k_{11})_n K_n X_{\text{HF}}^n p^{n-1} , \quad (6)$$

where X_m and X_{HF} are the mole fractions of argon and HF, is applicable.

Figures 1–3 present deactivation rate data for a low temperature (205 °K) and a higher temperature (~275 °K). Figure 1 illustrates the linear dependence of deactivation rate on HF(DF) mole fraction observed for all temperatures above about 220 °K. As the temperature was reduced below 220 °K, the dependence of $(p\tau)^{-1}$ on X_{HF} became increasingly nonlinear, as Figs. 2 and 3 indicate.

In principle data such as those of Figs. 2 and 3 could be analyzed by means of Eq. (6) to estimate values for the rate constants $(k_{11})_2$, $(k_{11})_4$, $(k_{11})_6$, etc., for deactivation by HF dimers, tetramers, hexamers, etc. The equilibrium composition of HF polymers at the tempera-

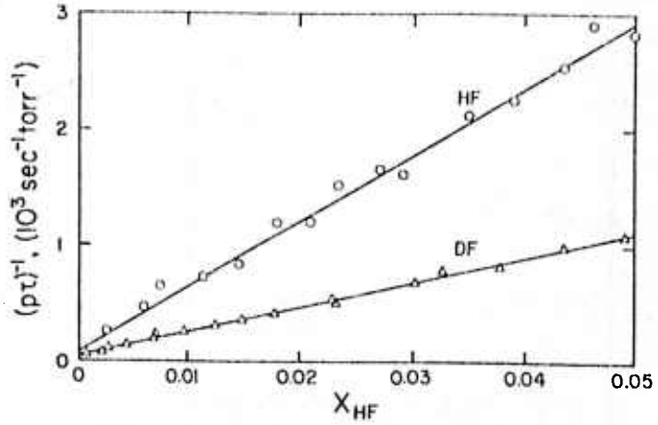

FIG. 1. Observed HF(DF) fluorescence decay rates for HF(DF)–argon mixtures. The HF data are for $T = 279$ °K; the DF data for $T = 275$ °K.

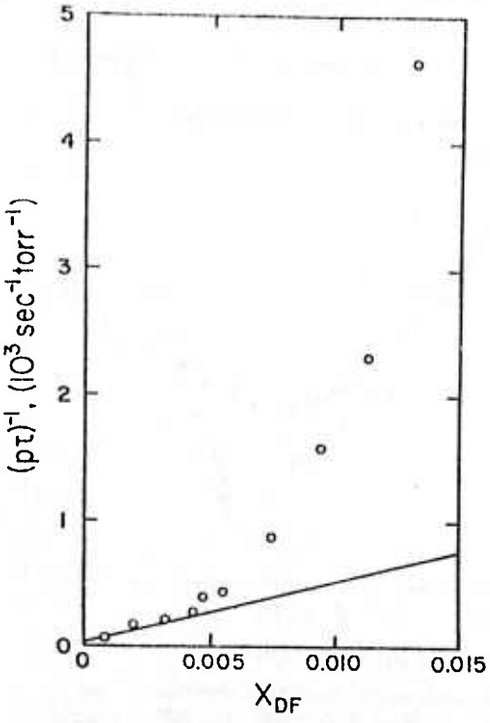

FIG. 3. Observed DF fluorescence decay rate as a function of DF mole fraction for DF–argon mixtures at $T = 205$ °K.

tures and pressures of present interest is, however, not well characterized and has been the subject of several conflicting analyses during the past 20 years.[24–27] Thus only the linear term, $k_{11}X_{HF}$, can be unambiguously determined from the present data. The solid lines shown with the data of Figs. 2 and 3 indicate the approximate contributions to the relaxation rate from this linear term.

In contrast to the HF data, the DF data exhibit pronounced nonlinear contributions for $X_{DF} \gtrsim 0.01$. The deactivation rate for DF observed for values of $X_{DF} \gtrsim 0.01$ is so large that the fraction of deactivating polymers in the DF would have to exceed about 10^{-2}. The data can be represented with Eq. (6) provided that large contributions to deactivation caused by $(DF)_4$ and $(DF)_6$ are assumed, but that virtually no contribution from $(DF)_2$ is present. This result is puzzling since, according to the most recent analysis[24] of P–V–T data for HF,[26] only the DF dimers would be present in a concentration large enough to give a major contribution to deactivation. It should be noted, however, that in an earlier analysis based upon infrared absorption studies Smith[25] concluded that the equilibrium concentration of $(HF)_2$ would be small relative to those of $(HF)_4$ and $(HF)_6$ at the temperatures of interest here.

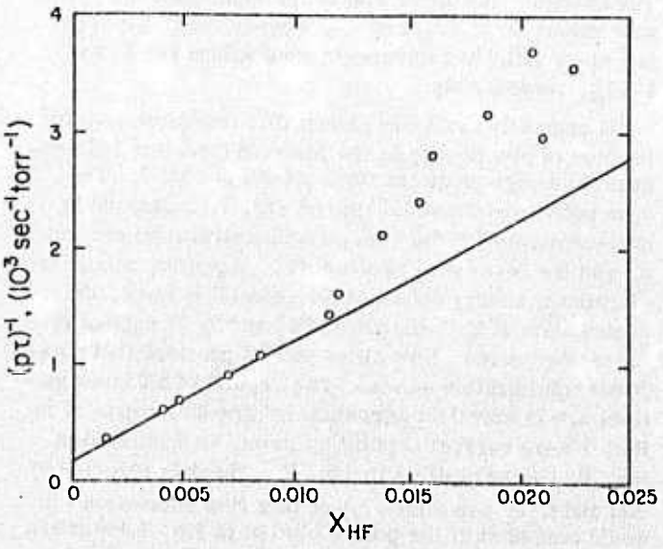

FIG. 2. Observed HF fluorescence decay rates as a function of HF mole fraction for HF–argon mixtures at $T = 205$ °K.

The present measurements of probabilities for the self-deactivation of HF and DF by processes (1) and (2) are given along with previous results in Figs. 4 and 5. The present results and the corrected data of I are seen to be in good agreement with the work of Bott[12] and Hinchen,[15] who worked with premixed gases, and with the measurement of Osgood *et al.*[22] performed with a static system.

The data of Refs. 2, 6, 14, 19, and 20 were all obtained with flow-mixing apparatus similar to that used here. These data are presumably subject to some correction because of compressible flow and viscous effects at the fluorescence cell exhaust valves. For the data of Airey and Fried,[2] Hancock and Green,[20] Fried *et al.*,[14] Stephens and Cool,[19] and Ahl and Cool,[6] taken with HF(DF)–argon mixtures, the compressible flow correction would result in a 19% downward shift in the reported probabilities which are plotted in Figs. 4 and 5. If we assume that no additional correction of significance needs to be made for viscous flow effects for the values used in these studies, then all of the fluorescence cell measurements are in reasonably good agreement with the shock tube measurements of Bott.[12] Unresolved systematic differences yet exist, however, between the shock tube data for HF of Bott,[13] Bott and Cohen,[10] Blair *et al.*,[13] and of Solomon *et al.*[8]

The dashed lines shown with the probability data of

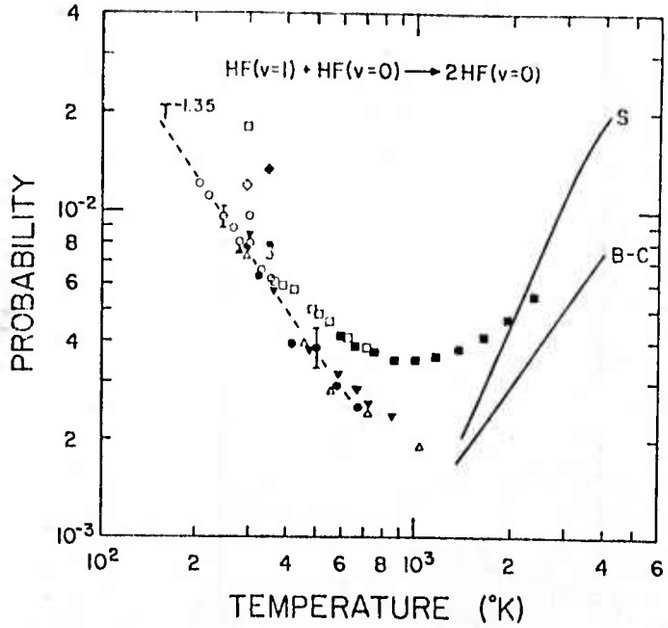

FIG. 4. Temperature dependence of the probability for self-deactivation of HF: line B–C, Bott and Cohen, Ref. 10; line S, Solomon *et al.*, Ref. 8; ■, Blair *et al.*, Ref. 13; Δ, Bott, Ref. 12; ▼, Hinchen, Ref. 15; □, Fried *et al.*, Ref. 14; ●, Lucht and Cool, Ref. 1; ○, present data; ♦, Airey and Fried, Ref. 2; ◐, Stephens and Cool, Ref. 19; ○, Ahl and Cool, Ref. 6; ◇, Hancock and Green, Ref. 20; ▲, Osgood *et al.*, Ref. 22.

Figs. 4 and 5 indicate the approximate temperature dependence of the present data and the corrected measurements of I over the range from 200 to 400 °K.

B. Vibrational energy transfer in HF-DF mixtures

Measurements of the rate constant sums, k_e+k_{12} and $k_e'+k_{21}$, for the processes

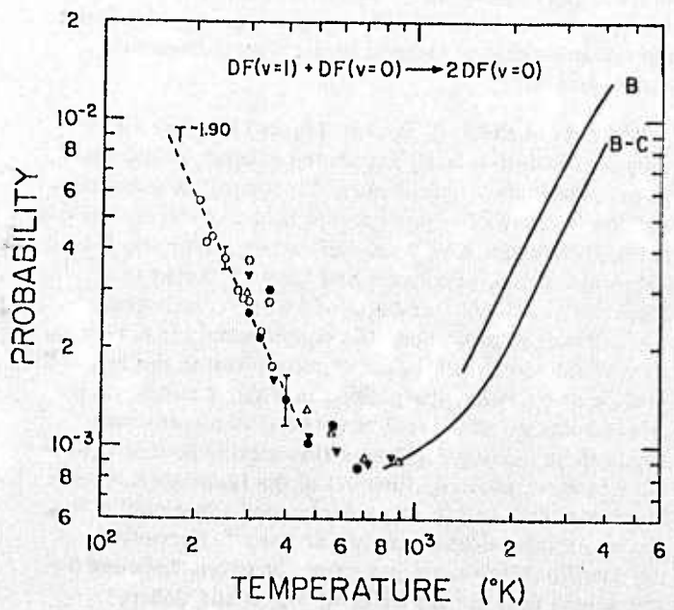

FIG. 5. Temperature dependence of the probability for self-deactivation of DF: line B, Blauer *et al.*, Ref. 9; line B–C Bott and Cohen, Ref. 11; Δ, Bott and Cohen, Ref. 16; ▼, Hinchen, Ref. 15; ○, Ahl and Cool, Ref. 6; ●, Stephens and Cool, Ref. 19; ●, Lucht and Cool, Ref. 1; ○, present data.

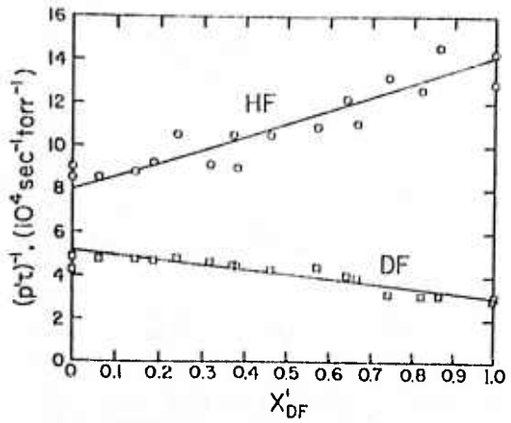

FIG. 6. Observed HF and DF fluorescence decay rates from HF–DF–argon mixtures at 250 °K as a function of the reduced mole fraction of DF; $X'_{DF}=X_{DF}/(X_{HF}+X_{DF})$.

$$HF(v=1)+DF(v=0)\underset{k_e'}{\overset{k_e}{\rightleftharpoons}}HF(v=0)+DF(v=1)+\Delta E_v=1055\ \text{cm}^{-1} \tag{7}$$

$$HF(v=1)+DF(v=0)\xrightarrow{k_{12}}HF(v=0)+DF(v=0)+\Delta E_v=3962\ \text{cm}^{-1} \tag{8}$$

and

$$DF(v=1)+HF(v=0)\xrightarrow{k_{21}}DF(v=0)+HF(v=0)+\Delta E_v=2907\ \text{cm}^{-1} \tag{9}$$

were performed over the temperature range 205–364 °K. Previous measurements[4–7,9,21] cover the range 297–4100 °K.

Figure 6 gives typical HF and DF fluorescence relaxation rate data for HF–DF mixtures at a temperature of 250 °K. The upper data of Fig. 6 are HF fluorescence relaxation rates; the lower data are observations of the relaxation of DF fluorescence. The intercepts of data plots such as that of Fig. 6 yield the desired rate constant values for processes (7)–(9) after small corrections are made for the influence of argon deactivation.[1,7] For example, the upper and lower right-hand intercepts give values for k_e+k_{12} and k_{22}, respectively; the upper and lower left-hand intercepts give values for k_{11} and $k_e'+k_{21}$, respectively.

All presently available probability measurements for the sum of process (7) in the forward direction and process (8) are given as the dark points in Fig. 7. The open points and the solid line of Fig. 7 correspond to measurements for the sum of probabilities for process (9) and the reverse of process (7). However, since the vibrational energy defect of process (7) is large, the contribution of k_e' to the sum of k_e' and k_{21} is negligible for temperatures below about 500 °K provided that rotational equilibration exists. The results of all investigations are in excellent agreement. The data reported in Ref. 7 were corrected point by point, as described in Sec. II, before plotting in Fig. 7. The data reported by Ahl and Cool[6] are also subject to a flow correction which would tend to shift the points plotted in Fig. 7 downward in better agreement with the other data.[20]

The dashed lines of Fig. 7 indicate the similar inverse temperature dependence, at low temperatures, for

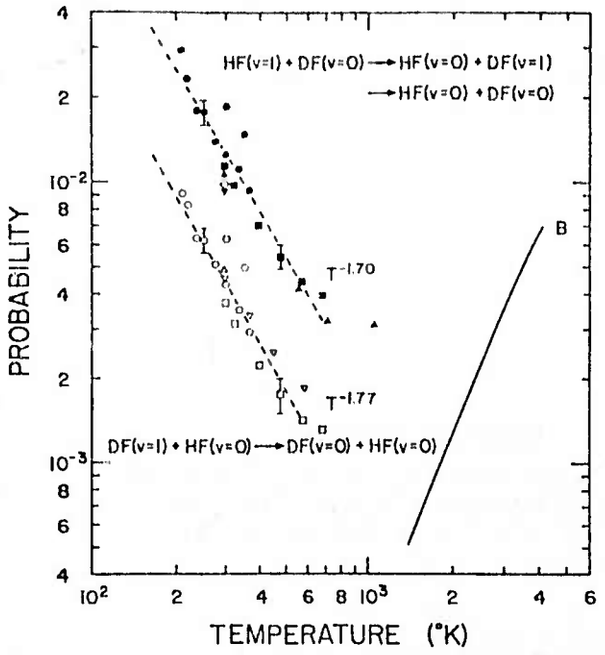

FIG. 7. Temperature dependences of probabilities for energy transfer in HF–DF mixtures: line B, Blauer *et al.*, Ref. 9; ▲, △, Bott and Cohen, Ref. 4; ○, ●, Ahl and Cool, Ref. 6; ◇, Airey and Smith, Ref. 21; ▼, Hinchen, Ref. 5; ▽, Hinchen, Ref. 15; ■, □, Lucht and Cool, Ref. 7; ●, ○, present data.

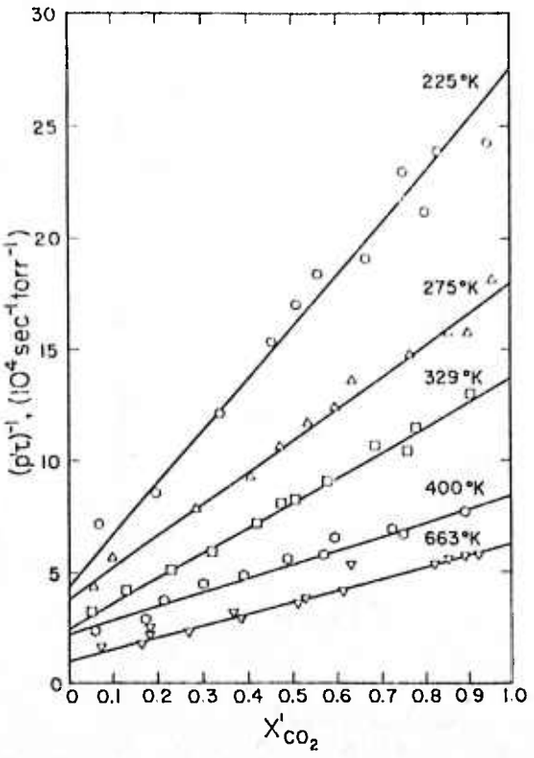

FIG. 9. Observed DF fluorescence decay rates for DF–CO_2–argon mixtures for several temperatures as a function of the reduced mole fraction of CO_2; $X'_{CO_2}=X_{CO_2}/(X_{DF}+X_{CO_2})$.

the probabilities corresponding to both of the rate constant sums k_e+k_{12} and k'_e+k_{21} of processes (7), (8), and (9).

C. Vibrational energy transfer and deactivation in the HF-CO_2 and DF-CO_2

It was shown in I that plots of the decay rates, $(p'\tau)^{-1}$, of HF fluorescence from HF–CO_2 mixtures varied linearly with CO_2 reduced mole fraction; p' is the sum of HF and CO_2 partial pressures. Measurements of the relaxation rate of HF fluorescence, $(p'\tau)^{-1}$, for the limiting case of HF–CO_2 mixtures with a mole fraction of HF approaching zero were used to obtain the rate constant sum k_e+k_{12} for the processes

$$\mathrm{HF}(v=1)+\mathrm{CO_2}(00^\circ0)\underset{k'_e}{\overset{k_e}{\rightleftharpoons}}\mathrm{HF}(v=0)+\mathrm{CO_2}(00^\circ1)+\Delta E_v=1612\ \mathrm{cm^{-1}} \qquad (10)$$

and

$$\mathrm{HF}(v=1)+\mathrm{CO_2}(00^\circ0)\xrightarrow{k_{12}}\mathrm{HF}(v=0)+\mathrm{CO_2}(nm^\prime0)\ . \qquad (11)$$

This linearity in the variation of relaxation rate with mixture composition was also observed at lower temperatures. Because of the influence of HF polymers, it was not possible to obtain data amenable to unambiguous interpretation for temperatures below about 220 °K. Figure 8 shows the linear variation of $(p'\tau)^{-1}$ with the reduced mole fraction of CO_2, $X'_{CO_2}=X_{CO_2}/(X_{HF}+X_{CO_2})$, observed for several temperatures. The data for 420 and 580 °K are those reported in I, but with flow corrections applied point by point.

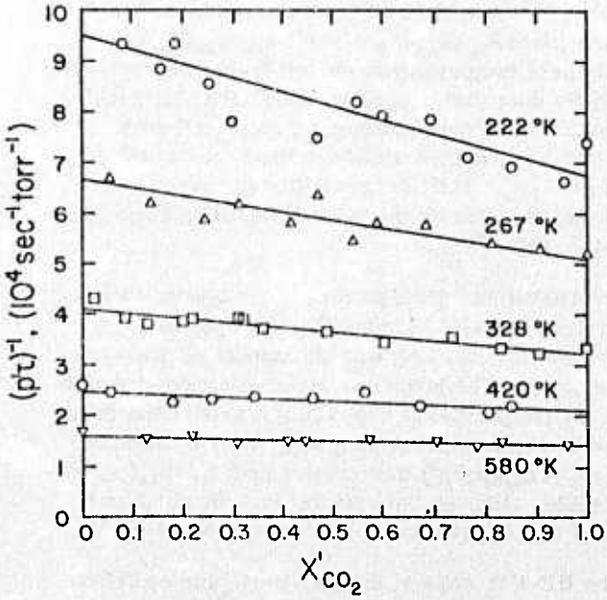

FIG. 8. Observed HF fluorescence decay rates for HF–CO_2–argon mixture for several temperatures as a function of the reduced mole fraction of CO_2; $X'_{CO_2}=X_{CO_2}/(X_{HF}+X_{CO_2})$.

Figure 9 displays an analogous set of data taken for the DF–CO_2 system for temperatures ranging from 225 to 663 °K. Here again, an essentially linear variation in DF relaxation rate with mixture composition was observed for all temperatures.

Figure 10 indicates the temperature dependence for the sum of probabilities for processes (10) and (11) for the HF–CO_2 system and for the analogous processes for

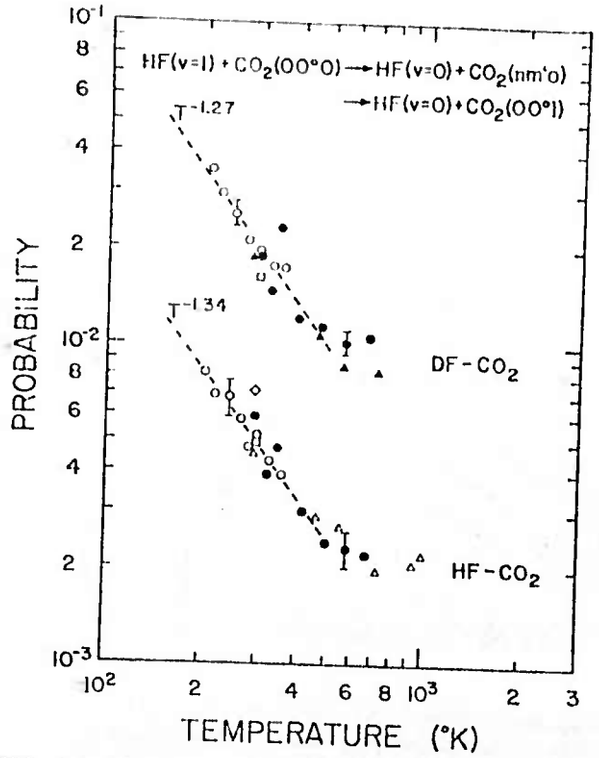

FIG. 10. Temperature dependence of the probabilities for energy transfer between HF(DF) and CO_2: △, Bott and Cohen, Ref. 4; ▲, Bott and Cohen, Ref. 16; ◇, Hancock and Green, Ref. 20; ●, Stephens and Cool, Ref. 19; ●, Lucht and Cool, Ref. 1; ○, present data; □, Airey and Smith, Ref. 21.

the DF–CO_2 case. These measurements were obtained from the right-hand intercepts of graphs similar to those of Figs. 8 and 9, as explained in I. The present results and the corrected measurements of I are in excellent agreement with the overlapping results of previous studies in the temperature range 300 °K–700 °K. The low temperature (200–400 °K) variation in probability with temperature, indicated by the dashed lines, is similar for both the HF–CO_2 and DF–CO_2 systems.

Observations were also made of the decay of $CO_2(00°1)$ fluorescence to provide measurements of the rate constant sum, $k'_e + k_{21}$, for the reverse of process

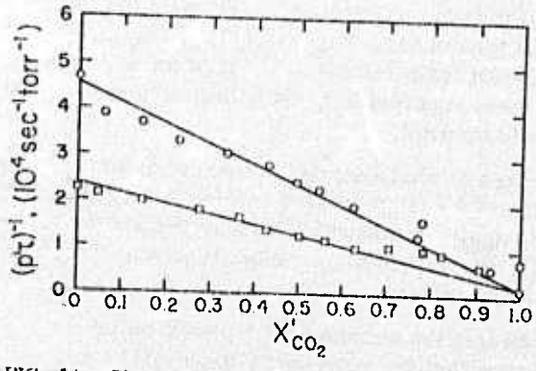

FIG. 11. Observed CO_2 fluorescence decay rates for the final stages of relaxation for HF–CO_2–argon and DF–CO_2–argon mixtures at 248 °K as a function of the reduced mole fraction of CO_2.

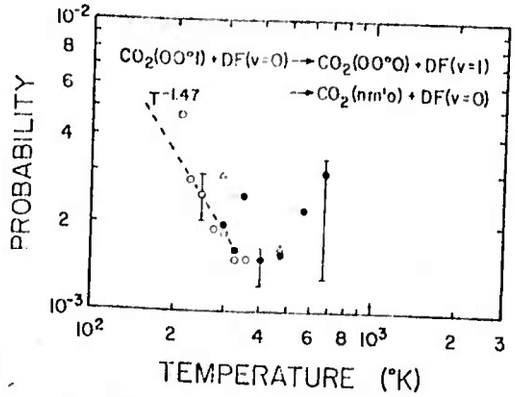

FIG. 12. Temperature dependence of the probabilities for $CO_2(00°1)$ deactivation by DF: △, Bott and Cohen, Ref. 16; ●, Stephens and Cool, Ref. 19; ●, Lucht and Cool, Ref. 1; ○, present data.

(10) and the CO_2 deactivation process,

$$CO_2(00°1) + HF(v=0) \xrightarrow{k_{21}} CO_2(nm'0) + HF(v=0)\,. \quad (12)$$

The procedure by which measurements of $k'_e + k_{21}$ were obtained was based upon observations of the dependence of the decay rate, $(p'\tau)^{-1}$, of $CO_2(00°1)$ fluorescence in the latter stages of relaxation upon the reduced CO_2 mole fraction, X'_{CO_2}. It was shown in I that when X'_{CO_2} approaches zero, that $(p'\tau)^{-1}$ for the CO_2 fluorescence decay has the smaller of the two limiting values $k_{11} + k_{1m}(p_m/p')$ or $k'_e + k_{21} + k_{2m}(p_m/p')$. Here k_{11} is the rate constant for self deactivation of HF(DF), k_{1m} and k_{2m} are the respective rate constants for vibrational deactivation of HF(DF) and $CO_2(00°1)$ by argon, p_m is the partial pressure of argon, and p' is the sum of HF(DF) and CO_2 partial pressures. For HF–CO_2 mixtures at temperatures below 700 °K and DF–CO_2 mixtures below 400 °K, it was found that $k_{11} + k_{1m}(p_m/p') > k'_e + k_{21} + k_{2m}(p_m/p')$; thus, for these temperatures the left-hand intercepts ($X'_{CO_2} = 0$) for data plots, such as that of Fig. 11, yield values for the rate constant sum, $k'_e + k_{21}$. All such data plots exhibited a substantially linear variation[1] of $(p'\tau)^{-1}$ with X'_{CO_2}. This fact permitted the assignment of useful upper bonds on the values of k_e to be made for the DF–CO_2 data.[29]

The probabilities corresponding to the measured rate constant sums, $k'_e + k_{21}$, for the DF–CO_2 system are presented in Fig. 12 along with the results of previous measurements. The large uncertainties associated with the data for temperatures above 500 °K arise from difficulty[30] in the determination of $k'_e + k_{21}$ under conditions when $k'_e + k_{21} + k_{2m}(p_m/p')$ was greater than $k_{11} + k_{1m}(p_m/p')$. It is possible, although not certain, that the combined probability $P'_e + P_{21}$ reaches a minimum at about 400 °K.

For the HF–CO_2 case k'_e makes a negligible contribution to $k'_e + k_{21}$ in the temperature range represented by the probability data of Fig. 13. All of the presently available data are in good agreement and have a simple inverse temperature dependence in the range from 200–700 °K.

TABLE I. Rate constants and probabilities for vibrational energy transfer in the HF–DF system.

Temperature (°K)	Rate constants (10^4 sec^{-1} · Torr^{-1})		Probabilities[a]	
T	$k_e + k_{12}$	k_{21}	$P_e + P_{12}$	P_{21}
210	25.3 ± 3.0	7.8 ± 1.5	0.030	0.0091
219	19.6 ± 2.0	7.0 ± 1.0	0.023	0.0033
235	14.5 ± 1.0	5.1 ± 0.5	0.018	0.0063
250	14.0 ± 1.5	4.9 ± 0.5	0.018	0.0062
274	10.4 ± 1.3	3.8 ± 0.5	0.014	0.0051
297[b]	8.2 ± 0.8	2.7 ± 0.4	0.011	0.0037
298	9.0 ± 1.5	3.1 ± 0.5	0.013	0.0043
321[b]	6.75 ± 0.5	2.15 ± 0.4	0.0097	0.0031
333	7.6 ± 0.8	2.35 ± 0.4	0.011	0.0035
364	6.3 ± 0.8	1.95 ± 0.4	0.0093	0.0029
395[b]	4.4 ± 0.3	1.4 ± 0.2	0.0070	0.0022
475[b]	3.1 ± 0.3	1.0 ± 0.15	0.0054	0.0018
570[b]	2.3 ± 0.2	0.75 ± 0.1	0.0044	0.0014
578[b]	1.85 ± 0.2	0.6 ± 0.1	0.0039	0.0013

[a]Computed as described in Ref. 1.
[b]Denotes corrected data from Ref. 7.

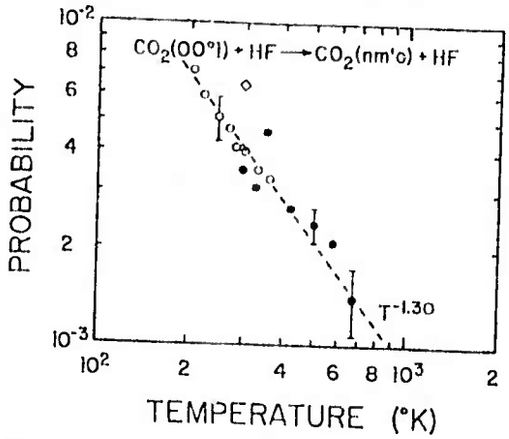

FIG. 13. Temperature dependence of the probabilities for $CO_2(00°1)$ deactivation by HF: △, Bott and Cohen, Ref. 4; ◇, Hancock and Green, Ref. 20; ●, Stephens and Cool, Ref. 19; ●, Lucht and Cool, Ref. 1; ○, present data.

D. Summary of experimental results

All of the corrected measurements of Refs. 1 and 7 are tabulated along with the present results in Tables I, II, and III. Upper bounds on the values of k_e for the DF–CO_2 system are given where possible; more accurate estimates of k_e for the DF–CO_2 and HF–CO_2 systems can in principle be gained from determination of the pre-exponential factors in the equations [e.g., Eqs. (11) and (12) of Ref. 19] for the temporal variations in HF($v=1$) or DF($v=1$) and $CO_2(00°1)$ populations. In practice this requires a precision in the determination of the relative intensities of HF(DF) and CO_2 fluorescences which is difficult to achieve.

E. Discussion

Figure 14 provides a comparison of the HF and DF self-deactivation data of Figs. 4 and 5 with data for HCl and HBr self-deactivation given in Ref. 31. The temperature dependence of self-deactivation for the DF, HCl, and HBr cases are well characterized with no large uncertainties of extrapolation between the high and low temperature data. The smooth curve drawn to represent HF self-deactivation data can be considered well-determined for temperatures below 700 °K, thanks to the application of gas-dynamic corrections, as discussed here and in Ref. 18. For temperatures above 700 °K the HF curve of Fig. 14 is dashed to indicate its approximate nature because of the unresolved discrepancies between the results of the various shock tube studies.

The curves of Fig. 14 indicate an HF isotope effect that merits further investigation. The minima in the probabilities for self-deactivation of HF and DF appear to occur at about 1000 and 700 °K, respectively. Since the intermolecular interaction potential is the same for HF and DF, the difference must be attributed to the dynamics of the vibration-to-rotation coupling responsible for deactivation. Accurate measurement of such isotope effects in the HF(DF), HCl(DCl), and HBr(DBr) systems presents a unique opportunity for tests of both the purely dynamical aspects of theoretical models, as well as those features dependent on the differences in interaction

TABLE II. Rate constants and probabilities for vibrational energy transfer in the HF–CO_2 system.

Temperature (°K)	Rate constants (10^4 sec^{-1} · Torr^{-1})			Probabilities[a]		
T	k_{11}	$k_e + k_{12}$	k_{21}	P_{11}	$P_e + P_{12}$	P_{21}
205	10.5 ± 1.0	8.0 ± 1.5	7.0 ± 1.5	0.0120	0.0081	0.0071
221	9.4 ± 1.0	6.6 ± 1.0	5.6 ± 1.0	0.0110	0.0059	0.0059
248	7.6 ± 0.5	6.1 ± 0.8	4.6 ± 0.7	0.0095	0.0068	0.0051
267	6.75 ± 0.5	5.0 ± 0.6	4.1 ± 0.5	0.0088	0.0058	0.0047
278	6.0 ± 0.5	4.0 ± 0.6	3.5 ± 0.6	0.0080	0.0047	0.0041
295[b]	5.6 ± 0.3	4.9 ± 0.3	2.9 ± 0.3	0.0077	0.0059	0.0035
299	5.67 ± 0.4	4.25 ± 0.6	3.28 ± 0.3	0.0078	0.0052	0.0040
324[b]	4.4 ± 0.3	3.1 ± 0.3	2.45 ± 0.3	0.0063	0.0039	0.0031
329	4.5 ± 0.4	3.38 ± 0.5	2.72 ± 0.4	0.0065	0.0043	0.0035
358	4.05 ± 0.3	2.9 ± 0.5	2.45 ± 0.4	0.0061	0.0039	0.0033
420[a]	2.4 ± 0.2	2.05 ± 0.2	1.85 ± 0.2	0.0039	0.0030	0.0027
500[a]	2.15 ± 0.3	1.55 ± 0.2	1.55 ± 0.2	0.0038	0.0024	0.0024
580[a]	1.5 ± 0.2	1.35 ± 0.2	1.25 ± 0.2	0.0029	0.0023	0.0021
662[a]	1.2 ± 0.2	1.2 ± 0.2	0.75 ± 0.2	0.0025	0.0022	0.0014

[a]Computed as described in Ref. 1.
[b]Denotes corrected data from Ref. 1.

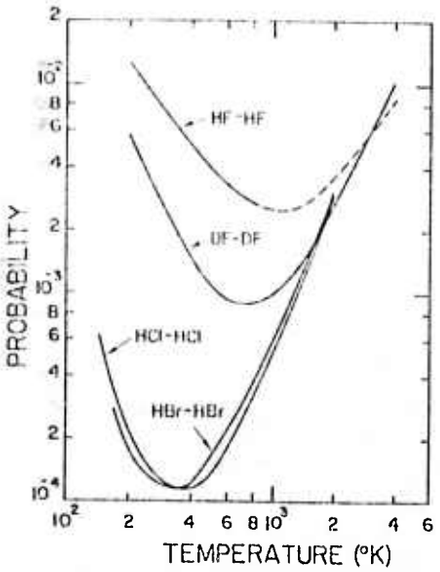

FIG. 14. Temperature dependence of the probabilities for self-deactivation of HF, DF, HCl, and HBr.

potentials for the HF, HCl, and HBr cases.

The over-simplified model for self-deactivation of HF and DF presented by Shin[32] does in fact predict the occurrence of a minimum in the DF probability at a slightly lower temperature than that for HF, in qualitative agreement with the results of Fig. 14.

The interactions between HF–HF, DF–DF, and HF–DF pairs and between HF(DF) and CO_2 are characterized by inverse temperature dependences for energy transfer probabilities that are stronger than T^{-1} (see Figs. 7 and 10). No presently available theories for energy transfer predict the strong inverse temperature dependence observed for these processes.[33] Until the effects of short range anisotropies in the intermolecular potentials can be included in a realistic way, it is doubtful that good agreement between experiment and theory will be obtained. Fortunately, progress in *a priori* calculations of energy surfaces has been rapid and perhaps reasonable interaction potentials for the F–H··· F–H and F–H··· O=C=O systems are near at hand.[34]

The existence of rapid deactivation of HF and DF by polymers at temperatures ~200 °K implied by the data of Figs. 2 and 3 and by similar data recently obtained by Hancock[35] sets a lower limit to conceivable operating temperatures for HF and DF chemical lasers. The sensitivity of the dependence of the observed self-deactivation rate for HF on the composition of $(HF)_n$ species inherent in Eq. (6) is well demonstrated in Fig. 3 for DF. If the $(HF)_n$ compositions were well characterized, then deactivation rates for one or two of the lowest order

TABLE III. Rate constants and probabilities for vibrational energy transfer in the DF–CO_2 system.

Temperature (°K)	Rate constants (10^{-8} sec^{-1} · Torr^{-1})				Probabilities[a]		
T	k_{11}	$k_e + k_{12}$	$k_e' + k_{21}$	k_e	P_{11}	$P_e + P_{12}$	$P_e' + P_{21}$
204	4.8 ± 1.5				0.0056		
208		34.0 ± 4.0	4.5 ± 0.7	≤30		0.035	0.0047
216	3.5 ± 0.5				0.0042		
225	3.55 ± 0.2	27.5 ± 3.0	2.6 ± 0.4	≤20	0.0043	0.030	0.0028
248	2.90 ± 0.2	22.5 ± 2.0	2.2 ± 0.4	≤16	0.0037	0.025	0.0025
275	2.20 ± 0.2	17.7 ± 2.0	1.6 ± 0.4	≤10	0.0030	0.021	0.0019
281	2.05 ± 0.2				0.0028		
298[b]	1.80 ± 0.2	15.0 ± 1.0	1.6 ± 0.2	≤8	0.0025	0.019	0.0020
300	1.95 ± 0.3	15.7 ± 1.0	1.5 ± 0.3	≤10	0.0028	0.020	0.0019
325[b]	1.55 ± 0.2	11.4 ± 1.5	1.25 ± 0.15	≤5	0.0023	0.015	0.0016
329	1.50 ± 0.15	13.5 ± 1.0	1.15 ± 0.2	≤6	0.0022	0.018	0.0015
359	1.12 ± 0.15	12.7 ± 0.3	1.10 ± 0.3	≤6	0.0017	0.017	0.0015
400[b]	0.86 ± 0.15	8.3 ± 1.0	$1.05^{+0.1}_{-0.2}$	≤4.5	0.0014	0.012	0.0015
473[b]	0.57 ± 0.06	7.3 ± 1.0	$1.0^{+0.1}_{-0.2}$	≤4.5	0.0010	0.011	0.0016
564[b]	0.60 ± 0.08	6.0 ± 0.5	$1.3^{+0.1}_{-0.5}$	≤4.5	0.0012	0.010	0.0022
673[b]	0.40 ± 0.10	5.7 ± 0.8	$1.6^{+0.1}_{-0.9}$	≤5.0	0.0009	0.011	0.0030

[a]Computed as described in Ref. 1.
[b]Denotes corrected data from Ref. 1.

polymer species could probably be estimated through use of Eq. (6). Alternatively, an accurate determination of the dependence of deactivation rate on HF pressure could yield information concerning $(HF)_n$ composition as a function of temperature which might be more accurate than that determined with conventional methods based on P–V–T relationships or on infrared absorption measurements.

*Supported by the Advanced Research Project Agency under ONR Contract N00014-67-A-0077-0006, by the U. S. Air Force Office of Scientific Research under Grant AFOSR-73-2550, and by the National Aeronautics and Space Administration under Grant NGL-33-010-064.

[1]R. A. Lucht and T. A. Cool, J. Chem. Phys. 60, 1026 (1974).
[2]J. R. Airey and S. S. Fried, Chem. Phys. Lett. 8, 23 (1971).
[3]H. L. Chen and C. B. Moore, J. Chem. Phys. 54, 4072 (1971).
[4]J. F. Bott and N. Cohen, J. Chem. Phys. 58, 4539 (1973).
[5]J. J. Hinchen, J. Chem. Phys. 59, 233 (1973).
[6]J. L. Ahl and T. A. Cool, J. Chem. Phys. 58, 5540 (1973).
[7]R. A. Lucht and T. A. Cool, J. Chem. Phys. 60, 2554 (1973).
[8]W. C. Solomon, J. A. Blauer, F. C. Jaye, and J. G. Hnat, Int. J. Chem. Kinet. 3, 215 (1971).
[9]J. A. Blauer, W. C. Solomon, and T. W. Owens, Int. J. Chem. Kinet. 4, 293 (1972).
[10]J. F. Bott and N. Cohen, J. Chem. Phys. 55, 3698 (1971).
[11]J. F. Bott and N. Cohen, J. Chem. Phys. 58, 934 (1973).
[12]J. F. Bott, J. Chem. Phys. 57, 96 (1972).
[13]L. S. Blair, W. D. Breshears, and G. L. Schott, J. Chem. Phys. 59, 1562 (1973).
[14]S. S. Fried, J. Wilson, and R. L. Taylor, IEEE J. Quantum Electron. QE-9, 59 (1973).
[15]J. J. Hinchen, J. Chem. Phys. 59, 2224 (1973).
[16]J. F. Bott and N. Cohen, J. Chem. Phys. 59, 447 (1973).
[17]We are indebted to Dr. J. K. Hancock for suggesting this technique for temperature measurement.
[18]J. F. Bott, J. Chem. Phys. 61, 3414 (1974).
[19]R. R. Stephens and T. A. Cool, J. Chem. Phys. 56, 5863 (1972).
[20]J. K. Hancock and W. H. Green, J. Chem. Phys. 56, 2474 (1972).
[21]J. R. Airey and I. W. M. Smith, J. Chem. Phys. 57, 1669 (1972).
[22]R. M. Osgood, Jr., A. Javan, and P. B. Sackett, Appl. Phys. Lett. 20, 469 (1972).
[23]Data discussed in Ref. 24, below, indicate that HF is predominantly in the monomer form for temperatures above 200 °K for pressures of interest in the present experiments.
[24]J. N. Maclean, F. J. C. Rossotti, and H. S. Rossotti, J. Inorg. Nucl. Chem. 24, 1549 (1962).
[25]D. F. Smith, J. Chem. Phys. 28, 1040 (1958).
[26]G. Briegleb and W. Strohmeier, Z. Electrochem. 57, 668 (1953).
[27]E. U. Frank and F. Meyer, Z. Elektrochem. 63, 571 (1959).
[28]Presumably this correction would be a 19% reduction in the probabilities given in Fig. 7; however, since the apparatus of Ref. 6 was no longer in existence, the magnitude of this correction could not be directly verified.
[29]The use of very large assumed values of k_e in calculations of the variation of relaxation rates with composition leads to curves which depart from the observed linear dependence of $(p'\tau)^{-1}$ on X'_{CO_2}. The upper bounds on k_e given in Table II represent values which would lead to nonlinear curves discernibly different from the experimental data.
[30]For further discussion of this point, see Ref. 1. The error bars of Fig. 12 represent limiting conceivable values of $k'_c + k_{21}$ that would be consistent with the measured dependence of $(p'\tau)^{-1}$ on X'_{CO_2} for the CO_2 fluorescence data.
[31]P. F. Zittel and C. B. Moore, J. Chem. Phys. 59, 6636 (1973).
[32]H. K. Shin, Chem. Phys. Lett. 10, 81 (1971).
[33]S. Ormonde, Rev. Mod. Phys. 47, 193 (1975).
[34]D. R. Yarkony, S. V. O'Neil, H. F. Schaefer III, C. P. Baskin, and C. F. Bender, J. Chem. Phys. 60, 855 (1974).
[35]J. K. Hancock (private communication, October 1974).

Chemical Laser Studies

Professor S. H. Bauer

STATEMENT OF OBJECTIVES

(i) To find conditions for generating rapidly (on the scale of 10-50 μs) very high levels of electronically/vibrationally excited BO^*, BF^*, $BC\ell^*$, BO_2^*, or other boron containing di or tri atomics, so that such systems may comprise the basis for lasing in the visible or near UV.

(ii) To measure the rates of reaction between B, BH, BH_2, or BH_3 radicals, generated by microwave stripping of boron containing precursors, with oxidizers, such as NF_3, N_2O, NO_2, and thus provide kinetic information for optimizing conditions for setting up lasing systems.

(iii) To test the utility of initiating rapid reactions between fuels, such as B_2H_6, H_3BCO, etc., and simple oxidizers by irradiating mixtures with intense pulses of CO_2 laser radiation; in general, SF_6 is added to the mixtures to serve as the energy absorbers-transmitter.

PERSONNEL

Dr. Josef Stricker, Post Doctorate Research Associate, terminated his tenure on this project on 15 August 1974. Mr. John Haberman was appointed while he was still at the University of Texas completing his Ph.D. program. He did not arrive in Ithaca until 1 April 1975. During that interval shop work continued on the construction, testing and revision of the pulsed CO_2 laser, and on the beam sampling system for the flow reactor, with TOF-MS diagnostic. No experiments were performed with this flow reactor during the report period.

DEVELOPMENT OF TECHNIQUES

A TEA pulsed CO_2 laser of a modified Seguin design, was constructed, extensively tested, reconstructed and finally developed into a reliable and reproducible device for generating approximately 20 J pulses. These show a rise time (which we estimate to be) of the order of 200 ns (it is too fast for our detector-recorder system to measure accurately), and a decay time (1/e) of approximately 1.5 μs; peak power are in the tens of megawatts. Triethylamine is an essential ingredient in the CO_2-N_2-He mixture for upgrading of the energy output. Good reproducibility is obtained with approximately 50 Kv excitation, when the gas mixture in the laser tube is fully replaced between shots; this is not essential for general operations. The burn pattern is clearly multi-mode, of rectangular shape (20 x 42) mm^2. About two months ago one of the condensers failed; it was replaced and we reduced the operating voltage from 55 to 48 Kv, to minimize the chances for other failures. The test cells (eight) are small, hollowed out Al blocks with rectangular front windows, 17 x 42 mm^2, and two round side windows, 15 mm I.D.; the cell volume is approximately 22 cm^2. In several cells a rear rectangular window was cut to permit measurement of the transmitted radiation intensity, or to provide access to the cell interior for insertion of powder samples. All cells have relief valves. We found that the pressures developed during the rapid onset of combustion occasionally burst the rock salt windows; even with the relief valves extensive crazing of the windows appears after half a dozen runs.

The operating procedure starts with several cells assembled, after careful cleaning of the walls, polishing the windows, etc. The cells are vacuum tested and conditioned with the fuel [B_2H_6, B_5H_9]. They are then re-evacuated and

filled with the reagents [fuel + oxidizer + SF_6] taken directly from their respective cylinders. [Lack of reproducibilities in recorded light intensity, as described below, have been traced to failures to properly condition the cells, insufficient care in mixing the reagents, and to impurities in the reagents.] Then, in rapid succession the cells are exposed to CO_2 laser pulses and the emissions recorded. The laser beam is not focused.

The experimental arrangement is shown schematically in Figure 1. The emitted chemiluminescence can be simultaneously recorded, both photographically $\left[\int I_t(\lambda)\, dt \right]$ and photoelectrically $[I_{\lambda 1}^{\lambda 2}(t)]$. The electrical recording devices are triggered by an amplified pulse from a LN_2 cooled IR detector, which views the reflected beam from a tilted NaCℓ cell entrance window.

The Four-channel, Broad Band Photometer [4 CP]

The arrangement of the photometer is illustrated in Figure 1; both the top view and an end view are shown. The light from one round window is incident on a polished square base prism, which directs the light onto 4 filter-phototube units. A sandwich of two colored glass filters limits the range of response for each phototube to a selected broad spectral region ($\lambda_1 \rightarrow \lambda_2$). The transmission curves for the filters multiplied by the corresponding photo-surface sensitivities are plotted in Figure 2. The output scope records provide rough but ready gauges of chemiluminosity $[I_{\lambda 1}^{\lambda 2}(t)]$, and permit the rapid comparison of intensities produced by various combinations of fuels and oxidizers, to determine the effect of total pressures, and thus serve as guides to those ranges of the spectrum which merit detailed examination. In order to obtain light intensity calibrations,

the reactor cell was replaced by a geometrically equivalent box which holds a GE-3M flashbulb, of known spectral intensity distribution and total light output [see below].

The Jarrell-Ash, 1 meter Spectrograph [JAS]

As is indicated in Figure 1, a tilted mirror directs the light emitted from the other end window of the cell onto the slit of the JA grating spectrograph, which has an effective aperture of f/7.8 and a dispersion of approximately 7 Å/mm. Each setting of the grating permits recording of a time integrated spectrum $\left[\int I(\lambda)\,dt\right]$ for a 2000 Å range from 2100 Å to 8000 Å. In these experiments the resolution was determined by the slit width, which in turn was set by the available light intensities. Generally we worked with slit-widths of approximately 80 μm; this gave a plate resolution of 0.5 Å. While single shots were often sufficient to record a diseernable spectrum, to enhance the photographic density 3-6 shots were sometimes superposed. Our reference spectra for wavelength calibrations were superposed utilizing a Hartmann disphragm. TRI-X professional film No. 4164 was used; these have a high sensitivity over a broad spectral range.

The Optical Multi-channel Analyzer [OMA]

We borrowed an OMA system to record the spectral dependence of chemi-luminescence on a time resolved basis. The SSRI model 1205A eontrol unit, with model 1205D video detector, and model 1210 high voltage pulser were kindly supplied by the Princeton Applied Research Corporation of Princeton, New Jersey for a one week evaluation. [We acknowledge with thanks this courtesy.] We were somewhat disappointed in that no significantly new data were developed during these trials. The following is a brief analysis of the limitation of OMA

for our application.

The detector tube was mounted on a 1/4m JA spectrometer, with fixed slits. Each channel of the OMA (approximate 2.5 μm wide) provides a summed signal covering 5 Å of spectral information. However, in actual performance we found that when it was free running the overall resolution [spectral plus electronic] was closer to 10 Å, and for a single shot the added electrical noise and background signals degenerated the attainable resolution to approximate 30 Å. In case of BO, where the band heads are double-double degenerate, the resulting OMA spectra revealed only coarse features. The wavelength response of the 1205D detector is limited and not sufficient for a full study of the spectral range of interest. The detection of efficiency of the tube falls off very rapidly below 400 nm; see Figure 3. The minimum gating pulse width for model 1210 pulser is about 8 μs which is too long to permit us to study several of the narrow emission "spikes" [refer to C and D data sets, below]. The most severe limitation of this device is a consequence of the digital nature of the OMA output which limits the possibility of obtaining statistically significant results with high resolution from a single intense (fast) event, in contrast to providing useful information by superposing many faint events, each with a low S/N < 1 characteristic. In our case the BO molecular transition bands are superposed on top of a large and almost continuous emission background, both of which are intense.

Fourteen Channel (Moderate Resolution) Spectrometer (14 CS)

A multi-channel phototube array for the output of the one meter JA spectrograph (refer to Figure 1) was constructed. Fourteen phototubes were aligned such that each viewed 9.5 mm aperture which corresponds to a band pass

of approximately 65 Å, across the entire focal plane of the spectrograph, thus covering a total of about 1750 Å. A precision mask was machined with 14 open and 13 closed sections each 9.5 mm wide. By rotating the grating we can bring the 13 previously blocked portions of the spectrum in front of the open slots. With this many channels the entire spectral output from the reaction can be quantitatively recorded, as a function of time, with a spectral resolution of 65 Å and with a minimum number of shots. Furthermore, the oscilloscope output can be placed on an absolute basis so that total photon numbers can be deduced. In practice, the number of channels was limited by the number of dual-beam oscilloscopes we can assemble. [This unit is not yet operational.] In addition we are designing a mask and a set of slender mirrors which will allow us to record, in a similar manner, the phototube outputs from selected portions of the spectrum (say 100 Å wide) with a resolution of approximately 7 Å. Thus, once an interesting molecular band has been identified, the time dependence of its intensity distribution on composition and pressure will be readily explored.

SUMMARY OF RESULTS

In the following seven combinations of reagents were tested utilizing the diagnostics described above. The results for each of these mixtures are briefly summarized.

A. $B_2H_6 + N_2O + SF_6$ (low pressure range)

Typical oscilloscope traces obtained with this mixture (4 CP) are presented in Figure 4. A substantial peak in intensity appears in the 400-500 nm channel. The output voltage at the peaks ranged from 15 to 20 volts across a 1 K ohm resistor; the background level underlying this peak is about 6 volts. This peak

occurs quite reproducibly 30-40 μs after the initiating laser pulse. For the particular run illustrated here the intensity recorded in channel 2 (300-400 nm) was for some reason enhanced by a factor between 5 and 10 over that normally observed; this may be due to Si contamination from either the cell or the gas-transfer line.

The photographic record of the spectrum show BO^* bands. Two shots on TRI-X film were sufficient to show (weakly) details of the BO band heads in the region 404 (1,0); 436 (1,1); 504 (0,2); and 555 (0,3) nm of the α system. A time resolved emission spectrum was then recorded with the OMA. The videcon tube was gated "on" for 10 μs intervals at selected times 10 μs post initiation, during the observed maximum, and 50 μs post initiation. In every case the violet end of 6 BO band heads ($A^2\Pi \rightarrow {}^2\Sigma$) between 400-600 nm could be identified, with an accuracy of 25 Å. Gating the OMA on during the pulse, as indicated in Figure 4, shows more emission at all wavelengths than when the OMA was gated on for the same period before or after peak emission. In other words, the emission maximum observed in channel 1 does not appear to arise from a single BO transition but from an overall enhancement of intensity. This may be due to a rapid rise in chain-carrier concentrations, initiated by the combustion. The relative intensity of the BO emission as recorded by the OMA during the intervals designated before, during and after the maximum are 3.5, 5.0 and 4.0, respectively. For comparison, the relative flashbulb calibrating intensity, measured in the same manner for a 10 μs gate [20 ms after flashbulb ignition] is about 3.0. On the basis of the manufacturer's rating of the equivalent black body color temperature for the GE-M3 flashbulb [Appendix II] the maximum peak output for this system indicates an emission from the sample which correspond to

approximately 4×10^{19} photons $cm^{-2} sec^{-1}$. We estimate that during the 11 μs excess-emission-peak $\approx 2 \times 10^{17}$ photons are produced, while the integrated emission is at least x 10 greater. The cell contains 2.8×10^{19} B atoms and 1.4×10^{19} oxygens.

B. $B_2H_6 + N_2O + SF_6$ (high pressure range)

The (4 CP) was used to evaluate the emission from samples at higher pressures. The results are illustrated in Figure 5; they are closely similar to the data shown in Figure 4. The time for appearance of the peak intensity is earlier somewhat than that for the lower pressure runs.

C. $B_2H_6 + NO_2$ (with and without SF_6)

Since NO_2 has an absorption band at 10.6 μ we tested whether any SF_6 is essential to serve as an energy transfer agent. Mixtures of fuel + oxidizers were run with and without added SF_6. Sample results are shown in Figures 6 and 7. The emission intensity (4 CP) differ by almost a factor of 2, with greater emission generated by samples that contain SF_6. However, most of the data were taken without SF_6 to remove the possibility of superposed S_2^* emission. The scope traces indicated no strong peak emissions; the emission time profiles do show several small peaks.

To obtain integrated spectral distributions (JAS) for $B_2H_6 + NO_2$, multiple exposures were taken ---- four exposures were superposed to record 350-550 nm range, and 6 exposures were superposed for the 450-650 nm range. The band systems for BO and BO_2 were clearly evident. Nine of the eleven BO bands ($A^2\Pi \rightarrow {}^2\Sigma$) are clearly identifiable over the 350-650 nm spectral region. On several plates the double-double degraded band heads of BO can be readily identified; all the observed bands were degraded to the red. The BO_2 maxima reported by Pearson and Gaydon were also recorded on these films. The results obtained with the OMA were identical with those found for the A and B mixtures. The violet

ends of seven BO bands were identified. The relative intensities of BO and flashbulb emissions are, respectively, 4 and 3. On the same scale, the relative intensity of the BO emission peaks from the $B_2H_6 + N_2O + SF_6$ mixtures (A) is 5. In addition, the OMA indicated several BO_2 maxima. When it was gated "on" at late times the sodium D lines were clearly observed (unresolved).

D. Mixtures of $B_2H_6 + O_2 + SF_6$

Figure 8 shows typical oscilloscope scans (4 CP) for such mixtures; no obvious sharp peaks in intensity appear.

E. $B_5H_9 + N_2O + SF_6$

Typical scans for this mixture (4 CP) are illustrated in Figure 9. The time evolution of the emission is similar to that observed for $B_2H_6 + N_2O$ samples, as shown in Figure 4. In this case, however, the emission intensity is 1/5 to 1/4 of that when B_2H_6 is used as a source. We were not successful in recording discernable emission spectra by superposing 2 shots from this mixture.

F. $B_5H_9 + NO_2 + SF_6$

The (4 CP) records for this mixture are shown in Figure 10. Interesting time dependent emissions appear in channels 1 and 4, covering the spectral range 400-640 nm. Further study of this sample is underway.

G. $B_5H_9 + O_2 + SF_6$

Typical (4 CP) traces are shown in Figure 11. Channel 1 (400-500 nm) reveals an interesting intense emission; additional studies are required to identify the emitter.

At this stage we made a direct test of the role of SF_6, in view of the observation that under some conditions [when SiH_4 is used as a fuel, etc.] intense

S_2^* emissions essentially dominated the spectral distribution. The question is whether in the case of the boranes, SF_6 acts solely as an energy transfer agent. The pressure of SF_6 in the sample cell determines how much energy is absorbed by the mixture. When too little is present initiation of the oxidation reaction is considerably delayed, and the total intensity is low. When the SF_6 pressure is too high the sample mixture is not uniformly irradiated. When low partial pressures of SF_6 (less than approximately 22 torr) were used, non-uniform and unreproducible emissions were recorded; specifically little emission was observed (4 CP) during the first 40-50 μs as indicated, in Figure 12. Compare these results with the scope traces shown in Figure 4.

CURRENT PROGRAM AND PROJECTIONS

The immediate task is to complete the installation of the 14 channel, moderate resolution attachment to the JA spectrometer, and to calibrate the spectral and electronic response for each of the channels over the entire wavelength range. This will require a significant number of hours; however, we are convinced that this time will be well invested. Meanwhile, we shall continue with the design and construction of a 10 channel, high resolution, mask consisting of 10 slits approximately 1 mm wide, each to provide 7 Å band pass.

In our search for an optimum fuel-oxidizer combination, we propose to focus on those BO bands for which the lower states have high v" values both in the α and β systems, and to select portions of the spectrum at which there are no underlying BO_2 bands. On the basis of experiments described above with B_2H_6 and B_5H_9, and correlary observations made by Dr. Graydon K. Anderson in his studies of attack on H_3BCO, it appears that H_3BCO and H_3BPF_3 are fuels of high potential for BO^* production. The problem here is to find oxidizers with which these reagents are compatible, so that mixtures could be prepared for laser irradiation. We plan to test N_2O, OF_2 and possibly NF_3. The use of these fuels suggest another intriguing possibility. If it is demonstrated that pulsed BO^* and BS^* lasers could be prepared, flame lasers could be developed based on mixing flows of BH_2 or BH radicals with suitable oxidizers in rapidly flowing streams. However, prior to setting up such experiments basic data on the rates of reaction between O, S, O_2, N_2O, or F_2O and BH and BH_2 will have to be obtained. This we could do with the flow reactor and TOF-MS diagnostic. The current status of the reactor, nozzle and beam chopper is illustrated in Figure 13.

We have on hand the components needed to construct a long narrow cell, with internal reflecting walls for near-axial irradiation of its content. A laser cavity for the visible and near IR range will be set up along the axis of the cell. We will thus have the facility for testing selected mixtures for the onset of lasing.

We also propose to look into the possibility of generating substantial concentrations of C, C_2, and C_3 by the pyrolysis of C_2O_3: SF_6 mixtures with incident 10.6 μ radiation, both under pulsed and cw conditions. If successful this could lead to lasing via reactions of C_n with OCS and S_2^*.

APPENDIX I

To test for uniformity of sample irradiation we set up the configuration shown at the top of Figure 14. The SF_6 pressure was varied and the transmitted power was measured. The results are plotted in the accompanying graph. Each sodium chloride window reduces the power by approximately 18%. Note that the test cell has a 3.8 cm path length and 2 windows, in contrast to a single window and 2.7 cm path length for the gas mixtures used in the emission experiments. Reduction of the data as illustrated in the graph, shows that approximately 60 torr of SF_6 almost completely absorbs the incident radiation. This was derived by extrapolating the curve in Figure 14 for detected power vs pressure of SF_6.

APPENDIX II

The M3 flashbulb derives its luminosity from the combustion of Zr ribbon in an atmosphere of oxygen. The spectral distribution, over the interval 350-725 nm, corresponds to a color temperature of $T_{M3} = 4050^{\circ}K$, (cited by the GE lamp division). The source is optically thick; $\epsilon(ZrO_2$ at ≈ 400 nm) = 0.40. Hence the equivalent black body temperature ($\epsilon = 1$) is $4850^{\circ}K$. From Wein's radiation law, for a $\Delta\lambda = 90$ nm (full width at half maximum for the filter transmission x phototube sensitivity curves) centered at 445 nm:

$$J_{\Delta\lambda} = 1.57 \times 10^{2} \epsilon \text{ , watts ster}^{-1}$$

The solid angle viewed by the detector is 0.056 ster. [Note: since the identical optical geometry was maintained for the flash bulb and reaction cell, this quantity eventually cancels]. The area of emitter is 2.0 cm^2. Also, at 445 nm, $E = 4.47 \times 10^{-12}$ ergs photon^{-1}.

We derive: $W_{\Delta\lambda}^{M3} = 3.90 \times 10^{18}$ photons sec^{-1}/cm^2 of receiver

Figure 15 presents the (4CP) oscilloscope output when a GE M3 flashbulb was ignited in the location of the reaction cell. The FWHM in channel 1 is ≈ 36 ms. The recorded maximum output (1.5 v) represents the above magnitude for $W_{\Delta\lambda}$.

For comparison, the chemiluminescent intensity produced by [$B_2H_6 + N_2O + SF_6$; Fig. 4] is a factor of 10 greater at its peak [i.e. 15 v signal]. Hence the corresponding

$$W_{\Delta\lambda}\ (B_2H_6) \approx 4 \times 10^{19} \text{ photons sec}^{-1}/\text{cm}^2 \text{ of receiver.}$$

Assuming the light emitted is isotropic, and that the gaseous reaction mixtures are optically dense (thus we under-estimate the photon emission), the <u>total</u> light

output is ≈225 times that picked up by the detector. Hence, during the brief interval of 11 μs [FWHM for the excess-emission-peak] $N_{\Delta\lambda}(B_2H_6) \approx 2 \times 10^{17}$ photons were generated. During the emission spike:

$$\frac{N_{\lambda}(B_2H_6)}{\#\,B's} \approx 0.014$$

We estimated the total emission is at least 10 times greater than that produced during the spike. Thus, we obtain approximately one photon per seven boron atoms.

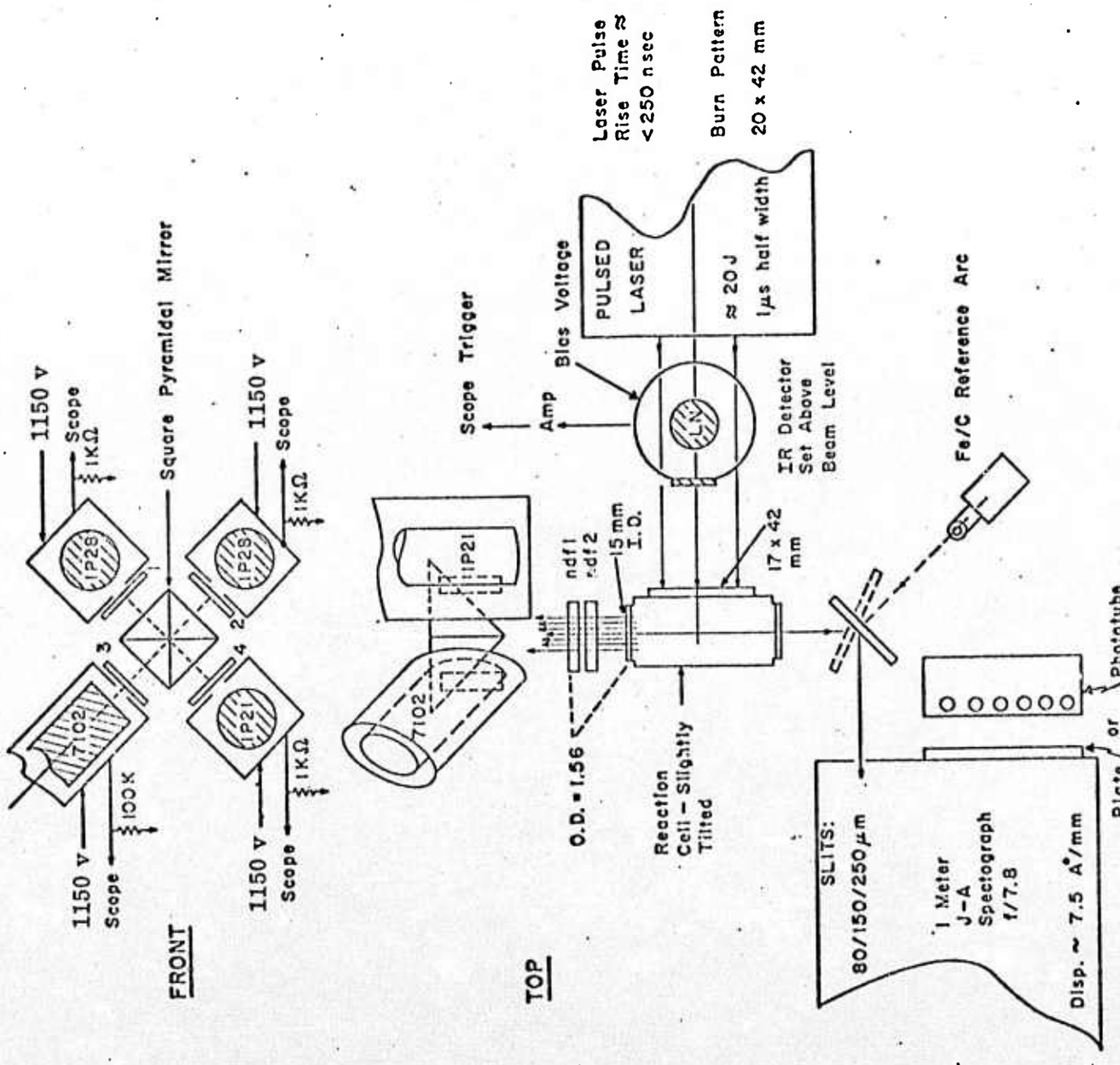
1150 v
Scope
1KΩ
Square Pyramidal Mirror
1150 v
Scope
1KΩ
1150 v
Scope
100K
1150 v
Scope
1KΩ
FRONT
Scope Trigger
Amp
Bias Voltage
PULSED LASER
Laser Pulse Rise Time ≈ <250 nsec
≈ 20 J
1μs half width
Burn Pattern
20 x 42 mm
IR Detector Set Above Beam Level
Fe/C Reference Arc
ndf1
ndf2
15 mm I.D.
17 x 42 mm
O.D. = 1.56
Reaction Cell – Slightly Tilted
SLITS:
80/150/250μm
1 Meter J-A Spectograph f/7.8
Disp. ~ 7.5 A°/mm
Phototube Assembly (14)
or
Plate Holder
TOP

FIGURE 1

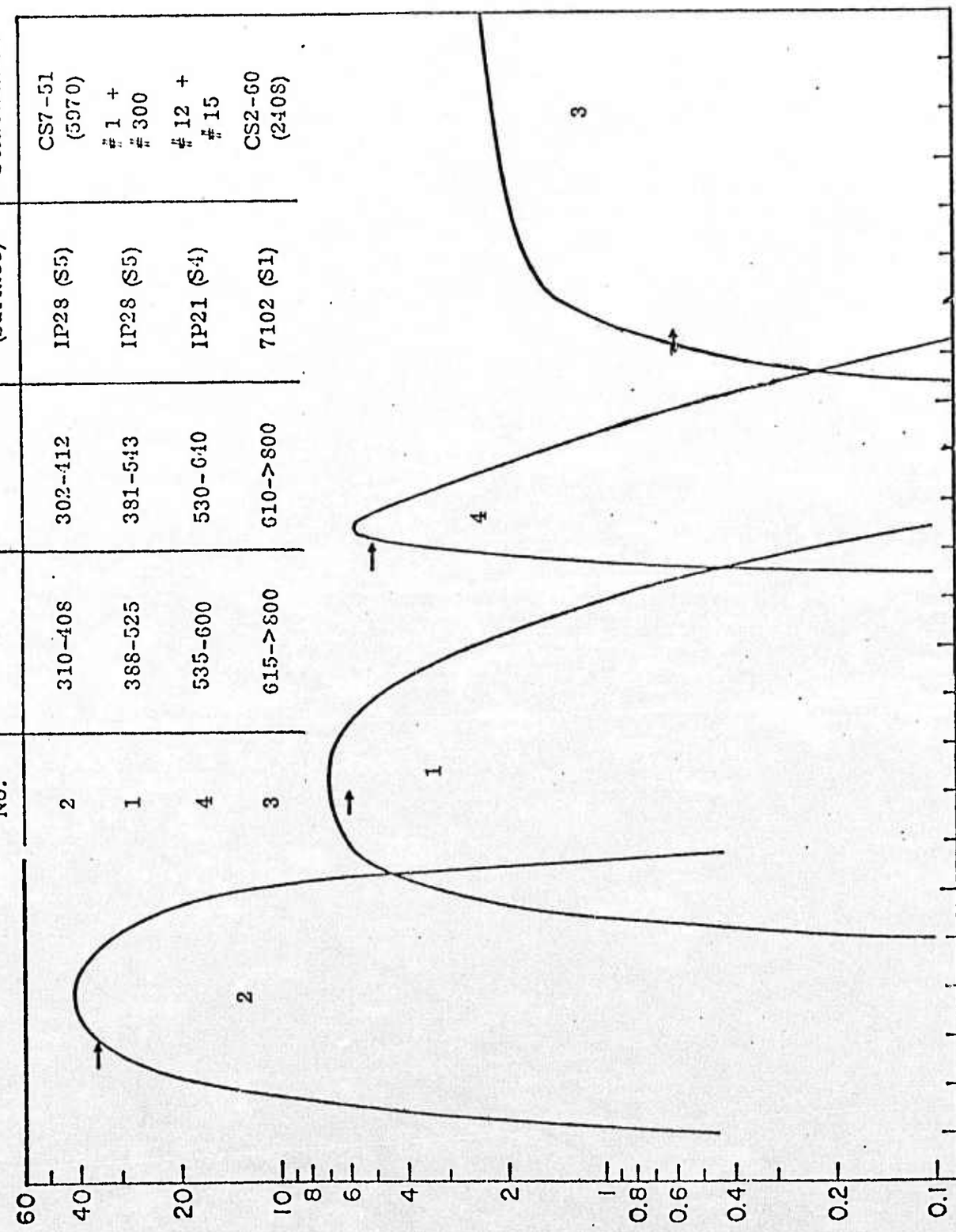

Channel No.	Δλ (nm) 10% of max	Δλ (nm) 2% of max	Phototube (Surface)	Filter Combination
2	310–408	302–412	IP28 (S5)	CS7-51 (5970)
1	388–525	381–543	IP28 (S5)	#1 + #300
4	535–600	530–610	IP21 (S4)	#12 + #15
3	615–>800	610–>800	7102 (S1)	CS2-60 (2408)

FIGURE 2

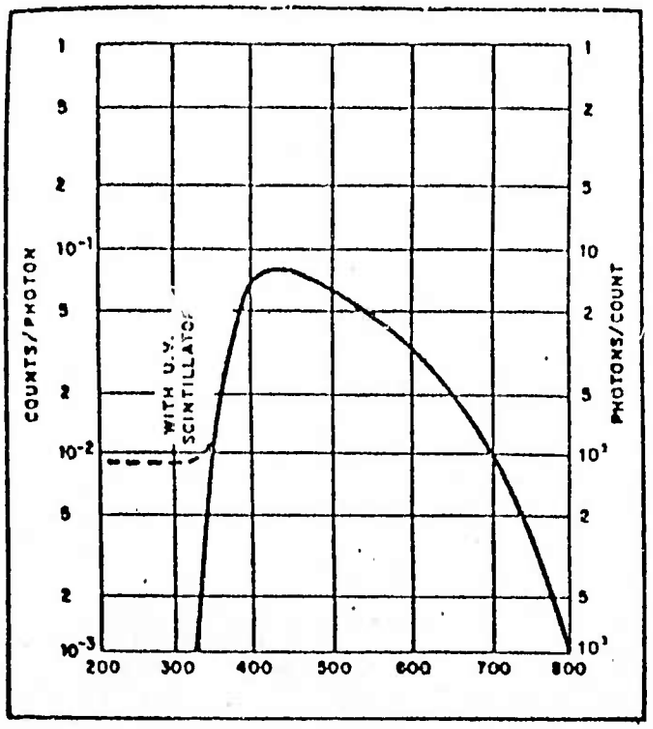

Figure I-3. RESPONSE vs WAVELENGTH FOR 1205D

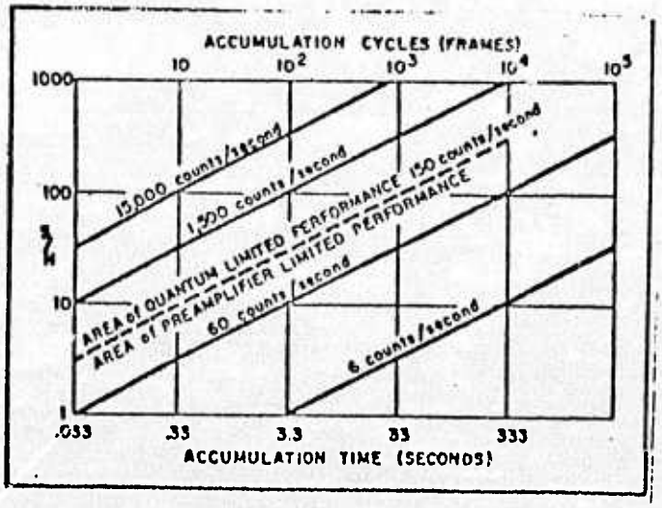

Figure I-5. SIGNAL-TO-NOISE RATIO vs TIME FOR 1205D

FIGURE 3

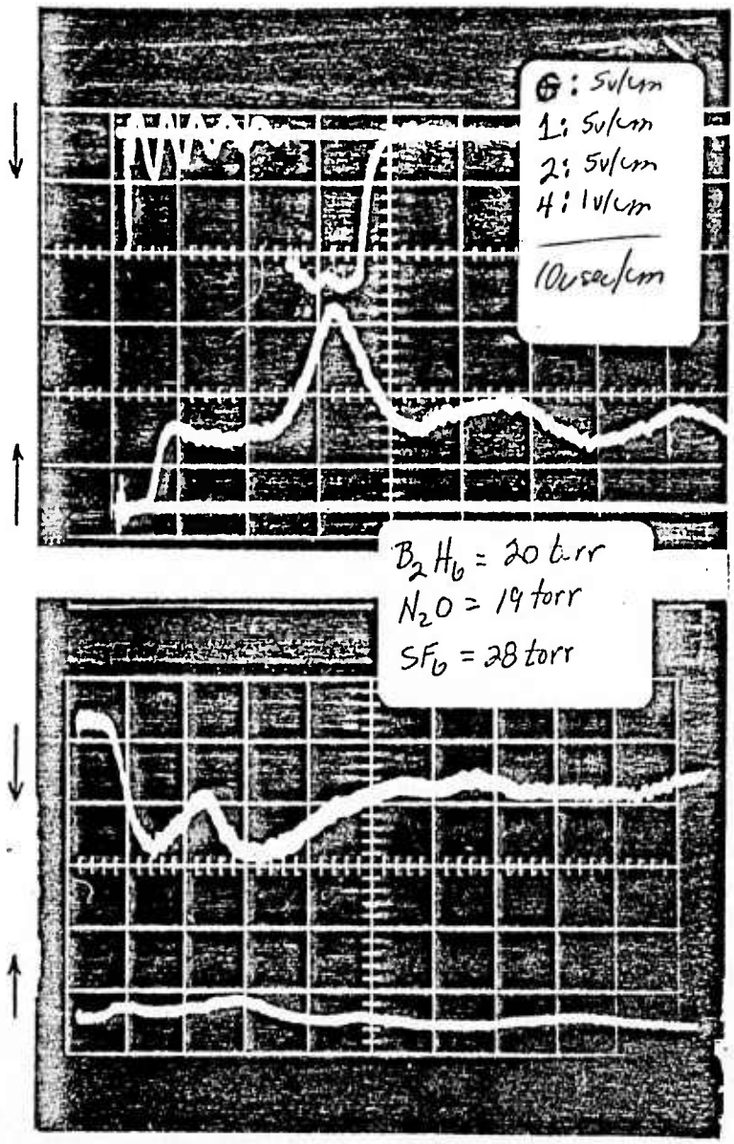
G: 5v/cm
1: 5v/cm
2: 5v/cm
4: 1v/cm
10 sec/cm
Gate (OMA)
Channel 1
B_2H_6 = 20 torr
N_2O = 19 torr
SF_6 = 28 torr
Channel 2
Channel 4

FIGURE 4

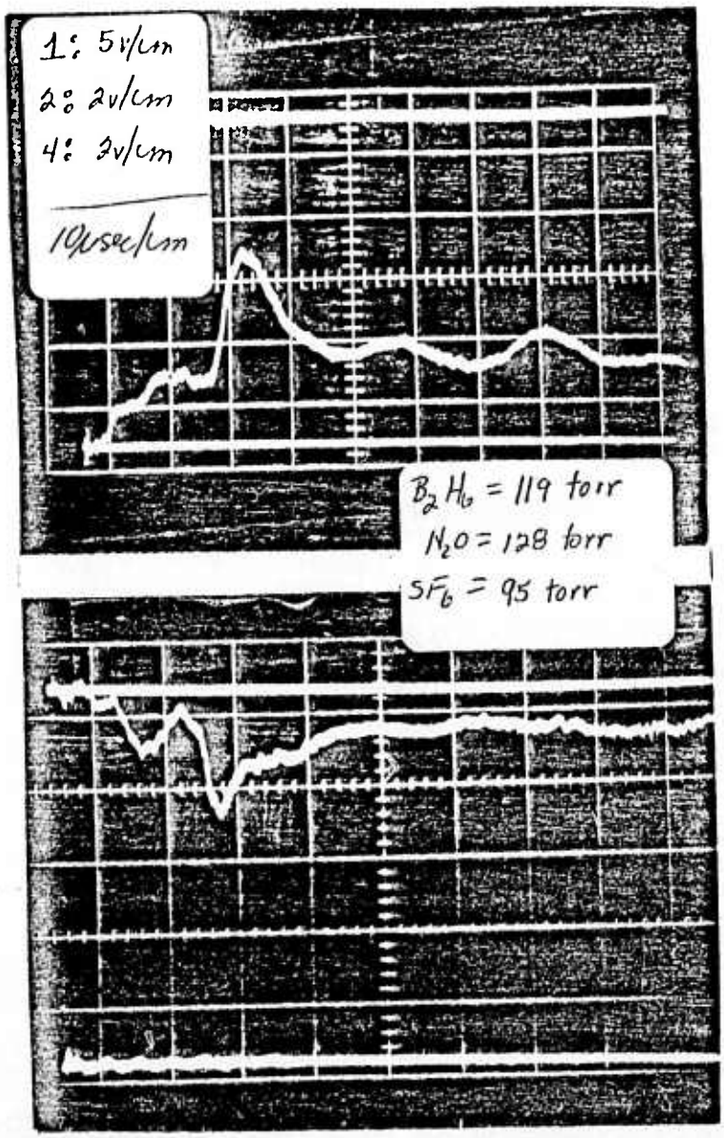

Channel 1

Channel 2

Channel 4

FIGURE 5

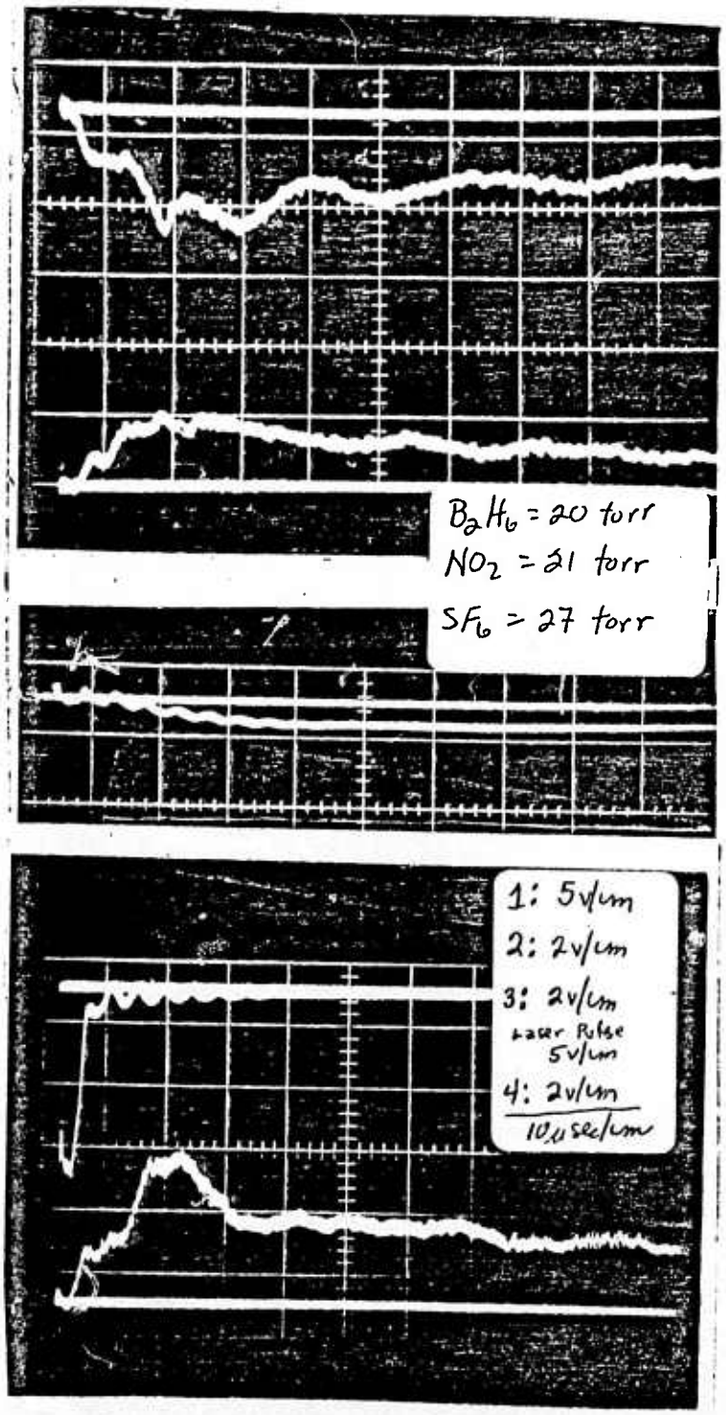

Channel 1

Channel 2

Channel 3

Laser Pulse

Channel 4

FIGURE 6

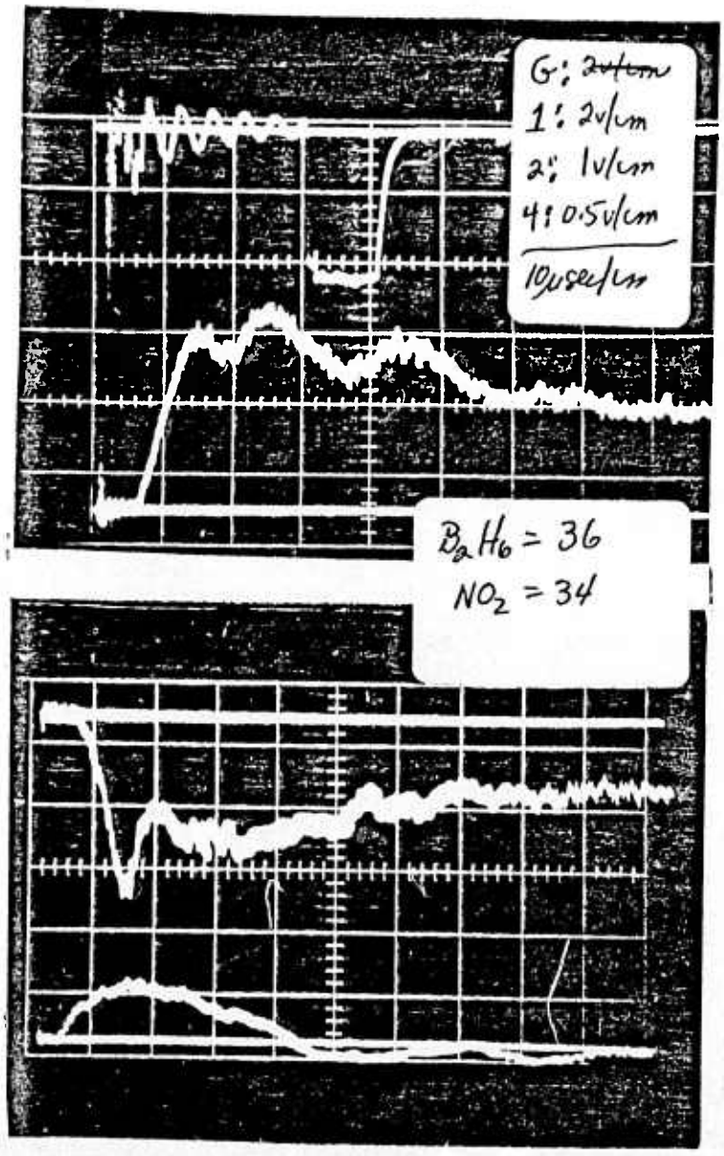

Gate

Channel 1

Channel 2

Channel 4

FIGURE 7

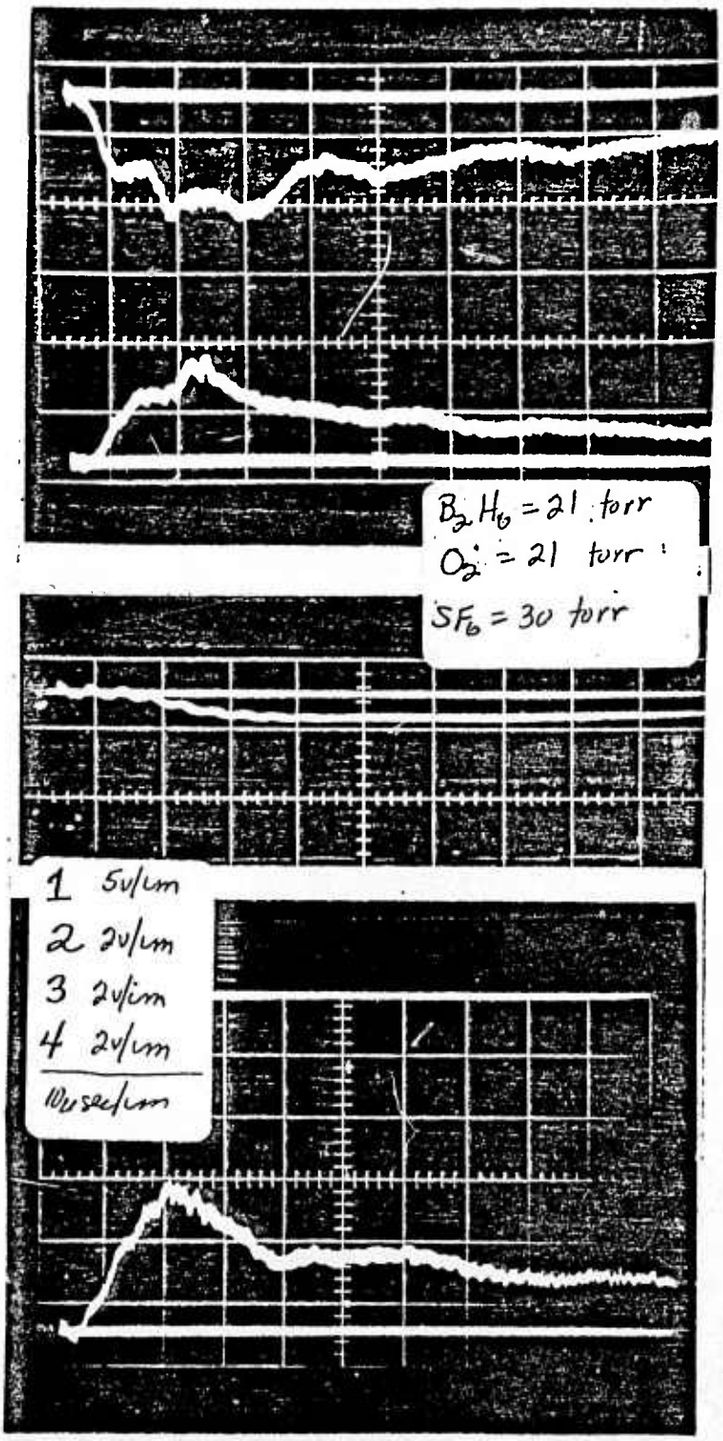
Channel 1
Channel 2
B_2H_6 = 21 torr
O_2 = 21 torr
SF_6 = 30 torr
Channel 3
1 5v/cm
2 2v/cm
3 2v/cm
4 2v/cm
10μsec/cm
Channel 4

FIGURE 8

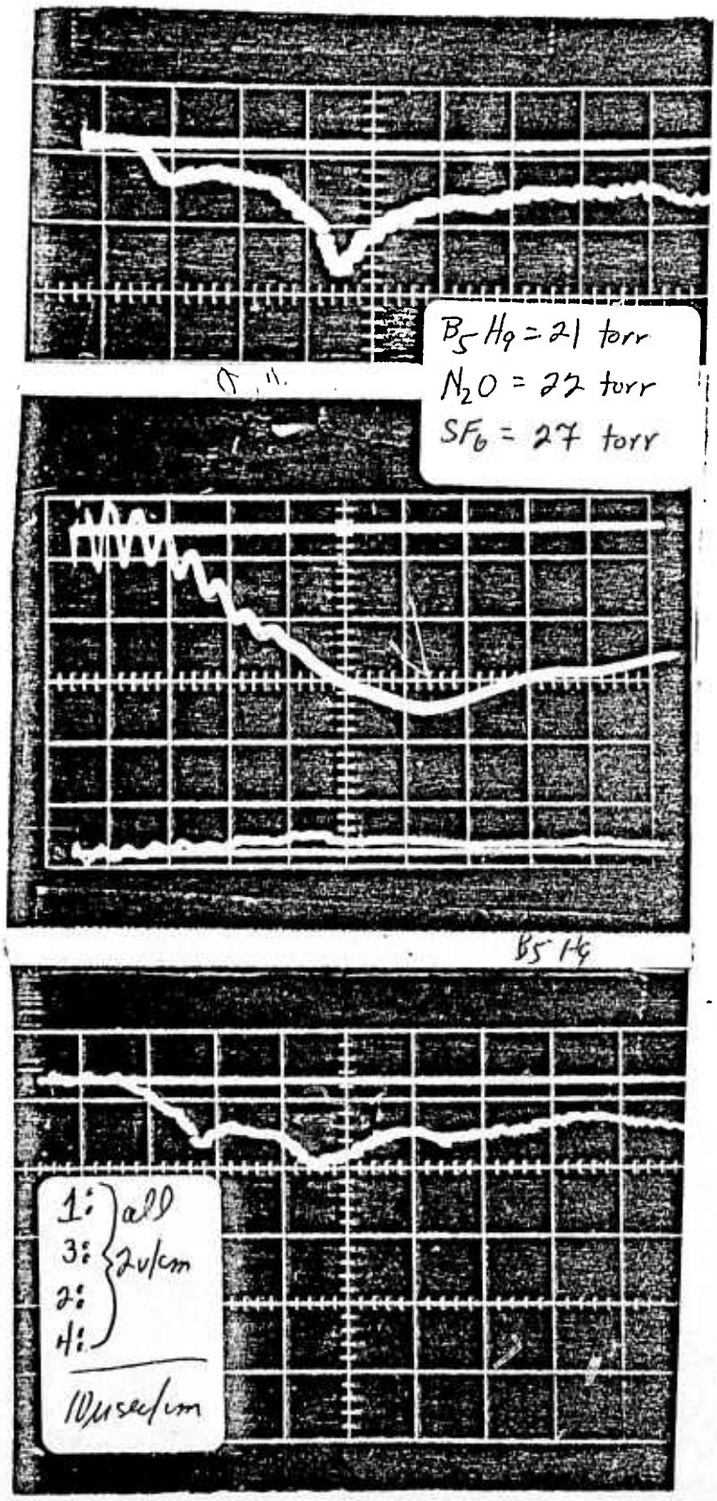

Channel 1

Channel 3

Channel 2

Channel 4

FIGURE 9

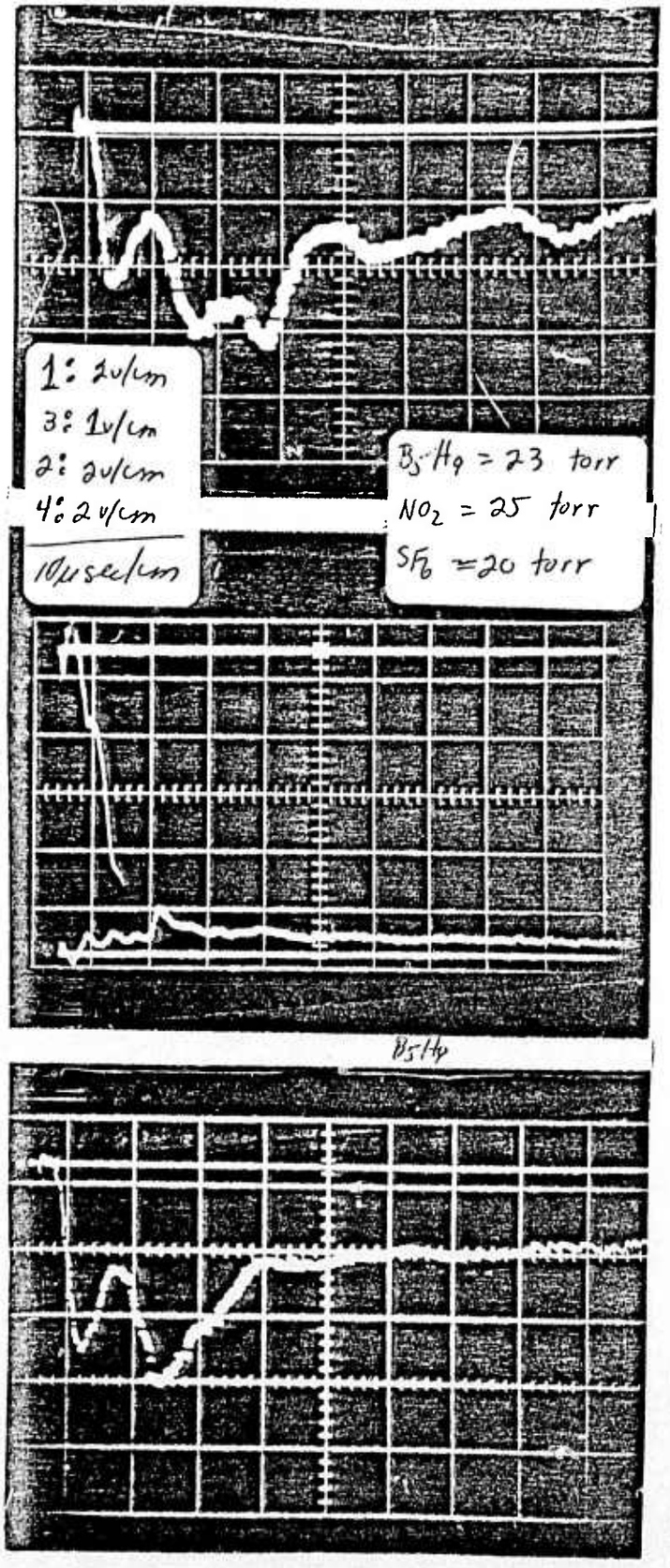

Channel 1

Channel 3

Channel 2

Channel 4

FIGURE 10

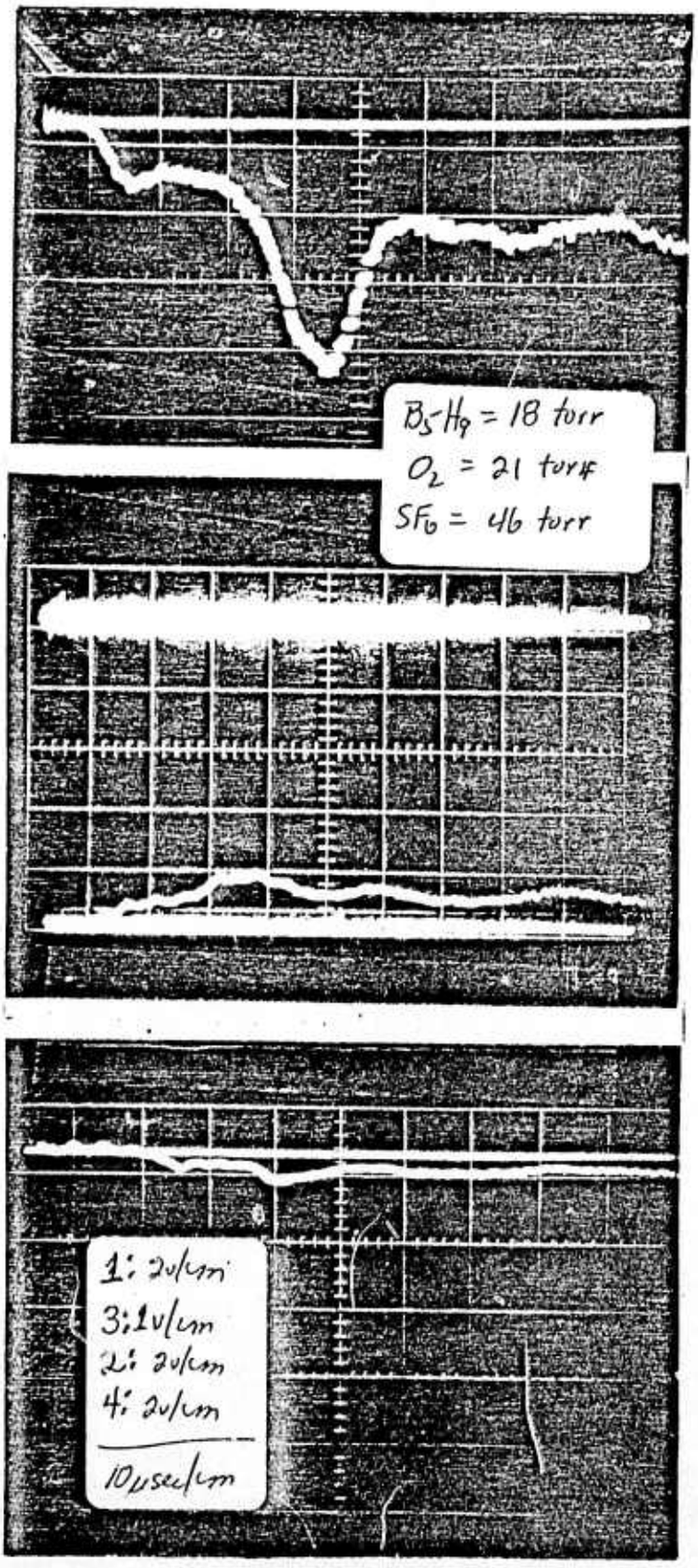

Channel 1

Channel 3

Channel 2

Channel 4

FIGURE 11

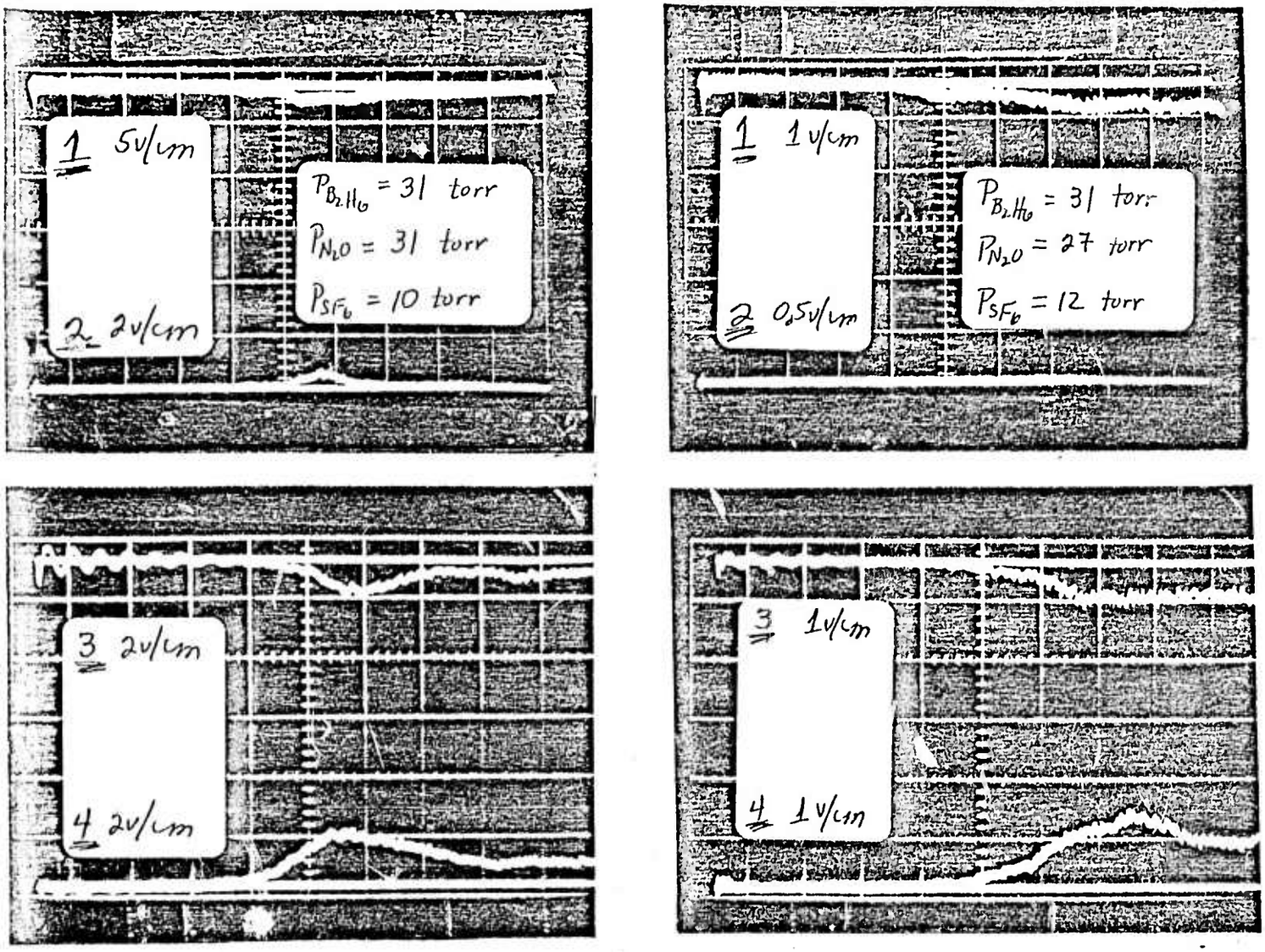

All time scales 10 μsec/cm

FIGURE 12

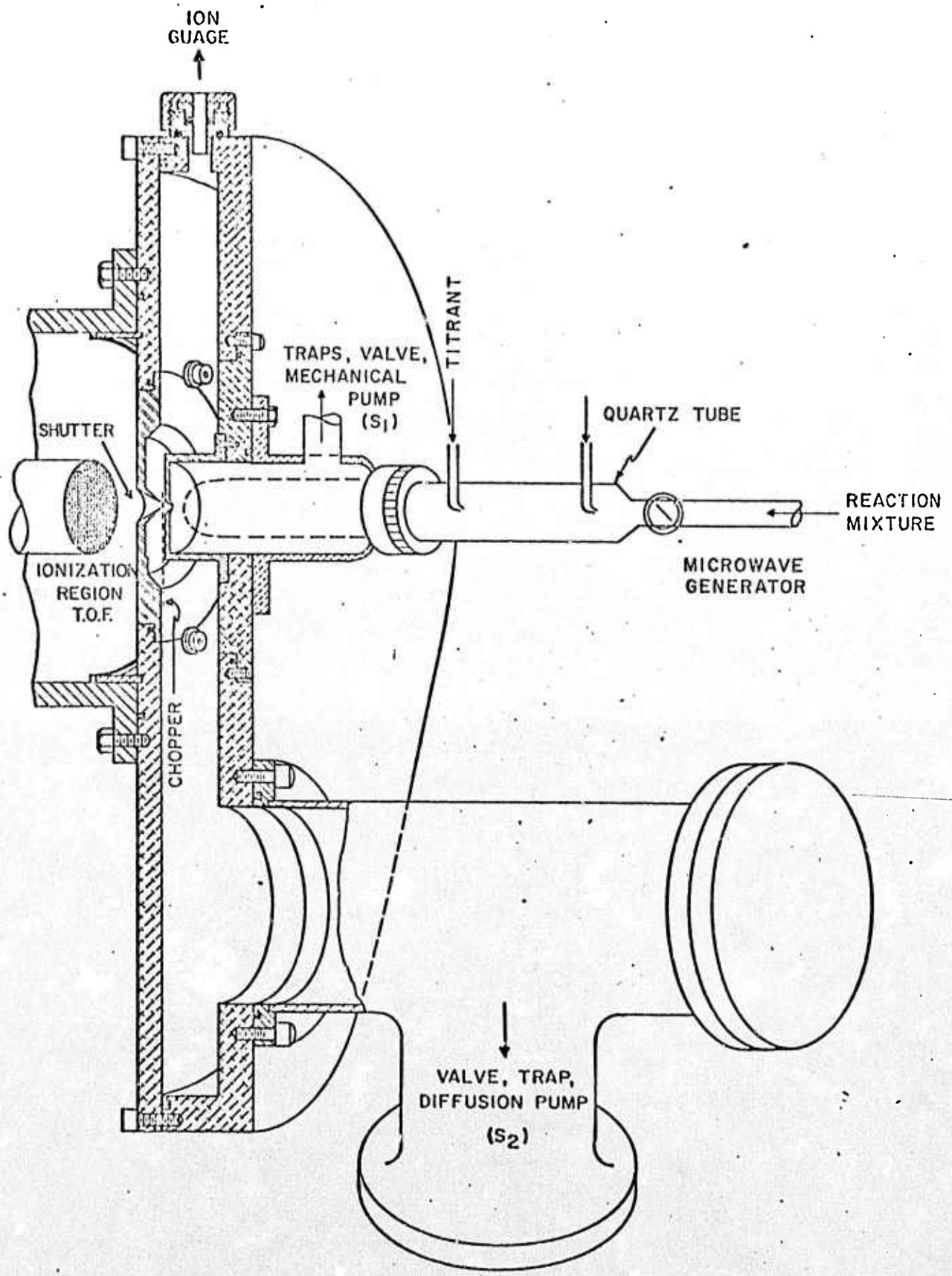
ION
GUAGE
TRAPS, VALVE,
MECHANICAL
PUMP
(S_1)
TITRANT
QUARTZ TUBE
SHUTTER
REACTION
MIXTURE
MICROWAVE
GENERATOR
IONIZATION
REGION
T.O.F.
CHOPPER
VALVE, TRAP,
DIFFUSION PUMP
(S_2)

FIGURE 13

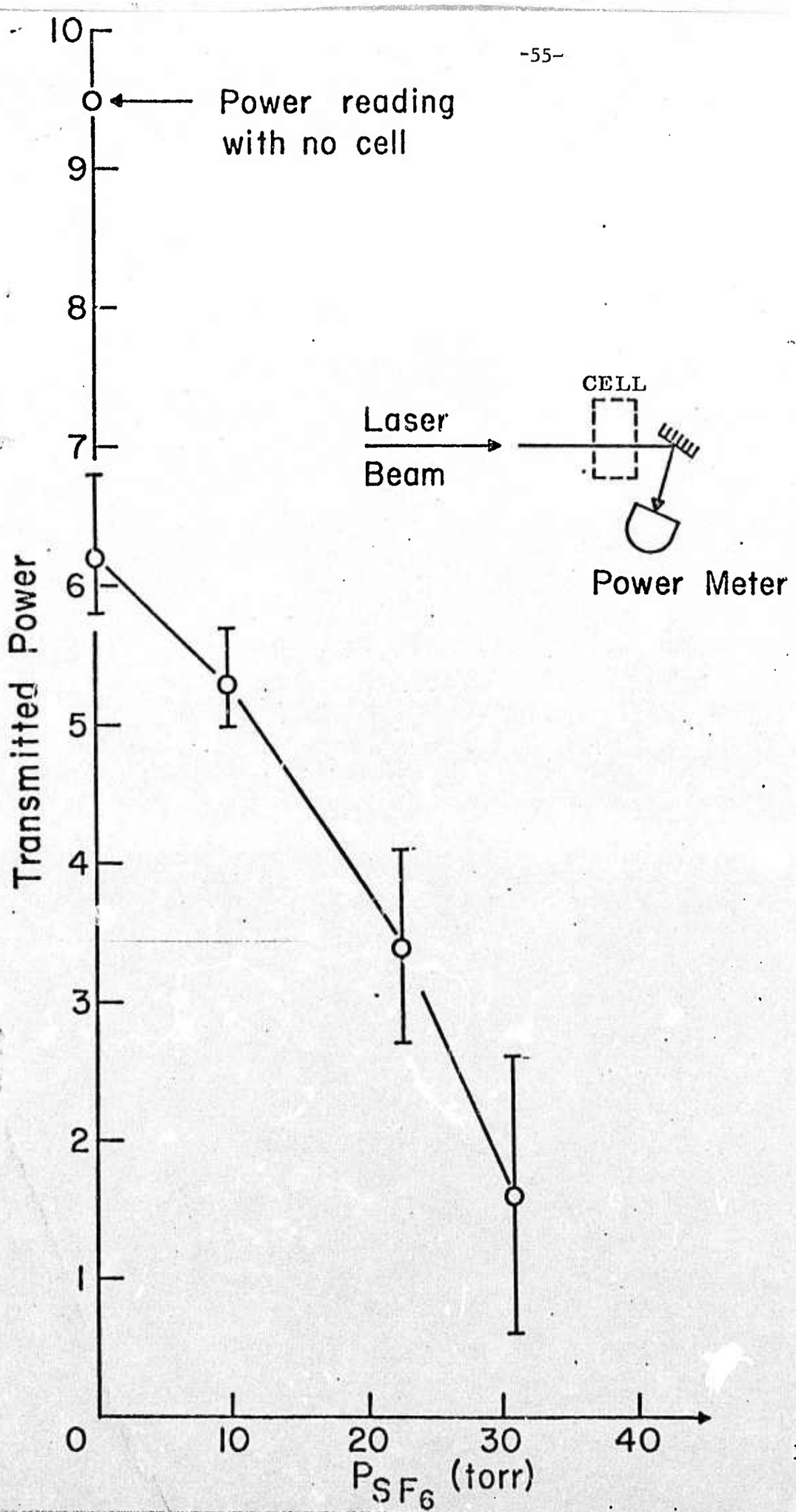
10
9
8
7
6
5
4
3
2
1
0
Power reading
with no cell
CELL
Laser
Beam
Power Meter
Transmitted Power
0
10
20
30
40
P_{SF_6} (torr)

FIGURE 14

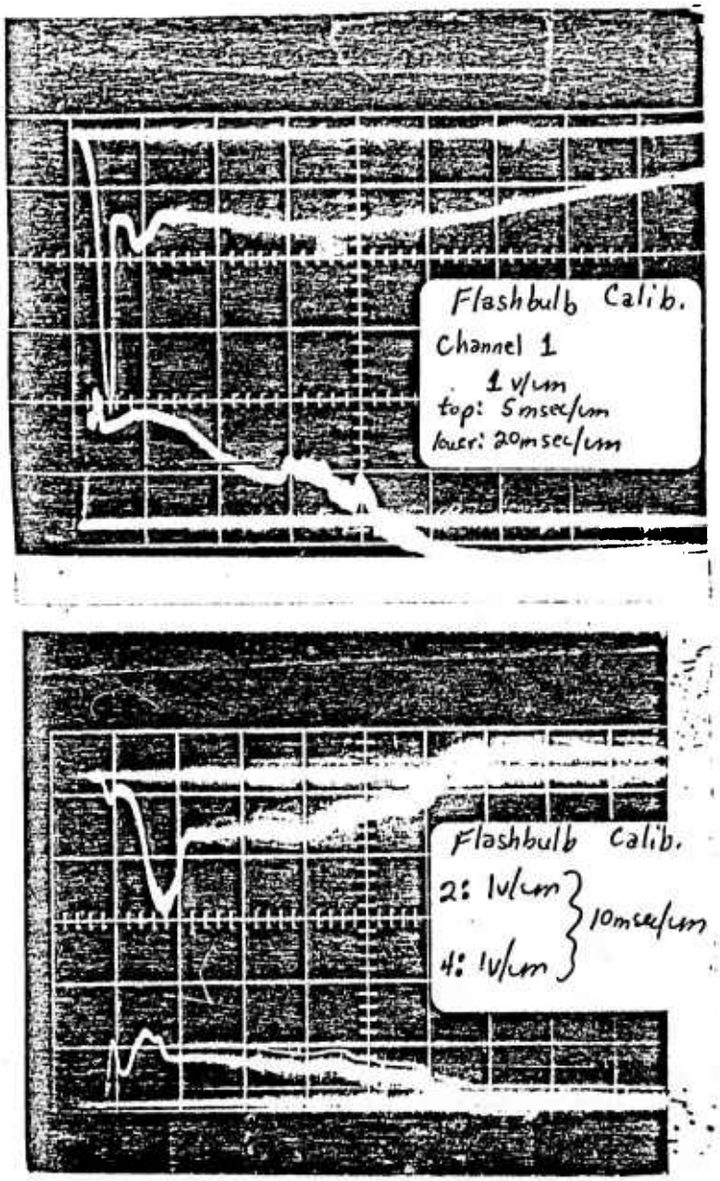

Channel 1

Channel 1

Channel 2

Channel 4

The above traces show the filtered phototube signals (4 CP) produced by a M3 flashbulb. The impressed voltage on the phototubes was 1150 v. The signal from the sample cell monitoring window (or calibration cell) is attenuated by a mask which is perforated by 11 (small) holes (attenuation factor 198) and by a sandwich composed of 1.2 density and 0.9 density neutral density filters (additional attenuation factor 126).

FIGURE 15